

System Design of an Integrated Terrestrial-Satellite Communications Network for Disaster Recovery

By

Suem Ping Loo

Thesis submitted to the Faculty of the
Virginia Polytechnic Institute and State University
in partial fulfillment of the requirements for the degree of
Master of Science
in
Electrical Engineering

Charles W. Bostian, Chairman
Timothy Pratt
Ahmad Safaai-Jazi

February 10, 2004

Blacksburg, Virginia

Keywords: Ka-band, LMDS, Integrated Network, 30/20 GHz, VSAT, TCP/IP, SPACEWAY

Copyright 2004, Suem Ping Loo

System Design of an Integrated Terrestrial-Satellite Communications Network for Disaster Recovery

Suem Ping Loo

(ABSTRACT)

This thesis describes a possible integrated terrestrial-satellite network system for disaster recovery and response. The motivation of this thesis was based on the adjacent spectrum allocations between the Virginia Tech terrestrial Local Multiple Distribution Service (LMDS) system and a Ka-band satellite system, and potentially being able to provide as an additional Ka-band satellite network backbone to the Virginia Tech terrestrial LMDS system for better and faster communications deployments. The Spaceway satellite system's design parameters were adopted typically for a Ka-band satellite system. The LMDS system was assumed to use IEEE 802.16 standard protocols although it currently uses its own proprietary protocols.

Four possible topologies integrating both terrestrial and satellite network were investigated. The study showed that the task was more problematic and complicated than anticipated due to incompatible network protocols, limitations of available hardware components, the high path loss at Ka-band, and the high cost of the equipment, although the adjacent frequency bands do suggest a possible integrated network.

In this thesis, the final selected topology was proposed and designed. The technical characteristics of the earth station used for coupling both terrestrial and satellite networks were determined by a link budget analysis and a consideration of network implementations. The reflector antenna used by the earth station was designed. In addition, other system design concerns and engineering tradeoffs, including adjacent satellite interference, rain attenuation, antenna pointing error, noise temperature, and modulation and multiple access selection, were addressed.

To My Parents

Acknowledgments

The first person that I would like to thank is Dr. Charles Bostian, who is not only my academic advisor, but also a father-like figure to me. He has made me smile during my most difficult times. I thank him for his support, guidance, and encouragement during my graduate study.

I thank Dr. Timothy Pratt's sincere guidance on my thesis. Dr. Pratt has trained me to think as an engineer. I also thank you, Dr. Ahmad Safaai-Jazi for reading my thesis and being a committee member in my master program.

I thank you, Mr. Tim Gallagher for his priceless help on my thesis. Without his assistance, I might not be able to complete this thesis. I also thank all the CWT faculties, staffs, and students. You all are just awesome! I thank you for all your help that you have provided me.

I also thank all my friends whom I have met over the past 7½ years in the U.S. All of you are surely the most wonderful gifts that I have ever received. I thank you for walking next to me during my academic life in the states. I treasure and value all of your given patience and support. I have already captured all your faces into my memory books.

I also would like to thank the most wonderful families that I have in the U.S., the Chua and Silvetre family. Without your unfailing love and support, my life in the states would not be as complete as I desired. You are definitely the angels whom HE has sent to me.

Obviously without the financial and unfailing loves from my parents, siblings, in-laws, nephews, and nieces, I would not be able to run to an endzone of a football field for a touchdown. Thanks for allowing me to achieve my dreams and goals.

The last person whom I would like to thank is HIM, Jesus as I met HIM during my academics years in Virginia Tech. HE indeed teaches me how to "*ask and it will be given to you; seek and you will find; knock and the door will be opened to you (Mathew 7:7)*". I thank HIM for his patience, love, and spiritual supports.

Table of Contents

System Design of an Integrated Terrestrial-Satellite Communications Network for Disaster Recovery.....	i
(ABSTRACT)	ii
Acknowledgments	iv
Table of Contents	v
List of Figures.....	ix
List of Tables	xi
Chapter 1: Introduction	1
1.1. Background.....	1
1.2. Virginia Tech LMDS Broadband Communications System	3
1.3. Problem Statement and Research Goals	4
1.4. Document Overview	5
Chapter 2: Ka-band Satellite Communications Systems	6
2.1. Ka-band Satellite History and Current Status.....	6
2.2. Ka-band Geostationary (GSO) Fixed Satellite System (FSS)	8
2.2.1. Spaceway Satellite System	9
2.2.2. Spaceway Satellite Space Segment.....	9
2.2.3. Spaceway Proposed Ground Segment	11
2.3. Satellite Communications Fundamentals.....	11
2.3.1. Bent-pipe Satellite System.....	12
2.3.2. On-board Processing (OBP) Satellite System.....	15
2.3.2.1. On-board Processing Switches	16
2.4. Satellite Link Multiple Access Techniques	18
2.4.1. Frequency Division Multiple Access (FDMA).....	18
2.4.2. Time Division Multiple Access (TDMA).....	19
2.4.3. Code Division Multiple Access (CDMA).....	20
2.5. Digital Modulation Techniques for Satellite Links	21

2.5.1. Coherent Versus Non-coherent Modulations.....	21
2.5.2. Phase Shift Keying (PSK).....	22
2.5.2.1. Binary Phase Shift Keying (BPSK).....	22
2.5.2.2. Quadrature Shift Keying (QPSK).....	23
2.5.2.3. M-ary Phase Shift Keying (M-PSK).....	23
2.5.3. Quadrature Amplitude Modulation (QAM).....	24
2.6. Forward Error Correction (FEC).....	26
2.7. Uplink Power Control (UPC).....	26
2.8. Summary.....	27
Chapter 3: Terrestrial-Satellite Integration Design Selections	28
3.1. Virginia Tech LMDS System Frequency Planning Allocations.....	28
3.2. Virginia Tech (VT) LMDS Modem Characteristics.....	29
3.3. Four Terrestrial-Satellite Integration Designs.....	31
3.3.1. Topology 1: RF-to-RF Coupling.....	33
3.3.1.1. Frequency Planning Aspects.....	33
3.3.1.2. Hardware Aspects.....	34
3.3.1.2.1. A Satellite-to-LMDS (STL) Frequency Converter.....	34
3.3.1.2.2. A LMDS-to-Satellite (LTS) Frequency Converter.....	36
3.3.1.3. Link Budget Aspects.....	37
3.3.1.4. Network Implementation Issues.....	41
3.3.2. Topology 2: Bandpass-to-bandpass (IF-to-IF) Coupling.....	41
3.3.2.1. Frequency Planning Aspects.....	41
3.3.2.2. Hardware Aspects.....	43
3.3.2.3. Link Budget Aspects.....	44
3.3.2.4. Network Implementation Issues.....	44
3.3.3. Topology 3: RF-to-IF baseband Coupling.....	45
3.3.3.1. Frequency Planning Aspects.....	46
3.3.3.2. Hardware Aspects.....	46
3.3.3.3. Link Budget Aspects.....	47
3.3.3.4. Network Implementation Issues.....	47

3.3.4. Topology 4: Baseband-to-Baseband Coupling	48
3.3.4.1. Frequency Planning Aspects	48
3.3.4.2. Hardware Aspects	49
3.3.4.3. Link Budget Aspects	49
3.3.4.4. Network Implementation Issues	49
3.4. Final Design Selection and Summary	50
Chapter 4: Final System Design Selection	51
4.1. System Design Block Diagram	51
4.2. VSAT Antenna	52
4.3. Elevation (EL) and Azimuth (AZ) Angle Calculations	54
4.4. Rain Attenuation Calculations	56
4.4.1. Prediction of Attenuation Statistics for an Average Year	57
4.5. Interference from Adjacent Satellite Systems	64
4.5.1. Uplink Adjacent Satellite Interference Analysis	65
4.5.2. Downlink Adjacent Satellite Interference Analysis	67
4.6. Other Losses	69
4.7. Uplink and Downlink Noise Temperatures	70
4.8. Link Budget	70
4.8.1. Inbound Link Design	71
4.8.2. Outbound Link Design	77
4.9. Summary	80
Chapter 5: System Network Issues and Hardware Selection	81
5.1. Terrestrial-Satellite Network and Protocols Concerns	81
5.2. Open System Interconnection (OSI) Layers	81
5.3. Overall Terrestrial-Satellite System Network Design	83
5.4. VSAT Commercial Hardware Components	85
5.5. Summary	87

Chapter 6: Conclusion and Future Work.....	88
6.1. Conclusion and Contribution.....	88
6.2. Future Work.....	89
References.....	90
Appendix A: Elevation and Azimuth Angle Calculations.....	94
Appendix B: (a) Uplink Rain Attenuation Calculations	95
Appendix B: (b) Downlink Rain Attenuation Calculations	96
Vita	97

List of Figures

Figure 1	Virginia Tech LMDS System Overview [Bos02].....	4
Figure 2	Spaceway North America Spotbeam Footprints [Fit95].....	10
Figure 3	Bent-pipe Transponder Satellite Link Overview	12
Figure 4	On-board Processing Transponder Satellite Link Overview	16
Figure 5	A Typical TDMA Frame [ITU02]	20
Figure 6	Different Digital Modulation BER Performance Comparison [Cou01].....	25
Figure 7	Virginia Tech LMDS System Building Blocks	30
Figure 8	A Satellite-Terrestrial System Linked by RF on Both Uplink and Downlink.....	34
Figure 9	A Block Diagram of the Satellite-to-LMDS (STL) Converter	35
Figure 10	A Block Diagram of the LMDS-to-Satellite (LTS) Converter	36
Figure 11	A Satellite-Terrestrial System Linked by IF on Both Uplink and Downlink Using a Single-Stage Frequency Converter	42
Figure 12	A Satellite-Terrestrial System Linked by IF on Both Uplink and Downlink Using a Dual-Stage Frequency Converter.....	43
Figure 13	A Satellite-Terrestrial System Linked by RF on Uplink and IF on Downlink.....	45
Figure 14	A Satellite-Terrestrial System Linked at baseband on Both Uplink and Downlink .	48
Figure 15	Integrated Terrestrial-Satellite Network Architecture	51
Figure 16	Theoretical Ka-band Reflector Antenna Pattern.....	53
Figure 17	The Geometry of Elevation Angle Calculation	55
Figure 18	Schematic Presentation of an Earth-to-Space Path Giving the Parameters to be Input into the ITU-R Rain Attenuation Prediction Procedures	57
Figure 19	Rain Climatic Zones for the Americas [ITU837]	60
Figure 20	Uplink Interference from an Adjacent Satellite System [Mar95].....	66
Figure 21	Downlink Interference from an Adjacent Satellite System [Mar95].....	68
Figure 22	Pointing Losses as a Function of VSAT Antenna Diameter.....	70
Figure 23	Inbound Data Rate vs. VSAT Transmitting Power	73
Figure 24	Inbound Data Rate Vs. Antenna Size for Given Various Pt.....	74
Figure 25	Inbound Data Rate vs. Antenna Size with $P_t=1w$ and Different Modulations.....	75
Figure 26	Inbound Link Availability vs. Antenna Size for Different Locations	76

Figure 27	Data Rate versus VSAT Antenna Size for the Outbound Link Design	79
Figure 28	A comparison of the TCP/IP and OSI protocol architecture [Ngu03].....	82
Figure 29	The Terrestrial-Satellite Integrated System OSI Model Architecture	84
Figure 30	Topology 4 VSAT Block Diagram.....	86
Figure 31	A Typical VSAT Commercial Reflector Antenna.....	86
Figure 32	Selected Commercial STL Frequency Up-converter (Left) and LTS Frequency Down-Converters (right).....	87

List of Tables

Table 1	Spaceway Satellite Frequency Allocation	9
Table 2	Spaceway Satellite Overview Characteristics [Fit95].....	10
Table 3	Comparison of different on-board switching technologies [Ngu03]	17
Table 4	Coherent Signal Modulation Methods [Cou01].....	25
Table 5	C/N of M-ary PSK and M-ary QAM [Cou01].....	26
Table 6	LMDS Radio Channel Assignment	28
Table 7	LMDS Frequency Plan Allocations	28
Table 8	Summary of Terrestrial and Satellite System Frequency Allocation Plans	29
Table 9	Virginia Tech LMDS Modem Characteristics	31
Table 10	Three Suggested Turbo Codes for Virginia Tech LMDS Modem [Esh02].....	31
Table 11	Topology 1: Inbound Link Budget Example (Blacksburg, VA -Los Angeles, CA).	38
Table 12	Topology 1: Outbound Link Budget Example (Los Angeles, CA-Blacksburg, VA)...	40
Table 13	Reflector Antenna Gain	54
Table 14	Calculations for Azimuth Angle	56
Table 15	EL and AZ Angles of Earth Stations Placed Across the United States	56
Table 16	Rainfall Intensity Exceeded in mm/hr Corresponded to Rain Climate Zones.....	59
Table 17	Regression Coefficients for Estimating Specific Attenuation, γ_R [ITU838]	61
Table 18	Uplink and Downlink α and k Regression Coefficient.....	62
Table 19	Parameter Status of p, ϕ , and θ to Find the β Value	63
Table 20	Uplink Estimated Rain Attenuation [in dB] for 99.5 % Link Availability	64
Table 21	Downlink Estimated Rain Attenuation [in dB] for 99.5 % Link Availability	64
Table 22	VSAT Maximum EIRP Levels	65
Table 23	Topology 4: Inbound Link Budget Example (Blacksburg, VA-Los Angeles, CA)..	72
Table 24	Topology 4: Outbound Link Budget Example (Los Angeles, CA-Blacksburg, VA)...	78
Table 25	An Overview of All Terminals/Stations Technical Specifications.....	80

Chapter 1: Introduction

1.1. Background

A disaster is defined as an extraordinary situation characterized by surprise, significant destruction or adverse consequences, a strong threat to important values, and a short decision-response time [Str02]. For instance, the Northridge earthquake, Hurricane Andrew, the September 11 terrorist attack, and the Iran earthquake each killed thousands of people, destroyed many buildings, and interfered with normal daily life.

In order to minimize casualties and protect public health, safety and property, government agencies must respond quickly with appropriate and effective recovery personnel and resources during a disaster. Communications is a critical element of an effective lifesaving response to a disaster because emergency responders need to exchange information with other responders, managers, technical experts, etc., at anytime from anywhere. Furthermore, rescue crews, police officers, and firefighters need reliable communications systems in order to access needed data, such as maps, blueprints, and photographs. On-site doctors and nurses also need contact with the nearby hospitals to report patients' health conditions. Hence, essential and standardized communication networks and equipment, providing wire-line and wireless voice, data, and video services, are needed. They must be deployed quickly to support such emergency management and disaster operations.

On April 5th, 1984, President Ronald Reagan signed Executive Order 12472 to direct the National Communications System (NCS) to ensure the availability of the National Security/Emergency Preparedness (NS/EP) telecommunications infrastructure. He required that the communications infrastructure should be capable of satisfying priority telecommunications requirements through the use of commercial, government, and privately owned resources in support of the President and federal departments, agencies, and other entities [Luk99]. In addition, the Federal Emergency Management Agency (FEMA) is responsible for improving disaster area communications capabilities by identifying the full range of communication requirements within the disaster area and implementing smart and effective solutions to improve those communications [Bar95].

Although cellular telephones conveniently provide voice communications, the cellular networks can quickly be congested with traffic. They fail easily due to high volumes of users operating simultaneously in an affected area. Wire-line telephone carriers can be used but often would be overloaded as well. For example, for the Oklahoma City bombing, 75% of the incoming calls were blocked. For the Loma Prieta earthquake, 90% of the incoming calls were blocked for a short period of time [Phi95].

Data and video communications require even higher bandwidth capacity since these services allow users to monitor and update the real-time situation within an affected area, especially in the large-scale disaster like the September 11th event. Many broadband network cables and wires are destroyed or malfunction during disasters. Although some surviving fiber and copper connections might be available nearby, it is not easy for the first responders to access the connections quickly. For example, at the Pentagon attack, it took about a week for a local fire department to establish and restore Internet access [Bos02].

Many private companies and government agencies have developed various types of communications systems to prepare for disaster response and rescue needs. However, many deployed communications systems are limited to low data rate services, which might not be the best solution to the disaster responses. In addition, police officers, firefighters, and rescue crews often deploy communications systems that are incompatible with each other. This results in difficulties and delays in transferring experts' advice and safety information. Guarnera, et al. have introduced a mobile ad-hoc network (MANET) architecture that can overcome the heterogeneous mix of communications systems and equipment [Gua02]. The MANET could significantly reduce the costs for responders since radio equipment no longer needs to be replaced or modified. The MANET is beyond the scope of this thesis, however, and will not be discussed further. For an ideal disaster communication response, [Bos02] has suggested that a communications system should

- *Support first responders within the broad framework of the Incident Command System.*
- *Be accessible to an unlimited number of users without any special hardware or software.*
- *Provide hierarchical security and restricted access.*
- *Be intuitive and easy to use – requiring no more than 15 minutes orientation.*
- *Tie into pre-existing databases and systems.*
- *Support the full integration of geospatial information and data management.*
- *Operate with wired and wireless media.*
- *Be affordable across the entire spectrum of potential users.*

As mentioned earlier, many communications systems have been deployed for disaster response and recovery but only low data rate communications were used. In addition, when many diverse systems operate simultaneously within the same coverage area, interference and delay can occur on individual networks. This not only provides poor quality communication services but also degrades the overall performance of all responders. Thus, a higher data rate broadband network and better interoperable network implemented into an existing communications system would be necessary, which can serve as a backup or improve communications systems' coverage in an affected area. Coincidentally, our current Virginia Tech Local Multipoint Distribution Service (LMDS) system has met some criteria of the ideal disaster communications system suggested by Bostian [Bos02] but improvements and added values of this terrestrial LMDS system can be done to provide better disaster responses and recoveries.

1.2. Virginia Tech LMDS Broadband Communications System

Virginia Tech has constructed a high capacity broadband communications system that can be deployed quickly on a disaster scene. The system, consisting of a base station (known as a hub) and two remote units, operates in the U.S. commercial Local Multipoint Distribution Service (LMDS) band (around 28GHz). The hub can be connected to an existing network infrastructure via a surviving fiber or copper coaxial cable. The two remote units can be placed in the disaster area as long as they are within a 2 to 5 kilometers radius from the hub.

Both hub and remote units are composed of identical RF front-end and baseband hardware. The remote units provide generic 10/100BaseT access to network devices or local hosts. This access can be extended and interoperated with other standard networks, such as commercial-off-the-shelf (COTS) Ethernet and IEEE 802.11 LAN by using Internet Protocol (IP) and standard network interfaces. The first responders can use small mobile electronics devices, such as cellular telephones, laptops, personal digital assistants (PDAs), and pagers, on the disaster scene to communicate with the remote units. The remote units would then communicate with the hub placed outside the disaster scene at a high speed connection known as a virtual Ethernet network. Figure 1 below provides a high level view of the Virginia Tech system.

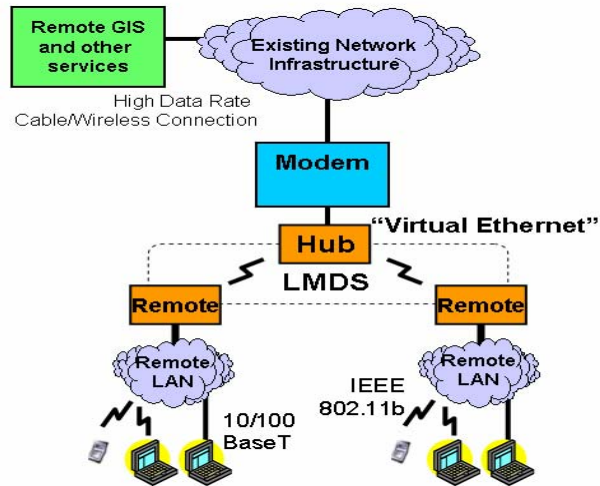


Figure 1 Virginia Tech LMDS System Overview [Bos02]

1.3. Problem Statement and Research Goals

The Virginia Tech LMDS system hub was designed and connected to an existing network infrastructure located at a relatively short distance away from the disaster scene via a high data rate wire connection, such as the surviving fiber cables. The problem of the current system is that the equipment setup time is a couple of hours at best or potentially much longer when the surviving fiber and cable are either far away from the disaster area or not accessible. This will surely degrade the usage and performance of the system. The gap may be bridged more quickly by a point-to-point microwave or optical link.

NS/EP recommended that a disaster communications system should provide voice band services, interoperability, survivability and durability, international interface, nationwide coverage, and intra or interagency emergency operation. Although the Virginia Tech system has met some of the disaster response communication needs, the system interoperability and the network accessibility are not sufficient to provide a flexible communication service for a disaster response.

The objective of this thesis is to provide an interoperable feature as an optional “satellite network backbone” to the LMDS system and to study possible network integrations between LMDS terrestrial system and the Ka-band satellite system since both systems spectrum allocations are adjacent to each other. In this thesis, four possible topologies of both terrestrial and satellite network integrations will be proposed and studied. The parameters of the Spaceway

satellite system will be taken as a typical Ka-band satellite system for analyzing the satellite link budgets and designing a satellite earth station. The standard IEEE 802.16 network protocols will be assumed for the current Virginia Tech 28 GHz LMDS system since the IEEE 802.16 protocols will ultimately be adopted for most of the LMDS systems in the U.S.

Among four proposed topologies, the most practical and feasible topology will be selected. Other consideration, including link power budget analysis, adjacent satellite interference, rain attenuation, path propagation effects, and hardware component selections, will also be studied to provide a more persuasive integrated system design. In addition, both terrestrial and satellite network implementations and transformations will be addressed to complete the system design of the terrestrial-satellite network.

1.4. Document Overview

Before discussing the design of a Ka-band satellite backbone to add an extra degree of interoperability to the Virginia Tech LMDS system, we will review the characteristics of Ka-band frequencies and Ka-band satellite system. The Hughes Network Ka-band Spaceway satellite system was selected to provide a good understanding of a generic Ka-band satellite system, and it was used to design the terrestrial-satellite network. The satellite communications system theory and fundamentals should be well understood; all of these will be described in Chapter 2. The added interoperability of the Virginia Tech LMDS system using Ka-band satellite was proposed in four topologies. These topologies will be thoroughly described in Chapter 3. The earth station antenna and link budget design for the selected topology will be given in Chapter 4. The overview network implementations of the selected integrated system design and selected earth station hardware components will be depicted in Chapter 5. Chapter 6 summarizes the overall contribution of this thesis and discusses potential future work.

Chapter 2: Ka-band Satellite Communications Systems

This chapter will review the literature of Ka-band satellite communications systems and the underlying fundamentals. The GEO Ka-band satellite history and current status are discussed briefly. The satellite transponders along with various types of modulation techniques and multiple access techniques used in satellite communications are introduced in this chapter.

2.1. Ka-band Satellite History and Current Status

As early as the 1970's, researchers from the United States, Europe, and Japan started exploring the Ka-band (from 26.5GHz to 40GHz) spectrum. Japan was the first country to provide Ka-band services, although only the basic technologies for transparent “bent-pipe” transponders were introduced at that time. For the last two decades, a number of experimental satellites have been launched to explore the use of Ka-band. European launches included ITALSAT 1 (1991) and 2 (1996); Kopernicus DFS-1 (1989), -2 (1990), and -3 (1992); and Olympus (1989). Japan has launched Sakura CS (1997), CS-2A (1983), CS-2B (1983), CS-3A (1988), and CS-3B (1988); N-STAR -1 (1995), and -2 (1996); ETS-6 (1994); and Superbird-1 (1989), -B1(1992), and -A1 (1992) [Eva00]. Satellites are no longer a “cable in the sky” based on transparent transponders but have become a network node.

In 1984 NASA formed an Advanced Communications Technology Satellite (ACTS) program to develop Ka-band satellite technologies. Its goals were to alleviate orbit congestion in lower bands; to promote effective utilization of the spectrum to increase communication capacities; and to ensure continued U.S. preeminence in satellite communications. The first Ka-band ACTS satellite that was launched in September 1993 demonstrated commercial-off-the-shelf (COTS) earth station equipment incorporating two-way frequency conversion and multimedia system integration technologies [Gar99].

In 1994 Vice President Al Gore introduced the concept of Global Information Infrastructure (GII) as a worldwide “network of networks” at the first World Telecommunications Development Conference in Argentina. This event stimulated a strong industrial interest in Ka-band in the USA. One year later the Federal Communications

Commission (FCC) licensed 13 geostationary (GEO) Ka-band fixed satellite systems (FSS) as parts of the first round filings. Licensees included Lockheed Martin (Astrolink), Loral Skyline (Cyberstar), Echostar Corporation (Echostar), Hughes Network (Spaceway), GE Americom (GE Star), KaStar Satellite Communications (KaStar), Motorola (Millennium), Morning Star Satellite Company (Morning Star), NetSat 28 Company (NetSat28), Orion Company (Orion), PanAmSat Corporation (PanAmSat), VisionStar Incorporated (VisionStar), and AT&T (VoiceSpace) [Eva00]. A summary of the systems that provide global coverage can be found in [Eva98] and [Eva00]. At that time Ka-band satellite communications systems became so popular because they could provide:

- **Large bandwidth:** The large amount of bandwidth availability in Ka-bands is the primary motivation for developing Ka-band satellite systems since lower frequency bands have become congested.
- **Small antenna size:** As the frequency goes up, the size of the antenna will decrease for a given gain and beamwidth. For a fixed antenna size, this will significantly reduce the interference from adjacent satellite systems. Obviously, the price of the smaller antenna will be lower, which makes broadband satellite service affordable to millions of commercial and residential end-users.
- **Larger system capacity:** Ka-band satellites provide smaller spot-beams to increase the satellite power density and allow large frequency reuses, which will lead to higher spectrum occupancy. Many user terminals can be served simultaneously.
- **Ubiquitous access:** Services are available at any location within the satellite footprint, especially in locations where terrestrial wired network are impossible or economically unfeasible.
- **Flexible bandwidth-on-demand capability:** This feature maximizes the bandwidth and resource utilization, and minimizes the cost to end-users.

On the other hand, Ka-band satellite links suffer degradation due to atmospheric propagation effects, which are more severe at the Ka-band than the degradation that happens at lower frequency bands. The primary propagation factors are rain attenuation, wet antenna losses, depolarization due to rain and ice, gaseous absorption, cloud attenuation, atmospheric noise, and tropospheric scintillation. Among those factors, rain attenuation is the most challenging obstacle to Ka-band systems.

Many Ka-band satellites have demonstrated that signal strength drops drastically during heavy rain, but many strategies and techniques are available to mitigate rain fading. For instance, the ACTS program introduced very small hopping spot-beams to focus the satellite signal power on a small area so that the signals can penetrate the rain. The satellite systems can also use coding to overcome transmission impairments. Another strategy is to lower bit rates during the period of rain. This approach would be unsuitable for many applications but might be satisfactory for some, such as Internet access. Uplink power control is another technique to mitigate the signal losses in heavy rain.

In recent years, due to the delayed market growth, attrition, consolidation, and immature Ka-band satellite industries, many companies with satellite licenses, like Lockheed-Martin (Astrolinks), and KaStar Corporation (KaStar), have either postpone or canceled their proposed satellite systems. Hughes Network Systems (HNS) is the only company with an FCC filing who did not cancel its proposed Ka-band satellite system. Hughes contracted Boeing to build the first Ka-band satellite of the Spaceway systems providing broadband communication services for the North American region. Boeing ultimately bought Spaceway. The satellite is proposed to be launched in early 2004. Since Spaceway is the only domestic Ka-band GEO FSS surviving satellite under construction, its characteristics that are studied and used in this thesis are believed to be similar to those of future Ka-band GSO FSS satellites.

2.2. Ka-band Geostationary (GSO) Fixed Satellite System (FSS)

A geostationary satellite is located on the geostationary orbit (GEO) that is a circular orbit in the equatorial plane, and is concentric with the Earth's radius [Gom02]. The geostationary satellite circles around the earth with a period of 23 hours 56 minutes and 4.1 seconds, which is the rotational period of the earth around its axis. As a result, the satellite is always in a fixed position in the sky related to any point on the earth's surface. This GEO satellite system is so-called fixed satellite system (FSS). The GEO FSS satellite is located at 35,786 kilometers above the earth. Hughes Network System's Spaceway satellite is one of those to be located in GEO.

2.2.1. Spaceway Satellite System

The Spaceway satellite system was licensed by the FCC to provide fixed satellite services in North America, Asia Pacific, Central/South America, and Europe/Africa. The first phase satellite was to be launched using Sea Launch’s rocket, Zenit 3SL, in early 2004 to provide cost-effective two-way voice, medium- and high-speed data, image, video and video telephony communications services to both business and individual users in the North America region.

The Spaceway satellite broadband system provides higher capacities, intelligent routing, bandwidth on-demand, and added value services that other Ku-band satellites, fiber optical cable, and DSL services cannot provide. Table 1 below presents the Spaceway satellite uplink and downlink operating frequencies. Only parts of the uplink and downlink spectra of the Spaceway system were selected for the system design in this thesis.

Table 1 Spaceway Satellite Frequency Allocation

	Uplink (Earth-to-space) Frequency Spectrum	Downlink (space-to-Earth) Frequency Spectrum
Spaceway (North American)	29.000-29.492 GHz 29.500-29.992 GHz	19.200-19.700 GHz 19.700-20.192 GHz

2.2.2. Spaceway Satellite Space Segment

The Spaceway satellite carries 48 multi-spot narrow beams. Each spot-beam support 125 MHz of bandwidth. The spot-beams provide higher capacities on desired populated areas to utilize available spectrum effectively. Of those spot-beams, 24 use left hand circular polarization (LHCP), and 24 use right hand circular polarization (RHCP). The spot-beam with 1-degree beamwidth provides a 650 km diameter footprint to cover most populated cities. A wide spot-beam with 3-degree beamwidth can cover a 1950-km diameter footprint in low populated density areas [Fit95]. Figure 2 presents the Spaceway spot-beam footprints of North America. Table 2 summarizes the basic characteristics of the Spaceway satellite.

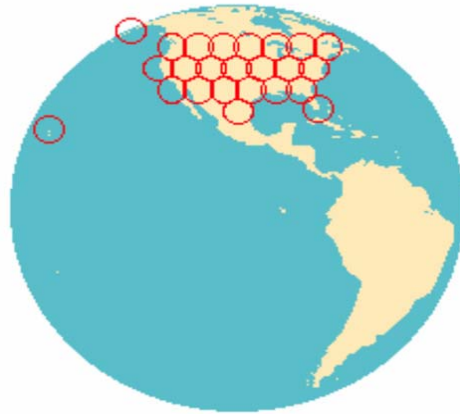


Figure 2 Spaceway North America Spotbeam Footprints [Fit95]

Table 2 Spaceway Satellite Overview Characteristics [Fit95]

Life Time	15 years
Dry Weight	3,785 pounds
Eclipse Capacity	100%
Number of Communication Beams	48
Bit Error Rate (BER) Performance	1×10^{-10}
Transmitter Redundancy	64 for 48
Satellite Modulation	QPSK
Uplink Data Stream	FDM/ TDMA
Downlink Data Stream	TDM
Data throughput	4.6 Gbps
Communication Beam Bandwidth	125 MHz
Narrow Spotbeam Uplink Antenna Gain	46.50 dB (Peak)/ 41.50 dB(Edge)
Wide Spotbeam Uplink Antenna Gain	35.00 dB (Peak)/ 30.00 dB(Edge)
Narrow Spotbeam Downlink Antenna Gain	46.50 dB (Peak)/ 41.50 dB(Edge)
Wide Spotbeam Downlink Antenna Gain	35.02 dB (Peak)/ 30.02 dB(Edge)
Proposed Downlink Data Rate	92 Mbps
Narrow Proposed Downlink EIRP	59 dbW (Peak)/ 54 dBW (Edge)
Wide Proposed Downlink EIRP	52.3 dbW (Peak)/ 47.30 dBW (Edge)
Inter Satellite links (if any)	60 GHz or 1Gbps

The Spaceway satellite will utilize a state of the art on-board processor (OBP) to route transmissions more intelligently within and between appropriate spot-beams, and provide end-users with immediate access to the space segment on demand. The satellite on-board processing is priced competitively with many basic terrestrial network services, especially in remote and underdeveloped areas, where basic terrestrial network services are neither economically feasible nor available.

2.2.3. Spaceway Proposed Ground Segment

Initially, Spaceway proposed very small aperture terminals (VSATs) that can provide direct access via satellites with on demand bandwidth. The proposed VSATs would range in size from 66 cm to 2 m on their antenna diameters. The uplink output power is between 0.1 watt and 2.0 watts. These proposed VSATs would provide 16 kbps to 2.048 Mbps uplink data rates, and 16 kbps to 92 Mbps downlink. A combination of Frequency Division Multiplexing (FDM) and Time Division Multiplex Access (TDMA) techniques was proposed for the VSAT uplink transmissions, and TDMA was used for the VSAT downlink transmissions.

On the other hand, in 2003 Hughes developed an advanced digital modem ASIC chip called Maxwell, which can provide up to 440 Mbps for uplink earth station transmissions. This chip would be used in DIRECTWAY terminals for the Spaceway broadband satellite system. The Maxwell chip will transmit and receive information to and from a Spaceway satellite that enables switching on-board the satellite. Thus, it eliminates the requirement for an expensive ground hub switching point, and reduces the cost of the end-user terminals. The Maxwell chip also enables TDMA/FDMA with transmitting capability at 512 kbps, 2 Mbps, and 16 Mbps. The Maxwell chip contains over 2.5 million gates, consumes less than 2 watts of power, and utilizes the state-of-the-art 0.13 micron ASIC's Radio Frequency Integrated Circuit (RFIC) technology.

2.3. Satellite Communications Fundamentals

To analyze the link characteristics for a satellite communications system, the characteristics of the satellite transponder should be studied first. There are two basic types of transponders, bent pipe and on-board processing (OBP). The early satellite transponders were based on analog transmission, but most modern satellite systems deliver signals digitally to ensure reliability and accuracy in information transmission. Digital switching techniques in OBP have facilitated a large scale deployment of affordable satellite-terrestrial networks. The OBP was adopted for the Spaceway systems..

2.3.1. Bent-pipe Satellite System

The bent pipe transponder acts as a transparent repeater. It consists of receiving and transmitting antennas, a low noise amplifier (LNA) receiver, a frequency converter, and a high power amplifier (HPA). The earth station transmitter will deliver signals to the satellite receiver. The uplink signals will be received at the receiving antenna, down converted, fed to the HPA, and then transmitted down to the receive earth station via the transmitting antenna. Usually, no change is made to the signal except an amplification to overcome the large path losses and a frequency conversion to separate the up and down links. Generally, the transponder is transparent to the users since the transmitting signal from one earth station will “bounce” and arrive at another earth station with its characteristics unchanged. Figure 3 shows the basic bent-pipe satellite link.

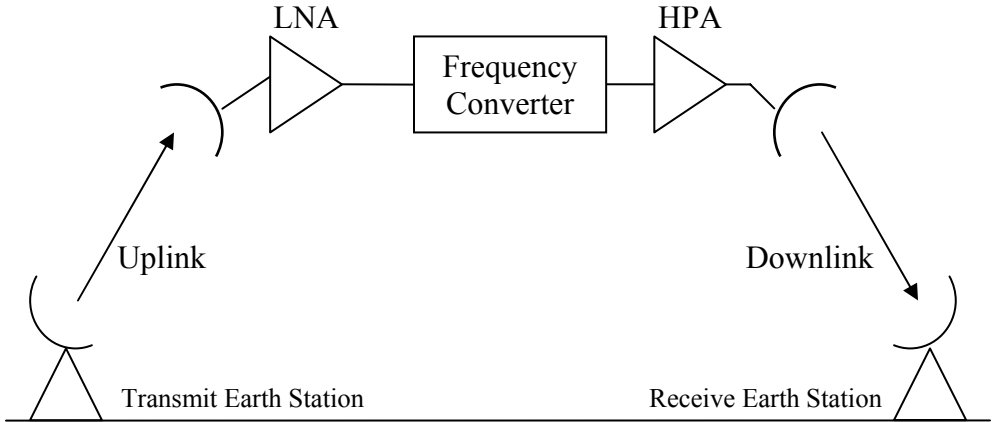


Figure 3 Bent-pipe Transponder Satellite Link Overview

The conventional way of characterizing the satellite link behavior using bent-pipe transponders is to use carrier-to-noise ratio (C/N). The C/N ratio represents the dB difference between the desired carrier signal power and the undesired noise power at the receiver. It also indicates the received signal quality for both analog and digital transmissions. In satellite communications systems the C/N calculation is often called a power link budget. The C/N calculation in decibels is shown in (Eq. 1) below.

$$\left. \frac{C}{N} \right|_{dB} = (P_t + G_t + G_r - L_p - A) - (k + T_n + B) - \text{OtherLosses} \quad [dB] \quad (\text{Eq. 1})$$

where

P_t = power transmitted [dBW]

G_t = gain of transmitting antenna [dB]

G_r = gain of receiving antenna [dB]

L_p = path loss = $10 \log\left(\frac{4\pi R}{\lambda}\right)^2$ [dB]

λ = wavelength of the signal [m]

R = transmission distance [m]

A = rain attenuation [dB]

k = Boltzmann's constant = 1.39×10^{-23} J/K = -228.6 dBW/K/Hz

T_n = noise temperature [dBK]

B = noise bandwidth in which the noise power is measured [dBHz]

OtherLosses = such as antenna point losses, atmospheric gaseous losses, power amplifier back-off, link margin, and implementation margin [dB]

The uplink refers to the signals delivered from an earth station to a satellite in space, and the downlink refers to the signal delivered from the satellite to the earth station, as shown in Figure 3 above. For the uplink, the transmitted power is the power transmitted from an earth station up to the satellite. The G_t is the power gain of the earth station transmitting antenna. G_r is the receiving antenna gain of the satellite.

The received signal is always much weaker than the transmit signal since the signals pass through a long path in the sky. Path loss, L_p , depends on the distance between the transmitter and the receiver, and the operating frequency. The path loss for Ka-band GEO satellites is large compared to those for satellites in lower orbits, and for those satellites operating in lower frequency bands.

The sum of P_t and G_t in decibels is presented as Effective Isotropic Radiated Power (EIRP). The EIRP is commonly specified in satellite communications and regulations. The International Telecommunications Union (ITU) and Federal Communication Commissions (FCC) have indicated the power limitations of transmitters in term of EIRP. The maximum EIRP permitted for an earth terminal will be provided in Chapter 4 when designing the outdoor unit (ODU) and indoor unit (IDU) of the earth terminal.

As mentioned in the previous section, as heavy rain will significantly degrade the link performance, the C/N ratio will decrease as well. The allowance of rain attenuation for a link

depends on many factors, such as the link availability in an average year, earth station geographical location, and link operating frequency. The estimation of the rain attenuation can be calculated using the ITU recommended rain model, which is presented in Chapter 4. Other factors affecting the link performance include antenna pointing losses, atmospheric gaseous losses, power amplifier back-off power, link margins, and implementation margins that will also be described briefly when the link budgets of the system are analyzed in Chapter 4.

The antenna gain for transmitting and receiving is a unitless quantity. It is the ratio of the power radiated (or received) by the antenna to the power radiated (or received) by an isotropic antenna fed with the same power in a given direction. When the antenna size or antenna beamwidth is known, the antenna gain can be obtained directly from (Eq. 2), or vice versa [Pra02 & Sko01].

$$G = \frac{4\pi A_e}{\lambda^2} = \frac{4\pi(\eta_A A_r)}{\lambda^2} \quad (\text{Eq. 2})$$

where

- A_e = effective aperture area [m^2]
- A_r = physical aperture area [m^2]
- η_A = aperture efficiency of the antenna

The decibel expression of the antenna power gain is

$$G_{dB} = 10 \times \log_{10}(G) \quad [dB] \quad (\text{Eq. 3})$$

In satellite communications, a parabolic reflector antenna usually is adopted for both space stations and earth stations. An earth station reflector antenna design and relevant theory will be provided in Chapter 4.

When a satellite uses a bent-pipe transponder, the C/N ratio for uplink and downlink are defined separately using (Eq. 1). $(C/N)_{UP}$ is used to present the uplink C/N value as a ratio, and $(C/N)_{DN}$ is used for the downlink C/N value. The overall C/N ratio that defines the satellite link performance should not be calculated by their dB values but by using the reciprocal formula where the C/N values are in power ratios shown in (Eq. 4) below.

$$\frac{1}{(C/N)_{Overall}} = \frac{1}{(C/N)_{UP}} + \frac{1}{(C/N)_{DN}} \quad (\text{Eq. 4})$$

The overall C/N value depends on both uplink and downlink designs. Engineering tradeoffs should be made to obtain an optimum overall C/N value. If the overall C/N is too small, the receiver will not detect the transmitted signals since the noise overpowers the desired signals. The larger the C/N value, the better the reception of the system; however, the system becomes unaffordable because the physical sizes of both space and earth stations or transmitted powers would be undesirably increased. For a particular modulation format, C/N is directly related to bit error rate (BER).

Eq. 4 is normally adopted when an analog transparent bent-pipe transponder is used. The uplink signals with noise will reach the space station receiver. The signals with noise will be amplified and translated to the downlink signal via a frequency converter, shown in Figure 3. This will directly impact the received downlink signal power and overall C/N ratio.

In contrast to a bent pipe system, the performance of a satellite system with a regenerative transponder is usually described in terms of the overall bit error rate (BER) in the end-to-end satellite link rather than C/N. This will be discussed after a digital on-board processing (OBP) transponder is discussed in the next section.

2.3.2. On-board Processing (OBP) Satellite System

The conventional bent-pipe satellite delivers signals on the same route; from the receiver to the transmitter, all signals on that specific transponder will usually be together, coming from the same transmitting earth station and going to the same receiving earth station [Rob97]. This limits the flexibility of the satellite network application. The OBP satellite system, consisting of regenerative transponders and on-board switching with multiple spot-beams, provides bandwidth on demand with low processing delay, flexible interconnectivities, and lowered ground station costs. The Spaceway satellite system carries OBP transponders; however, the Spaceway transponder will be assumed as a bent-pipe transponder.

In an OPB satellite system, both the uplink and the downlink of the OBP system are independent to each other. The uplink signals with distortions or noise reaching the space station receiver are down-converted and demodulated, and de-multiplexed and reconstructed. The reconstructed signals are then modulated, multiplexed, and up-converted to be transmitted at the downlink. Thus, the uplink degradation will have no effect on the downlink transmission. This

process, called base-band (BB) processing, significantly improves the overall link performance at the receiving earth station. Figure 4 shows the basic OBP system architecture and its link. Because demodulation is applied in the regenerative transponder digitally, it is necessary to represent the C/N ratio in terms of bit error ratio (BER). BER used in digital signals is to measure the probability of bit error that will occur in a given amount of time in the system. Different modulation schemes used in digital communications provide different BER performances, as described in Section 2.4. The overall error budget of the digital satellite systems using OBP is defined in (Eq. 5) [ITU02], shown as:

$$BER_{Overall} = BER_{UP} + BER_{DN} \quad (Eq. 5)$$

where BER_{UP} = probability of bit error for uplink
 BER_{DN} = probability of bit error for downlink

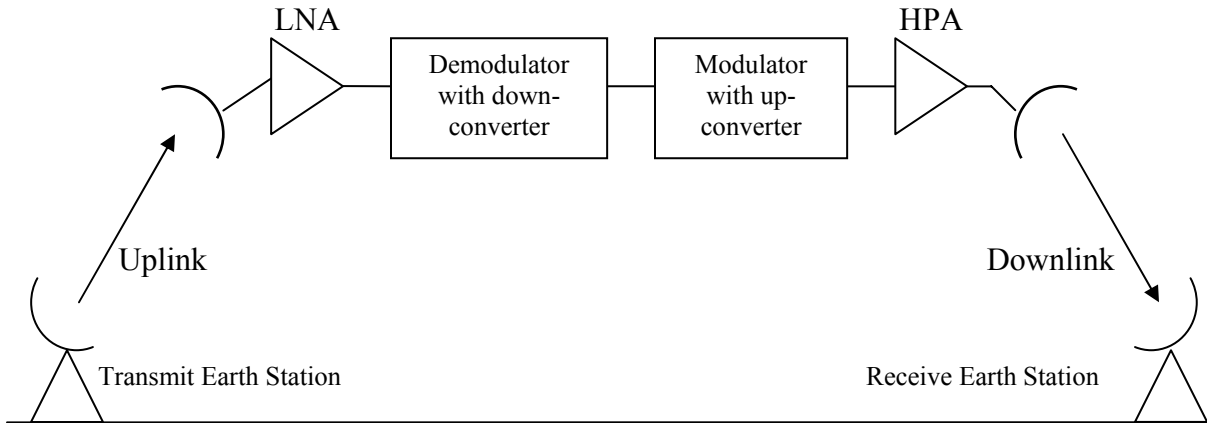


Figure 4 On-board Processing Transponder Satellite Link Overview

2.3.2.1. On-board Processing Switches

There are four types of proposed on-board switches: circuit switch, cell switch, fast packet switch, and hybrid switch. Each on-board processing switch has its own particular features and technologies. Circuit switches adopted by on-board processing transponders are efficient for bandwidth utilization; however, when the circuit switched network is used to support packet-based traffic, the bandwidth allocation is wasted because the bandwidth allocation is fixed. Thus, circuit switches are not suitable for broadband services. Cell switches are known as asynchronous transfer mode (ATM) switches. The bandwidth utilization is higher compared to other switches. In addition, ATM overhead requires 5 bytes in a 53-byte cell, which

is large for the limited bandwidth of wireless links. Hybrid switches are just the combination of circuit and packet switches; however, at the current technology, there are no products available for hybrid switches.

Among four switches, the packet switch is the most popular selection for satellite networks because it provides both packet-based traffic and circuit-based traffic in Internet Protocol (IP)-based networking environments. The Ka-band satellite Spaceway system adopted for this research carries a packet-switch OBP in order to provide broadband Internet services. Some advantages and disadvantages of these four switching technologies are summarized in Table 3 below.

Table 3 Comparison of different on-board switching technologies [Ngu03]

	Advantages	Disadvantages
Circuit Switching	<ul style="list-style-type: none"> • Excellent solution for circuit-based service provisioning • Easy congestion control by limiting access into the network 	<ul style="list-style-type: none"> • Reconfiguration of earth station time/frequency plans for each circuit set-up • No fixed bandwidth assignment • Low bandwidth utilization • Difficulty of implementing autonomous private networks
Fast packet switching	<ul style="list-style-type: none"> • Self-routing/auto-configuration abilities • Flexible and efficient bandwidth utilization • Can accommodate circuit-switched traffic • Easy to implement autonomous private network 	<ul style="list-style-type: none"> • For circuit switched traffic, higher overhead is required than circuit switching due to packet headers. • Contention/congestion may occur
Hybrid switching	<ul style="list-style-type: none"> • Able to support different types of traffic • Lower complexity of on-board processing than fast packet switch 	<ul style="list-style-type: none"> • Cannot maintain maximum flexibility for future services because the future distribution of satellite circuit and packet traffic is unknown • Waste of satellite resources in order to be designed to handle the full capacity of satellite traffic
Cell switching (ATM switching)	<ul style="list-style-type: none"> • Self-routing with a small overhead and auto configuration abilities • Easy to implement autonomous private networks • Provides flexibility and efficient bandwidth utilization for all traffic sources • Can accommodate circuit-switched traffic • Speed comparable to Fast packet switching 	<ul style="list-style-type: none"> • For circuit switched traffic higher overheads are required than packet switching due to 5 byte ATM header. • Contention and congestion may occur

2.4. Satellite Link Multiple Access Techniques

Since large amounts of bandwidth are available on GEO Ka-band satellites, an appropriate bandwidth management technique is necessary. One of the best ways is to use a multiple access technique. In satellite communications systems, multiple access allows many earth stations to share a transponder even though their carriers have different signal characteristics.

Three common types of multiple access deployed in satellite communications systems are frequency division multiple access (FDMA), time division multiple access (TDMA), and code division multiple access (CDMA). A common hybrid solution is used by combining techniques such as FDM/TDMA, and Spaceway has proposed the earth station to use FDM for uplink and TDMA for downlink to maximize the bandwidth efficiency. FDMA and TDMA will be presented in the next section. CDMA will be discussed briefly also because some CDMA satellite systems were proposed in recent years.

2.4.1. Frequency Division Multiple Access (FDMA)

FDMA is a popular multiplex access technique that was first used in satellite communications systems because of its simplicity and flexibility. In FDMA, signals can be analog or digital; however, analog signals with FDMA have become obsolete in the US, although some old satellite systems still operate with FDMA formats, particularly for TV.

In general, FDMA separates the total system bandwidth into smaller segments/channels, and assigns each channel to a user. Each user transmits at a particular allocated frequency. Filters are used to separate the channels so that they do not interfere with each other. The disadvantage of a filter is that it cannot easily be tuned to vary the bandwidth of channels or the channel frequency allocation. This makes inefficient use of transponder bandwidth and satellite capacity.

Another drawback of FDMA is the non-linearity of the transponder power amplifier that generates intermodulation products between carriers. This will degrade the link performance. In order to reduce such interference, the transmitted power of the satellite and earth station can be lowered. This is called back-off. Usually 2-3 dB back off power is needed when FDMA is used

[ITU02]. On the other hand, FDMA becomes useful for uplink transmission when a hub network is used, since only one carrier occupying the total transponder bandwidth will be transmitted to the satellite.

2.4.2. Time Division Multiple Access (TDMA)

TDMA is a digital multiple access technique that allows signals to or from individual earth stations to be received or transmitted by the satellite in separate, non-overlapping time slots, called bursts. For uplinks, each earth station must determine the satellite system time and range so that the transmitted signal bursts are timed to arrive at the satellite in the proper time slots, even though it is very hard to synchronize many earth stations on earth with proper synchronization times. For downlinks, such precise timing is not required.

Compared with FDMA, TDMA offers the following features [ITU02]:

1. Since only one signal is present at the receiver at any given time, there is no intermodulation caused by non-linearity of satellite transponders. The satellite transponder can be driven nearly at saturation in order to provide maximum satellite power.
2. The TDMA capacity does not decrease steeply with an increase in the number of accessing stations
3. The introduction of new traffic requirements and changes is easily accommodated by altering the burst length and position.

Each TDMA frame is formed by slots containing a preamble, guard time, and data information. The preamble contains synchronization and other essential data to operate the network. The guard time is used to prevent one station's transmissions from overlapping with another station's following transmission time slot. For uplinks, the transmitted bursts/times of users are critical. They should arrive at the transponders in the required slots so that the required information can be extracted at the received earth stations without errors.

A typical time length of a TDMA frame is 2 ms, which reduces the proportion of overhead to message transmission time. Sixteen 8-bit words are typically used in a digital terrestrial channel. Figure 5 shows two TDMA frames consisting of preamble and satellite channel at each frame.

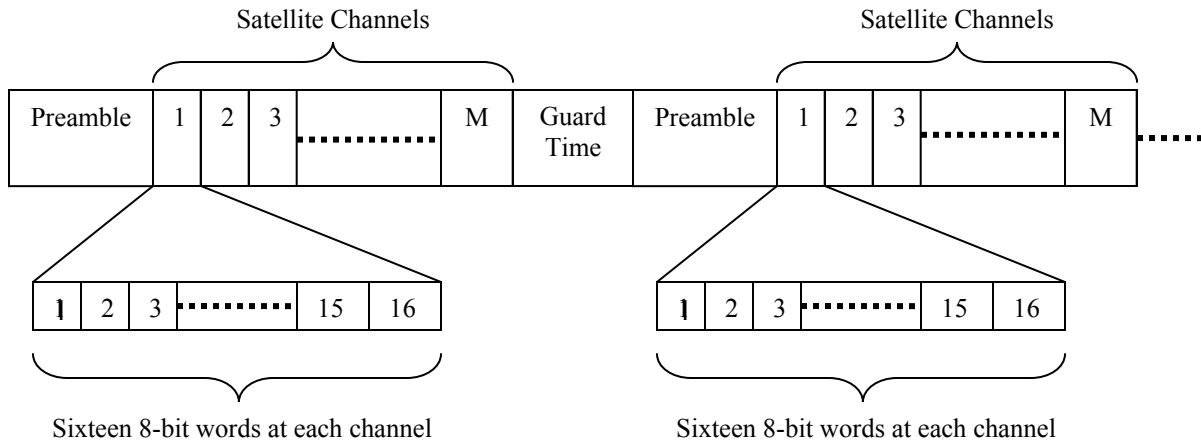


Figure 5 A Typical TDMA Frame [ITU02]

At the receiver, higher data bit streams must be recovered using modulation techniques discussed in Section 2.5, which requires demodulation of RF signals, generation of a bit clock, sampling of the receive waveform, and recovery of bits. This process requires large storage of bits (at preamble and guard time slots), so that original signals can be reconstructed even though signal transmissions are delayed. In a GEO Ka-band satellite system, the delay time for one-way transmission is around 240-250 ms at the distance of 35,786 km between an earth station and the satellite. The earth station would have to be on the equator at the sub-satellite point.

2.4.3. Code Division Multiple Access (CDMA)

CDMA was first designed for military uses in the 1960s. CDMA was designed to spread the energy of information signals across the wide bandwidth. The spread signals are usually below the noise floor, which makes detecting or jamming signals then more difficult. CDMA allows signals to be transmitted from multiple earth stations to a satellite at the same frequency and time. Since multiple signals are spread over a given allocated bandwidth, a specific encoding process is needed. Two common modulation processes adopted in CDMA are direct sequence (DS), so-called pseudo-code (PN) modulation, and frequency hopping (FH) modulation. As the result of either technique, the transmitted signal bandwidth is much larger than the information signal bandwidth at baseband. That is why these processes are known as a spread spectrum or a spread spectrum multiple access technique.

DS is the only type of spreading process being used in satellite communications. The user information signal is spread using a large bandwidth pseudo-random code; this makes the final bandwidth of the signals 10 to 100 times larger than the original bandwidth as mentioned above. The receiver can decode each signal by the user's unique code.

FH is commonly used in Bluetooth systems and was not commonly used in satellite systems, although a combination of DS and FH has been proposed. Instead of spreading information signals over a wide bandwidth with a pseudo-random code, the original signals can hop or change frequency based upon a unique PN code.

Many CDMA networks were proposed to be used especially in satellite communications systems when low data rate, low transmitted power, and small portable terminals are desired. This is usually done at a lower frequency band, such as L, C, and S bands.

2.5. Digital Modulation Techniques for Satellite Links

Over many years, a number of modulation techniques have been developed to optimize particular features of a digital transmission link. The desired bit error rate will determine the minimum required C/N values for each modulation technique. The different types of digital modulations are divided into coherent and non-coherent types.

2.5.1. Coherent Versus Non-coherent Modulations

Coherent modulation techniques will be described in this section. At a given minimum C/N requirement, the BER performance of a coherent system is better than a non-coherent system. In addition, coherent modulation can incorporate both amplitude and phase information, although synchronization circuits and phase-locked loop circuits increase the complexity of the system. On the other hand, non-coherent modulation is insensitive to the phase information, which degrades the BER performance [Cou01]. Since none of the satellite systems today uses non-coherent modulation, coherent modulation, such as binary phase shift keying (BPSK), quadrature phase shift keying (QPSK), M-ary phase shift keying (M-PSK) modulations, and quadrature amplitude modulation (QAM), will be adopted for the IDU design in Chapter of this thesis.

2.5.2. Phase Shift Keying (PSK)

Phase shift keying modulation is the most commonly used digital modulation in digital satellite communications systems. BER is the parameter used to measure the link performance of a satellite link. The BER is often referred to the probability of bit error, P_e . Probability of bit error is calculated from the characteristics of the type of modulation used and the energy per bit per noise density (E_b/N_o), which can also be obtained directly from the C/N values. The greater the E_b/N_o value, the lower the probability of bit error. For an ideal system, the E_b/N_o can be represented as:

$$\frac{E_s}{N_o} = \left(\frac{C}{N}\right)\left(\frac{B_n}{R_s}\right) \quad (\text{Eq. 6})$$

where E_s = energy per symbol [J]
 N_o = single sided noise power spectral density [W/ Hz]
 C = carrier power [W]
 N = noise power [W]
 R_s = symbol rate [symbol per second (sps)] = $1/T_s$, where T_s = symbol duration [sec]
 B_n = noise bandwidth [Hz]

To simplify the BER calculation, intersymbol interference is assumed to be zero and that ideal root raised cosine (RCC) filters are used at the transmitter and receiver.

2.5.2.1. Binary Phase Shift Keying (BPSK)

Binary phase shift keying consists of one bit per symbol. The probability of error for BPSK can be found in (Eq. 7)

$$P_e = Q \left[\sqrt{\frac{2 E_b}{N_o}} \right] = \frac{1}{2} \text{erfc} \sqrt{\frac{C}{N}} \quad (\text{Eq. 7})$$

where E_b = energy in a single bit [J]
 N_o = single sided noise power spectral density [W×Hz]
 C = carrier power [W]
 N = noise power [W]

The BER usually will be computed either with Q-function or with the complimentary error function (erfc). Many computational software packages, such as Matlab, already have the built in function features for both Q and erfc. BPSK is used in some satellite links although it is

considered to have low bandwidth efficiency compared to Quadrature Phase Shift Keying (QPSK), presented in the next section.

2.5.2.2. Quadrature Shift Keying (QPSK)

QPSK is widely used in satellite links. QPSK transmits two bits per symbol. Since two bits are sent per symbol, the symbols have four possible states. (Eq. 8) presents the probability of error as

$$P_e = Q \left[\sqrt{\frac{2E_b}{N_o}} \right] = \frac{1}{2} \operatorname{erfc} \sqrt{\frac{C}{2N}} \quad (\text{Eq. 8})$$

Comparing both (Eq. 7) and (Eq. 8), since QPSK carries twice as much information per symbol as BPSK, it needs an extra 3 dB of C/N to achieve the same P_e of BPSK. As a result, the symbol rate for the QPSK carrier is

$$R_s = \frac{R_b}{2} \quad [\text{sps}] \quad (\text{Eq. 9})$$

where R_b = data rate [bits per second (bps)]
 R_s = symbol rate [symbol per second (sps)]

BPSK transmits one bit per symbol and QPSK transmits two bits per symbol. Higher numbers of bits per symbol can also be sent using an M^{th} order modulation scheme, called M-ary Phase Shift Keying (M-ary PSK), described in the next section.

2.5.2.3. M-ary Phase Shift Keying (M-PSK)

If a symbol represents more than one bit, the system is known as M-ary. M stands for the number of possible states. M has to be greater or equal to 4, so that (Eq. 10) can be used to obtain the probability of error for M-PSK modulation [Cou01].

$$P_e \approx \operatorname{erfc} \left[\sqrt{\frac{C}{N} \sin^2 \left(\frac{\pi}{M} \right)} \right] \quad (\text{Eq. 10})$$

M is also related to l , the number of bits per symbol. (Eq. 11) shows the relationship between the number of bits per symbols and the number of states (M).

$$l = \log_2 (M) \quad (Eq. 11)$$

(Eq. 11) can generally be used for any multi-level modulation scheme. Bandwidth efficiency is a critical consideration when a higher level of modulation schemes is adopted. The bandwidth efficiency for any modulation usually is defined as

$$\eta = \frac{R_b}{B} \quad (Eq. 12)$$

where η = bandwidth efficiency [bits/s/Hz]
 R_b = bit rate [bit/sec]
 B = bandwidth of transmitted signal [Hz]

2.5.3. Quadrature Amplitude Modulation (QAM)

QAM basically is a modulation that combines four phase states of QPSK with multiple carrier amplitudes. For instance, 16-QAM is a modulation in which each symbol represents 4 bits and has 16 possible states. The M possible states can be calculated from (Eq. 11) above when the number of bits per symbol, l , is known. The probability of error in QAM modulation is calculated as [Cou01]

$$P_e = \frac{2(\sqrt{M}-1)}{\sqrt{M}} \operatorname{erfc} \left[\sqrt{\frac{3}{2(M-1)}} \left(\frac{C}{N} \right) \right] \quad (Eq. 13)$$

Taking M=16 as an example, 16-PSK needs an extra 4 dB of C/N to achieve an error probability of 10^{-6} compared to 16-QAM. Thus, the BER performance of 16-QAM is much better than 16-PSK, as shown in Figure 6. Therefore, many new generations of Ka-band satellites designed for Internet access will use 16-QAM between the satellite and hub, so that lower BER values can be maintained. Table 4 below presents the summary of all the possible modulations' theoretical equations and symbol rate relationships that will be used for the system design later in Chapters

3 and 4. Table 5 provides the required C/N values for M-ary PSK and M-ary QAM at the given probability of errors equal to 10^{-6} .

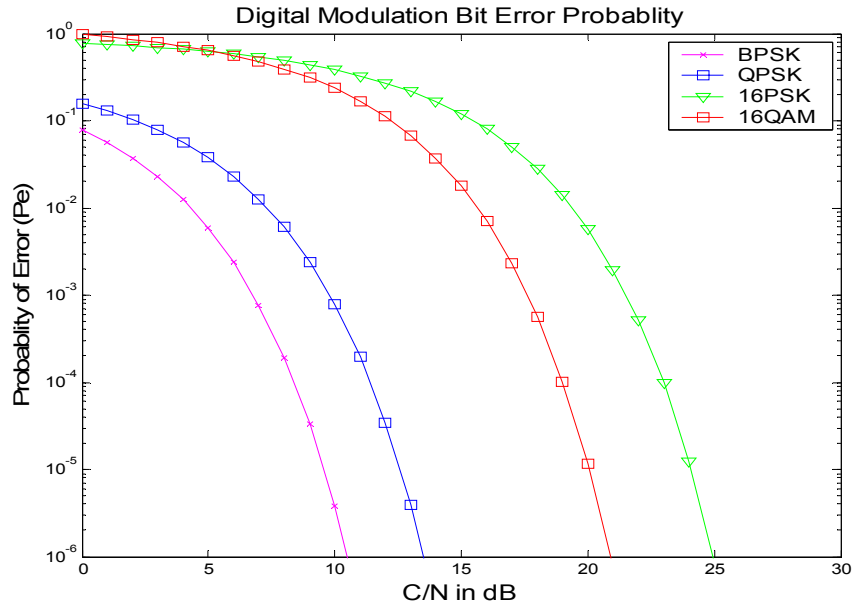


Figure 6 Different Digital Modulation BER Performance Comparison [Cou01]

From Figure 6 above, it can be concluded that when a higher number of bits per symbol in a type of modulation is used, a higher C/N value is required to achieve the same probability of error compared to those in lower number of bit per symbol.

Table 4 Coherent Signal Modulation Methods [Cou01]

Modulation Type	Bit Error Rate	R_s [symbol rate]
BPSK	$P_e = Q \left[\sqrt{\frac{2 E_b}{N_o}} \right] = \frac{1}{2} \text{erfc} \sqrt{\frac{C}{N}}$	R
QPSK	$P_e = Q \left[\sqrt{\frac{2 E_b}{N_o}} \right] = \frac{1}{2} \text{erfc} \sqrt{\frac{C}{2N}}$	$\frac{1}{2} R$
M-ary PSK (MPSK)	$P_e \approx \text{erfc} \left[\sqrt{\frac{C}{N} \sin^2 \left(\frac{\pi}{M} \right)} \right]$ for $M \geq 4$	R_b/N
M-ary QAM (MQAM)	$P_e = \frac{2(\sqrt{M} - 1)}{\sqrt{M}} \text{erfc} \left[\sqrt{\frac{3}{2(M-1)} \left(\frac{C}{N} \right)} \right]$	R_b/N

Where E_b = energy in a single bit [J], N_o = single sided noise power spectral density [J×Hz], C = carrier power [W], N = noise power [W], R_s =symbol rate, R_b =data rate

Table 5 C/N of M-ary PSK and M-ary QAM [Cou01]

M-ary PSK Modulation	Desired C/N (dB) @ BER = 10^{-6}	M-ary QAM Modulation	Desired C/N (dB) @ BER = 10^{-6}
2-PSK(BPSK)	10.76	-	-
4-PSK(QPSK)	13.53	4-QAM	13.77
8-PSK	19.12	8-QAM	17.53
16-PSK	24.97	16-QAM	20.02
32-PSK	30.95	32-QAM	24.36

The higher order modulations in Table 5 require higher C/N values that may be more difficult to achieve in a satellite link. Thus, using forward error correction (FEC) or uplink control power to get better BER for a given C/N maybe a preferable method, as described in the next section.

2.6. Forward Error Correction (FEC)

FEC not only can be used to optimize the link budget and maximize the power bandwidth efficiency, but also can provide a flexible tradeoff between the BER and the occupied bandwidth. With various selections of coding and code rates, FEC can be used to relax the link budget parameters or to improve the BER of a given link, especially at a small earth station with limited antenna size.

FEC is an error correcting method for a transmission link. Using redundancy added to the information bits, the receiver can detect and correct transmission errors and corrupted signals. In addition, no feedback is required from the receiver. The common codes that are used in satellite modems include Viterbi codes, Reed Solomon codes, Turbo codes, convolutional codes, etc. Turbo codes with $\frac{1}{2}$ FEC rate are adopted for the IDU design of the VSAT in Chapter 4.

2.7. Uplink Power Control (UPC)

As mentioned earlier, satellite links operating in the 20/30 GHz frequency band can be degraded severely by heavy rain. This degradation can be compensated by over-sizing the earth station equipment, i.e. by building a larger antenna and higher power transmitter[Dis97], which might not be the best technique to combat the rain attenuation because of the cost. Uplink power control technique can combat rain fades without incorporating excessive static margin to the link

power budget [Saa89]. Other potential techniques for fade mitigation, including orbital diversity and selective use of a lower frequency channel, will not be discussed in this study.

Uplink power control can be implemented in several forms, including closed loop, feedback loop, and open loop. In a closed loop implementation, the transmitting earth station will use its own transponded carrier to estimate the uplink fade [Ega82]. This closed loop technique is not always realizable since an earth station's ability to receive the transponded carrier depends on the satellite network configuration. With feedback loop control, the earth stations can measure the received signal strength and send this information to a control central station. Each station then will adjust its power to compensate for fading on its own uplink.

The open loop is the least complex among the three techniques. The open loop generally uses a beacon signal close to the downlink frequency to estimate the uplink fade. This method is less accurate compared to the closed and feedback loops, but careful design can provide an acceptable power control accuracy level to overcome rain fades. If the power level is too much above the true rain fade level, it might saturate the power amplifiers and create additional interference to adjacent satellites and other systems on the ground. There are many papers in the literature which show the advantages of using UPC. For instance, [Dis97] used an open loop uplink control power system to overcome the rain fading effect via the ACTS satellite operating at Ka-band, and [Ega82] provided a close loop technique to improve the link budget quality level.

2.8. Summary

This chapter provided a literature review of satellite communications technology. It presented comparisons between the conventional bent-pipe transponder and on-board processing transponders. It introduced different types of multiple access techniques: FDMA, TDMA, and CDMA. Coherent modulations were compared, such as BPSK, QPSK, M-PSK, and QAM. QPSK will be adopted for the system design in this thesis. Different modulation selections with link power budget design will be presented when the terrestrial-satellite integration network is determined in Chapter 3. FEC and UPC are alternative solutions in providing a desired BER performance.

Chapter 3: Terrestrial-Satellite Integration Design Selections

As introduced in Chapter 1, Virginia Tech’s LMDS broadband communications system can be quickly deployed at disaster scenes. In order to provide a nearly ideal disaster response service suggested by Bostian, et al [Bos02], additional flexibility and interoperability should be added. The extra feature is to provide an alternative Ethernet backbone network connection (other than for the existing optical fiber Ethernet connections) via a Ka-band satellite communications system. This requires a transportable earth station, including a receiver and a transmitter, to be interconnected with the LMDS system. Four possible system designs for integrating the existing LMDS terrestrial system and a Ka-band satellite system are presented and discussed in this chapter.

3.1. Virginia Tech LMDS System Frequency Planning Allocations

The Virginia Tech LMDS system was designed to have four channels and operates in the US commercial LMDS frequency band. The bandwidth of each channel is 100 MHz, shown in Table 6. Since the radios were initially designed for a frequency band slightly higher than the U.S. allocation, it was decided to utilize Channel 4 for demonstration purposes [CWT01]. Table 7 provides the US commercial LMDS frequency band defined by the FCC.

Table 6 LMDS Radio Channel Assignment

Channel Number	Uplink Frequency (GHz)	Downlink Frequency (GHz)
1	27.95 – 28.05	27.50 – 27.60
2	28.05 – 28.15	27.60 – 27.70
3	28.15 – 28.25	27.70 – 27.80
4	28.25 – 28.35	27.80 – 27.90

Table 7 LMDS Frequency Plan Allocations

LMDS Block A Frequencies	LMDS Block B Frequencies
27.500 GHz – 28.350 GHz	31.000 GHz – 31.075 GHz
29.100 GHz – 29.250 GHz	31.225 GHz – 31.300 GHz
31.075 GHz – 31.225 GHz	

For RF design purposes, channel 4 uplink and downlink frequencies are selected for the terrestrial LMDS systems. The Ka-band satellite uplink frequency band is chosen to be from 29.5 GHz to 29.6 GHz, and the downlink frequency band is from 19.7 GHz to 19.8 GHz complying with the ITU and FCC Ka-band frequency spectrum allocations. The bandwidth of the satellite links is also selected to be 100 MHz, equivalent to the LMDS system bandwidth, although wider bandwidth can be used. The Spaceway frequency allocation plans can be found in Table 1. Table 8 gives the summary of the pre-selected frequency bands used in this thesis for both terrestrial and satellite systems.

Table 8 Summary of Terrestrial and Satellite System Frequency Allocation Plans

	Uplink Frequency (GHz)	Downlink Frequency (GHz)
Terrestrial LMDS System	28.25 – 28.35	27.80 – 27.90
Ka-band Satellite System	29.50 – 29.60	19.70 – 19.80

3.2. Virginia Tech (VT) LMDS Modem Characteristics

The VT LMDS system consists of two remote units and a hub. The remote units and the hub are identical to each other, except that the remotes incorporate additional routers and hosts. Figure 7 shows the LMDS system blocks. Either the remote unit or the hub consists of a radio subsystem, a modem subsystem, a sounder subsystem, a monitor computer, and optional routers that can be connected to end-users. The radio subsystem consists of a dual-stage frequency up-converter for the radio transmitter, a dual-stage frequency down-converter for the radio receiver, and the transmitting and receiving antenna.

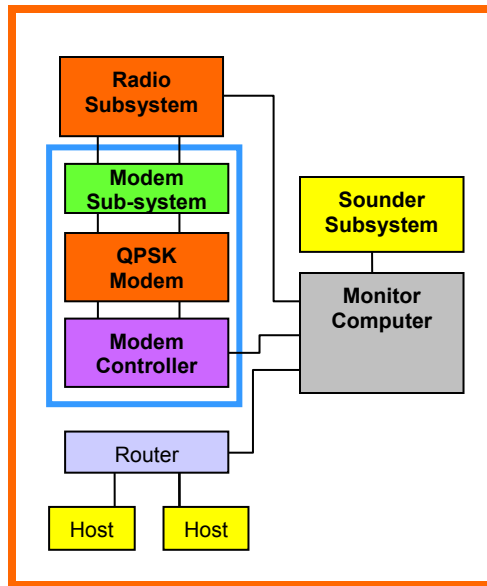


Figure 7 Virginia Tech LMDS System Building Blocks

The modem subsystems consist of a QPSK modulator, a QPSK demodulator, and a modem controller subsystem. Table 9 below presents the Virginia Tech LMDS modem technical characteristics. The modem operates at a maximum symbol rate of 60 Msps (data rate of 120 Mbps). The symbols are shaped with square root raised cosine filters resulting in an occupied signal bandwidth of 84 MHz. Turbo code and Reed-Solomon code are adopted for the modem. Eshler has claimed additional coding gains from Turbo Code for the LMDS systems shown in Table 10 [Esh02]. In addition, the modem has a baseband 100Base-T interface that is connected directly to the Ethernet network infrastructure from the hub unit. The maximum required input power of the modem is -15 dBm, and the output power of the modem is +4 dBm. The detailed functionalities of the modem can be found in [Loc01].

Table 9 Virginia Tech LMDS Modem Characteristics

Parameter	Virginia Tech LMDS Modem
Nominal Bit Rate	120.832 Mbps
Modulation	QPSK
Demodulation	Coherent
Encoding	Absolute
Data Filtering	Square Root RC 40% ($\alpha=0.4$)
Input Signal Level Range	30dB
BER better than 10^{-6}	@ $E_b/N_0=12.6$ dB
Carrier On/Off Ratio	50 dBc
Transmit and Receiver IF	140 MHz
Clock and Data Interface	Differential ECLL
Controller	External Board
Baseband Interfaces	100Base-T
Auxiliary Port	Sounder Interface
FEC Coding	Turbo Code Variable Rate
ODU Requirement	Tx/Rx IF, Power Control
Tx Level	+4 dbm
RX Level	-15 dbm
Transmit	Mute Sync to Sounder

Table 10 Three Suggested Turbo Codes for Virginia Tech LMDS Modem [Esh02]

Code	Block Size (b)	Data Size (b)	Data Size (B)	Coding Rate	Coding Gain (dB)
TB Code 1 (128,120)x(128,120)	16384	14400	1800	0.88	6.6
TB Code 2 (128,120)x(128,126)	16384	15120	1890	0.923	5.5
TB Code 3 (128,127)x(128,126)	16384	16002	2000.25	0.977	4.0

3.3. Four Terrestrial-Satellite Integration Designs

There are four possible topologies for integrating the existing Virginia Tech LMDS system with a Ka-band satellite system realized as a terrestrial network link. **Topology 1** is to up-convert LMDS transmitted (uplink) frequency signals to the Ka-band transmitted (uplink) frequency signals, and down-convert the Ka-band received (downlink) frequency signals to the LMDS received (downlink) frequency via a single or dual stage up and down frequency converter. This topology is called RF-to-RF coupling since both the LMDS transmitted and received signals are converted at their RF bands. This RF-to-RF coupling design is attractive for integrating both terrestrial and satellite systems due to the adjacent spectrum locations occupied

by the terrestrial LMDS band and the satellite Ka-band. A single or dual stage conversion between the LMDS RF signals and Ka-band satellite RF signals can be done in an earth station.

In general, a parabolic dish antenna with a diameter less than 2 meters would be deployed in the earth station, making it a very small aperture terminal, abbreviated VSAT. A VSAT usually consists of an outdoor unit (ODU) and an indoor unit (IDU). The ODU of the VSAT consists of a satellite-to-LMDS band converter (STL converter) and a LMDS-to-satellite band converter (LTS converter). The usual VSAT IDU includes a baseband modem and sub-controllers. In this particular topology, the transmitting and receiving modem in the IDU are eliminated.

Topology 2, providing an IF-to-IF coupling, is very similar to Topology 1, except that the received LMDS IF frequencies are up-converted to the Ka-band uplink RF frequencies, and the Ka-band RF downlink (received) frequencies are down-converted to the LMDS IF frequencies. Neither a transmitting nor a receiving modem is used in this topology, and hence no IDU is necessary.

Topology 3 is called a hybrid coupling of RF and IF. Basically, the received LMDS RF signals are up converted to Ka-band RF signals via a single or dual stage LTS frequency converter and sent to Ka-band satellites. The received signals at the VSAT from the satellite are down-converted by a STL converter. The signals are fed into a receiving modem. Then, these baseband signals will be bridged onto the LMDS modem via a router or switch before the LMDS hub communicates with the remote units.

Topology 4 provides a baseband-to-baseband coupling between the LMDS modem and the VSAT transmitting and receiving modem. The LMDS hub will receive the RF signals from the remote units. These RF signals will be down-converted and demodulated at the LMDS modem. The demodulated signals will then couple onto the VSAT transmitting modem by a router or a switch at the IDU before being re-modulated. The signals will then be transmitted to the satellite via the LTS converter. Conversely, the receiving signals at the VSAT will be down converted by the STL converter, and then demodulated by the VSAT receiving modem. These baseband signals will be modulated again at the LMDS modem before being transmitted to the remote units.

3.3.1. Topology 1: RF-to-RF Coupling

Since Ka-band frequency allocations are adjacent to the U.S. LMDS fixed wireless A-block allocation (see Table 1 and Table 6), both spectra appear to offer an opportunity to interconnect the terrestrial and satellite networks at the RF bands.

3.3.1.1. Frequency Planning Aspects

In this topology, the LMDS received signals at 27.85 GHz are converted to Ka-band satellite signals at 29.55 GHz. The satellite system serves as a network backbone, replacing the existing fiber cable terrestrial network backbone of the VT LMDS system. The Ka-band downlink frequency signals at 19.75 GHz will convert to the LMDS transmitted frequency signals at 28.30 GHz. The LMDS transmitted frequency signals at the hub unit will communicate with the remote units at 28.30 GHz to complete the satellite-terrestrial link transmission. Figure 8 below shows the overall frequency conversions and RF-to-RF couplings between the satellite and terrestrial systems.

Both up and down frequency conversions between the LMDS and Ka bands can be done by a one-stage mixer fed by a local oscillator (LO) signal. For the LMDS to Ka-band RF frequency conversion, the local oscillator is selected to be 1.7 GHz; and for the Ka-band to LMDS RF frequency conversion, the LO is set to be 8.55 GHz, shown in Figure 8 above. The left hand dotted-line square block can be viewed as a simplified VSAT, and the right hand solid square block illustrates the LMDS hub with its RF front-end dual IF frequency conversion stages and a satellite modem (including a modulator and a demodulator).

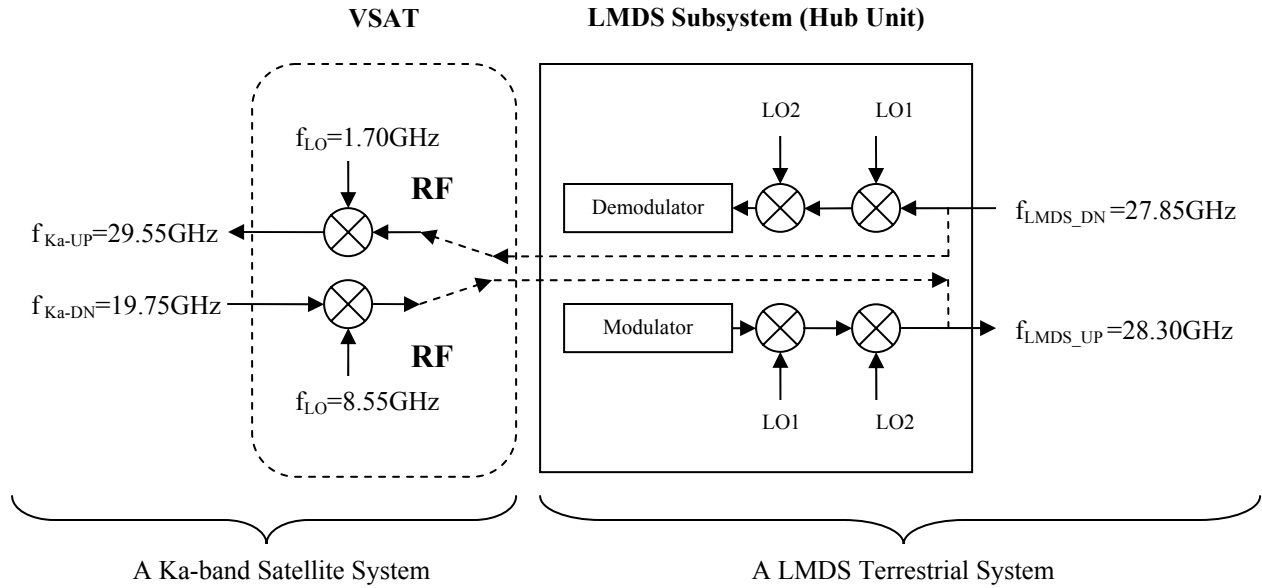


Figure 8 A Satellite-Terrestrial System Linked by RF on Both Uplink and Downlink

This VSAT consists of both satellite-to-LMDS (STL) and LMDS-to-satellite (LTS) frequency converters without baseband processing. The LMDS RF frequency is converted to the Ka-band RF frequency via a single stage frequency converter. Neither a transmitting nor a receiving modem is included at the VSAT. Instead, the received Ka-band RF spectra at the VSAT will be converted directly to the LMDS frequency spectra. These LMDS spectra will then be retransmitted to the remote units of LMDS system at the disaster areas via the system transmitting antenna.

The advantage of single-stage conversion at the VSAT is that it requires relatively few microwave components and is therefore inexpensive. The architectures and functionality of the STL and LTS are given in the following section.

3.3.1.2. Hardware Aspects

3.3.1.2.1. A Satellite-to-LMDS (STL) Frequency Converter

The STL frequency converter can be viewed as a heterodyne converter, consisting of a radio frequency (RF) section and an intermediate frequency (IF) section. Figure 9 below gives a general block diagram of a STL frequency converter.

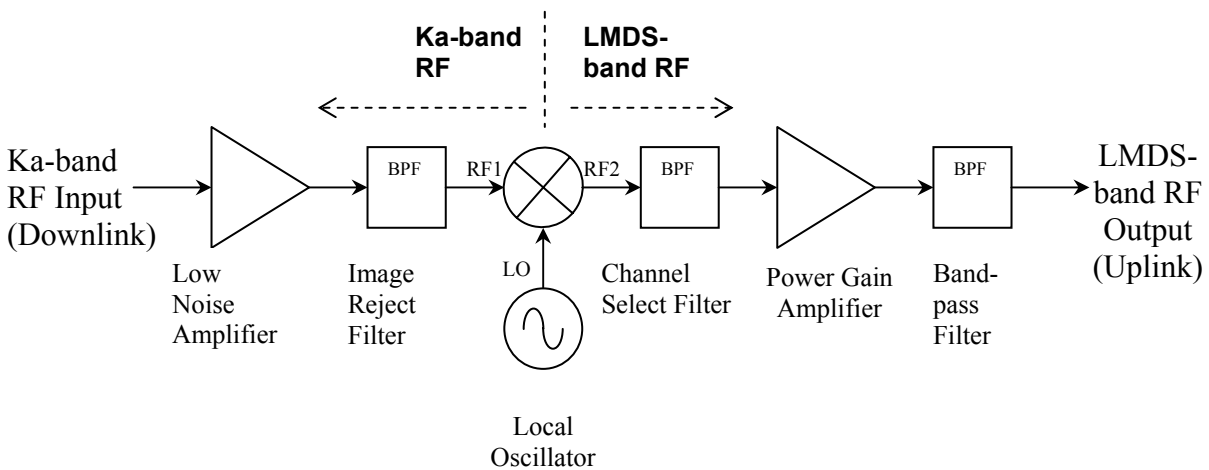


Figure 9 A Block Diagram of the Satellite-to-LMDS (STL) Converter

Commonly the Ka-band RF section is known as the front-end section of the receiver. In the front-end section, a RF low noise amplifier (LNA) plays a major role in determining the sensitivity and dynamic range of the converter. A band pass filter (BPF) could be placed before the LNA for frequency band selections, although the BPF will degrade the overall performance of the receiver [Raz98].

A mixer following the LNA will do the required frequency conversions. In addition, unwanted frequency carriers will mix with the LO signal and fall into the desired bands and degrade the desired signals. The BPF will filter out the unwanted channels but allow the desired channel to pass through. Since the desired channels are weak at this point, the IF amplifier is needed. The BPF also provides image rejection.

The combination of LNA and mixer is often known as a Low Noise Block (LNB) converter. As the received Ka-band signals have been filtered properly to remove images, the Ka-band signals can then be combined with the LMDS signals at the hub unit. Then, the clean LMDS RF signals (without images) can be retransmitted to the remote units.

In contrast, when the heterodyne STL converter operates at very high frequency bands, it is very hard to build filters with the required narrow bandwidths and associated with high Q values. Common filters are built for typically operating frequencies less than 1 or 2 GHz. In Topology 1, if the above heterodyne STL converter is adopted, the BPF must operate around 20

GHz and 8 GHz. This makes the design difficult. In addition, no commercial microwave mixers for such high IF frequencies are available, and they would be expensive to custom build.

3.3.1.2.2. A LMDS-to-Satellite (LTS) Frequency Converter

In order to allow LMDS uplink signals to communicate directly with the satellite, a heterodyne LTS converter is proposed, shown in Figure 10 below. The LTS consists of a single or a dual stage frequency converter. Power amplifiers are added at the LTS in order to strengthen the signals to the satellites.

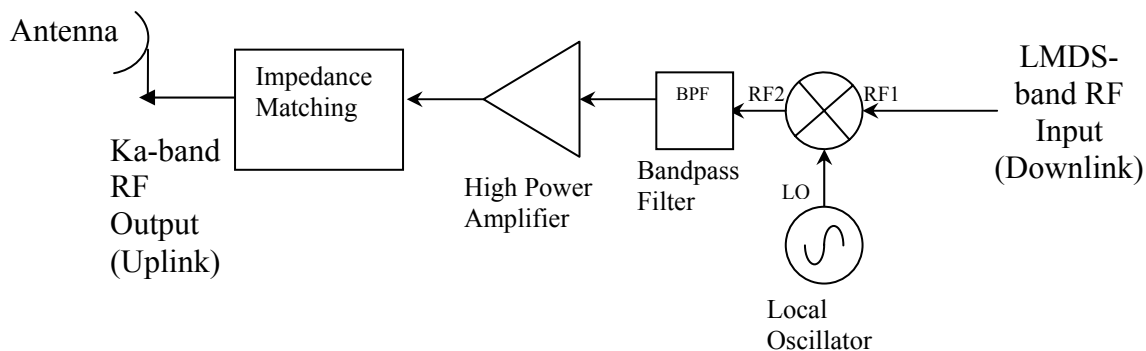


Figure 10 A Block Diagram of the LMDS-to-Satellite (LTS) Converter

The LMDS RF signals are directly fed onto the LTS converter. The LMDS RF signals will mix with the LO frequency signals via a transmitting mixer, which results in Ka-band RF transmitted signals. A BPF filter is used to eliminate undesired mixing components. The Ka-band signals are raised to a desired power level by a high power amplifier chain. Usually an impedance matching circuit will be added between the power amplifier chain and the antenna for maximizing power transfer. The matching network also helps to remove harmonics and other spurious signals from the transmitter output [Raz98].

As mentioned earlier, the LMDS RF received signals are delivered to the satellite via a VSAT transmitter without any signal filtering and image rejection processes at the LMDS hub. The original noise, distortion, and harmonics from the LMDS systems can carry onto satellite receivers, and this could significantly degrade the performance of transmission links. In order to overcome this problem, the received LMDS signals should be filtered at an IF band or baseband. This will be discussed in the next two topologies.

3.3.1.3. Link Budget Aspects

The link budget for this topology has been studied and analyzed. When the VSAT is desired to provide continuous broadband services, the typical BER value is expected to be around 10^{-6} for any given modulation scheme. Since no modem is provided at the VSAT, and the LMDS RF signals from the remote units are received by the hub antenna, the hub RF signals transmitted to the satellite are treated as if they are transmitted directly from the remote units. The modem used in the remote units, the same as the modem used in the hub, provides a fixed data rate of 120 Mbps. As the Spaceway transponder was treated as a conventional bent-pipe transponder as described in the previous chapter, and, since the modem uses QPSK modulation, both satellite and hub receiver bandwidth will be 60 MHz for the link budget analysis.

Table 11 shows the inbound link budget for this topology. The VSAT is placed at Blacksburg, Virginia, and the 8-meter center hub of the Spaceway system is located at Los Angeles, California. Since QPSK modulation, providing a required C/N value of 13.6 dB, is adopted for this topology, the minimum desired C/N threshold is 8.0 dB when 6.6 dB forward error coding and 1 dB implementation margins are included in the inbound link budget analysis.

For uplink power budget analysis, under clear sky and adjacent satellite interference, the $C/(N+I)$ is 10.3 dB when a 10-W 1.2-m VSAT is adopted. This value is achievable since it is more than the desired C/N threshold value of 8.0 dB.

Nevertheless, the uplink of inbound link budget will barely be feasible under moderate rain attenuation. Although the $C/(N+I)$ value equals 28.9 dB for the downlink of the inbound link design, the overall $C/(N+I)$ value is dominated by the uplink unachievable $C/(N+I)$ value. Thus, the link budget of this topology is still not feasible. This also shows that smaller antenna and/or lower transmitting power of the VSAT will not achieve the C/N threshold value due to the large path loss. The details of how the parameters of the link budget are obtained and the C/I calculation is calculated will be explained in the next chapter.

Table 11 Topology 1: Inbound Link Budget Example (Blacksburg, VA -Los Angeles, CA)

Major Parameters	Rain	Clear Sky	
Uplink Frequency (Hz)	29.55E+9	29.55E+9	Hz
Downlink Frequency (Hz)	19.75E+9	19.75E+9	Hz
VSAT Diameter	1.20	1.20	m
VSAT Transmitting Antenna Gain	50.53	50.53	dB
VSAT Receiving Antenna Gain	47.03	47.03	dB
UPLINK: VSAT to satellite			
	Rain	Clear Sky	
VSAT Pt	10.0	10.0	dBW
VSAT Gt	50.5	50.5	dB
Satellite Gr	41.5	41.5	dB
Free Space Path Losses	-212.9	-212.9	dB
Atmosphere Gaseous Losses	-1.0	-1.0	dB
Antenna Pointing Losses	-0.5	-0.5	dB
Other Losses	-0.5	-0.5	dB
Rain Attenuation Losses (0.5% outage at Blacksburg)	-7.2	0.0	dB
Pr (Received Power at Satellite Transponder Input)	-120.1	-112.9	dBW
Boltzmann's constant k	-228.6	-228.6	dBW/K/Hz
Satellite Input Noise Temperature Ts = 575K	27.6	27.6	dBK
Satellite Receiver Bandwidth Bn = 60 MHz	77.8	77.8	dBHz
N (Noise Power at Satellite Transponder Input)	-123.2	-123.2	dBW
Uplink C/N	3.1	10.3	dB
Uplink C/I	32.6	32.6	dB
Uplink C/(N+I)	3.1	10.3	dB
DOWNLINK: Satellite to HUB			
	Rain	Clear Sky	
Satellite EIRP	54.0	54.0	dBW
HUB Gr	61.8	61.8	dB
Free Space Path Losses	-209.4	-209.4	dB
Atmosphere Gaseous Losses	-1.0	-1.0	dB
Antenna Pointing Loss	-0.5	-0.5	dB
Other Losses	-0.5	-0.5	dB
Rain Attenuation Losses (0.5% Outage at Los Angeles)	-1.4	0.0	dB
Pr (Received Power at Hub Input)	-97.1	-95.6	dBW
Boltzmann's constant k	-228.6	-228.6	dBW/K/Hz
HUB Input Noise Temperature Ts = 275K	24.4	24.4	dBK
HUB Receiver Bandwidth Bn = 60 MHz	77.8	77.8	dBHz
N (Noise Power at HUB Receiver Input)	-126.4	-126.4	dBW
Downlink C/N	29.4	30.8	dB
Downlink C/I	38.8	38.8	dB
Downlink C/(N+I)	28.9	30.2	dB
For Bent-Pipe Transponder:			
	Rain	Clear Sky	
QPSK Required C/N @ 10e-6	13.6	13.6	dB
Implementation Margin	1.0	1.0	dB
Turbo Code Coding Gain	6.6	6.6	dB
Threshold C/N	8.0	8.0	dB
Overall (C/N+I)	3.1	10.3	dB

With today's VSAT technology, no reasonable sized VSAT terminal is capable of transmitting very high data rates. The NASA ACTS program proposed a VSAT that can transmit up to maximum of 2 Mbps. The unchangeable high data rate of the satellite modem requires a dish antenna larger than 2 meters or higher transmitting powers to meet desired BER performance, and this will not longer be a VSAT.

The transmitted power can be increased to minimize the antenna size for a desired BER performance at 10^{-6} . However, larger transmitted power will violate the FCC's and ITU's EIRP limitations. The uplink power control mentioned in a previous chapter can be added to the system when heavy rain occurs. The turbo coding gain claimed to be around 6.6 dB can be added to the existing link, but the C/N values still do not meet the desired BER requirement for a reasonable size of VSAT (less than 2m) and transmitted power (within the ITU's and FCC's EIRP requirements).

Table 12 below shows this topology's outbound link budget example. The hub is placed in Los Angeles, California and the VSAT is located at Blacksburg, Virginia. In most cases, the uplink of the outbound link will have adequate link margin since the large size antenna and high transmitting power of the hub provide high signal strength at the satellite. From the table, the overall uplink C/(N+I) for the outbound link is around 34.9 dB under rain or 37.3 dB under clear sky. The uplink rain attenuation was calculated to be -3.35 dB for the center hub placed at Los Angeles, and the downlink rain attenuation was -3.21 dB for the VSAT placed at Blacksburg. The 0.5% outage was assumed for moderate rain. This outage equals the total of 43.8 hours in an average year, which can be tolerated. The ITU rain model was used to calculate the rain attenuation for both uplink and downlink, and the details are given in Chapter 4.

On the other hand, the C/(N+I) value of the downlink of the outbound link depends on the antenna size of the VSAT. 1.2-meter VSAT antenna is assumed in this link budget example. The downlink C/(N+I) shown in Table 12 can be achieved because, with QPSK, the VSAT noise bandwidth is set to be 60 MHz. However, as the VSAT antenna size decreases, the feasibility of the outbound link will eventually become unrealizable, given the fixed data rate of 120 Mbps. If the VSAT is placed other than in Blacksburg, Virginia, the link might become impractical if the location's rain attenuation is higher. In addition, in this topology the network implementation between both satellite and terrestrial networks is another problem, which will be discussed in the next section.

Table 12 Topology 1: Outbound Link Budget Example (Los Angeles, CA-Blacksburg, VA)

Major Parameters	Rain	Clear Sky	
Uplink Frequency (Hz)	29.55E+9	29.55E+9	Hz
Downlink Frequency (Hz)	19.75E+9	19.75E+9	Hz
VSAT Diameter	1.20	1.20	m
VSAT Transmitting Antenna Gain	50.53	50.53	dB
VSAT Receiving Antenna Gain	47.03	47.03	dB
UPLINK: Hub to Satellite			
	Rain	Clear Sky	
HUB EIRP	89.5	89.5	dBW
Satellite Gr	41.5	41.5	dB
Free Space Path Losses	-212.9	-212.9	dB
Atmosphere Gaseous Losses (dB)	-1.0	-1.0	dB
Antenna Pointing Loss	-0.5	-0.5	dB
Other Losses	-0.5	-0.5	dB
Rain Attenuation Losses (0.5% outage at Los Angeles)	-3.3	0.0	dB
Pr (Received Power at Satellite Transponder Input)	-87.3	-83.9	dBW
Boltzmann's constant k	-228.6	-228.6	dBW/K/Hz
Satellite Input Noise Temperature Ts = 575K	27.6	27.6	dBK
Satellite Receiver Bandwidth Bn = 60 MHz	77.8	77.8	dBHz
N (Noise Power at Satellite Transponder Input)	-123.2	-123.2	dBW
Uplink C/N	36.0	39.3	dB
Uplink C/I	41.5	41.5	dB
Uplink C/(N+I)	34.9	37.3	dB
DOWNLINK: Satellite to VSAT			
	Rain	Clear Sky	
Satellite EIRP	54.0	54.0	dBW
VSAT Gr	47.0	47.0	dB
Free Space Path Losses	-209.4	-209.4	dB
Atmosphere Gaseous Losses (dB)	-1.0	-1.0	dB
Antenna Pointing Losses	-0.5	-0.5	dB
Other Losses	-0.5	-0.5	dB
Rain Attenuation Losses (0.5% outage at Blacksburg)	-3.2	0.0	dB
Pr (Received Power at VSAT Input)	-113.6	-110.4	dBW
Boltzmann's constant k	-228.6	-228.6	dBW/K/Hz
VSAT Input Noise Temperature Ts = 275K	24.4	24.4	dBK
Satellite Receiver Bandwidth Bn = 60 MHz	77.8	77.8	dBHz
N (Noise Power at VSAT Input)	-126.4	-126.4	dBW
Downlink C/N	12.8	16.0	dB
Downlink C/I	24.1	24.1	dB
Downlink C/(N+I)	12.5	15.4	dB
For Bent-Pipe Transponder:			
	Rain	Clear Sky	
QPSK Required C/N @ 10e-6	13.6	13.6	dB
Implementation Margin	1.0	1.0	dB
Turbo Code Coding Gain	6.6	6.6	dB
Threshold C/N	8.0	8.0	dB
Overall (C/N+I)	12.5	15.4	dB

3.3.1.4. Network Implementation Issues

In addition, network implementation issues are raised since both LMDS systems and Ka-band satellite systems use different types of information packets and protocols. The current Virginia Tech LMDS system uses its own proprietary protocols, which will not be compatible with any commercial Ka-band satellite systems. Thus, as mentioned earlier in Chapter 1, the IEEE 802.16 standard protocols are assumed to be used in our LMDS system because the standard IEEE 802.16 protocols will ultimately be adopted for most 28 GHz and 5-6 GHz U.S. LMDS systems in the near future.

As the LMDS system network operates at a standard IEEE 802.16 environment, the data bit streams are delivered in standard IEEE 802.16 protocols and packets. However, the proposed Ka-band Spaceway satellite operates on the standard IEEE 802.3 or TCP/IP environment. Different networks might be compatible only when the on-board processing transponders of the Spaceway systems are programmed to route or switch between the IEEE 802.16 and IEEE 802.3 environments. Otherwise, both LMDS and RF signals with different packets should be processed and implemented at the baseband before being delivered to the satellite. Topologies 3 and 4 will provide solutions to this implementation network impairment. More details on the network implementation issues between the terrestrial and satellite networks will be discussed in Chapter 5 when the final topology is chosen.

3.3.2. Topology 2: Bandpass-to-bandpass (IF-to-IF) Coupling

3.3.2.1. Frequency Planning Aspects

This topology is very similar to Topology 1 proposed in the previous section. The difference is that the second IF signal at 140 MHz from the hub unit is coupled onto the VSAT IF instead of the VSAT RF. The LMDS downlink frequency is converted to IF at 140 MHz via two mixers in the LMDS subsystem before connecting to the satellite modem. The LMDS second IF signal that is extracted will be connected to the IF ports of the VSAT.

For the LTS section of the VSAT, the initial 140 MHz LMDS second IF frequency will be converted to the Ka-band RF frequency with the LO frequency of 29.41 GHz. At the STL

section, the Ka-band frequency band at 19.75 GHz is down-converted to the 140 MHz IF through a LO frequency of 19.61 GHz.

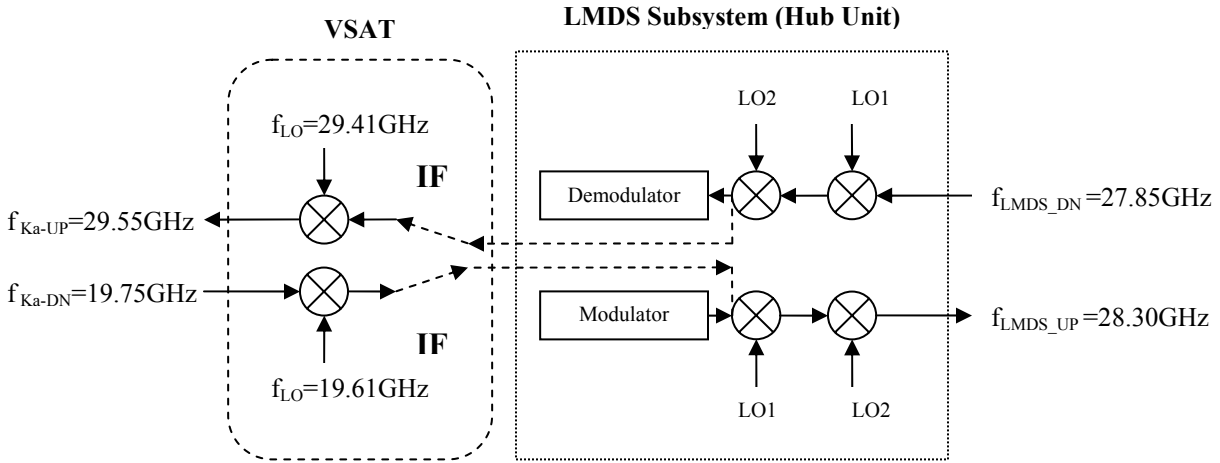


Figure 11 A Satellite-Terrestrial System Linked by IF on Both Uplink and Downlink Using a Single-Stage Frequency Converter

The LTS or STL converter can consist of two frequency conversion stages, as shown in Figure 12 below. For the LTS section, the incoming LMDS second IF frequency at 140 MHz will be converted to 910 MHz with the first LO running at 810 MHz. The second stage mixer will convert the first IF 910 MHz to the Ka-band RF frequency at 29.55 GHz running LO at 28.6 GHz. Moreover, the STL converter will convert the satellite downlink RF to the first IF frequency of 910 MHz with 18.80 GHz LO frequency. The first IF will convert again to the second IF frequency at 140 MHz with the given LO frequency of 810 MHz.

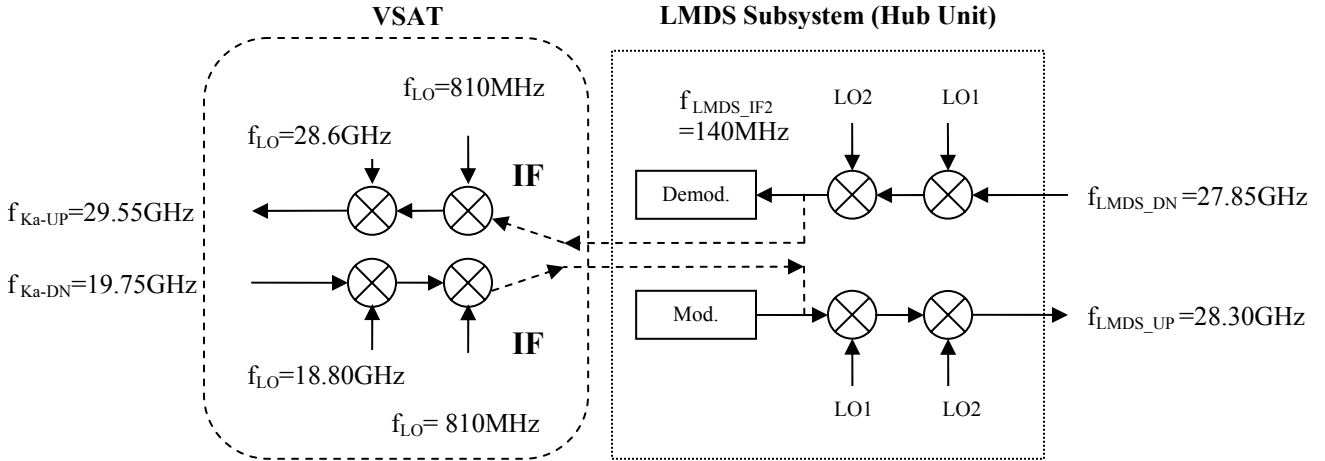


Figure 12 A Satellite-Terrestrial System Linked by IF on Both Uplink and Downlink Using a Dual-Stage Frequency Converter

The LO of STL and LTS can be shared since they are running at the same frequency. This frequency planning can save at least one LO component, and a total of three LO frequencies are necessary to build the VSAT.

3.3.2.2. Hardware Aspects

The dual stage frequency conversion of the VSAT can be viewed as a heterodyne STL and LTS converter similar to Figure 9 and 10, except that two-stage mixers should be incorporated in those figures. In this topology design, the VSAT does not have a modem to modulate and demodulate the transmitting and receiving signals.

The characteristics of the heterodyne LTS and STL converters are similar to those described in the Topology 1 RF-to-RF coupling design. The frequency converters in this topology are dual-stage instead of single-stage. For the dual stage heterodyne converter, the LNB can be purchased off-the-shelf. The BPF filters operating at 140 MHz and 910 MHz can be designed easily. The LO signals will be generated by a frequency synthesizer if the VSAT prototype is planned to be constructed for research purposes.

The functionalities of the amplifiers and BPFs were described earlier in Topology 1. That material applies as well to this topology. In addition, coupling at the IF between both the terrestrial and the satellite systems increases the amount of baseband equipment and the complexity of the earth station.

The disadvantages of the dual conversion design are the added costs of the second oscillator, mixer, and filters. The chief advantages of the dual-conversion architecture are flatter IF response, higher image rejection, and better broadband impedance matching compared to those in single stage conversion. In addition, image frequencies are not a problem for dual conversion receivers since images are far away from the desired signal, and therefore, easily filtered out beforehand. Moreover, the elimination of spurious responses and stable LO signal generators are the key elements for converters. Thus, the power and frequency selectivity of the LO are also very critical. Other distortions, such as harmonics, might corrupt the desired signals. However, for most of the time, the harmonics are so far away from the desired signals that they are easy to filter out.

3.3.2.3. Link Budget Aspects

The link budget analysis is based on Ka-band VSAT uplink and downlink transmissions. The minimum bandwidth of the filters, data rates, symbol rates, modulation schemes, and physical antenna size will affect the link budget. This topology link budget analysis was very similar to the one in the previous topology design since no modem is provided at the VSAT.

The remote unit RF signals are received by the hub unit. The hub unit will convert the received RF signals to IF signals, which will not be demodulated before being sent to the VSAT transmitter. Thus, the satellite will treat the remote unit as an end terminal for uplink and downlink transmissions. This topology link budget will then be the same as described in Topology 1, as shown in Table 11, since the remote unit modem is the same as the LMDS modem. Unfortunately, the link budget shows that this topology will not be feasible due to the same issues that were addressed in the earlier topology.

3.3.2.4. Network Implementation Issues

The network implementation issues for Topology 2 are also the same as in Topology 1 since both networks operate in two different protocol environments. The LMDS terrestrial network system is assumed to operate in an IEEE 802.16 environments, and the satellite network is in an Internet TCP/IP environment. Both protocols cannot be compatible either in RF or IF.

Apparently, the satellite will reject uplink transmissions from VSAT IF coupling to the LMDS IF, and the VSAT will also decline downlink transmission signals from the satellite. Although the frequency planning has simplified the hardware design, the network design seems to be infeasible for this topology due to the incompatibility between both systems joining at the IF frequency bands. Therefore, this topology is not selected.

3.3.3. Topology 3: RF-to-IF baseband Coupling

Topology 3 presents the joint design of topologies one and two. Basically, the downlink LMDS frequency will be converted onto the Ka-band uplink frequency via a LTS frequency converter. The received Ka-band downlink frequency will be converted onto a typical IF at 140 MHz via either a single stage or a dual stage STL converter before being fed onto a demodulator of the VSAT. The VSAT demodulator at the VSAT receiver will couple to the LMDS modem at baseband. Thus, this design is called RF-to-IF baseband coupling.

Figure 13 below shows a possible single-stage of the STL and LST frequency converter of the VSAT. As mentioned in the previous section, a dual stage converter of the VSAT might be more favorable since standard components can be purchased off-the-shelf, although the system complexity is increased.

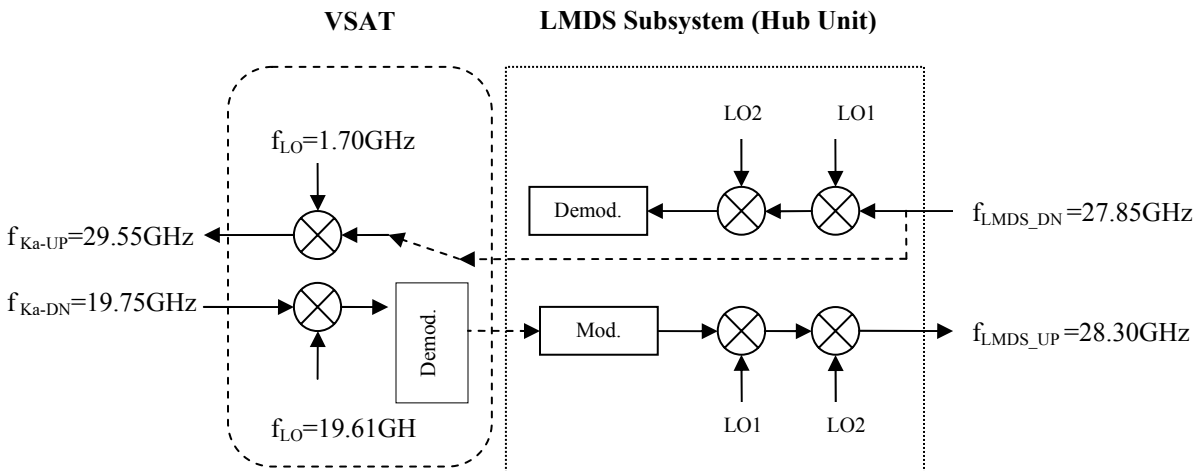


Figure 13 A Satellite-Terrestrial System Linked by RF on Uplink and IF on Downlink

3.3.3.1. Frequency Planning Aspects

The LMDS RF signals at 27.85 GHz are converted to the Ka-band uplink frequency at 29.55 GHz with a LO running at 1.7 GHz. Since the baseband coupling between the VSAT and LMDS subsystem is proposed in this design, a new demodulator should be added after the STL converter for baseband processing. The Ka-band downlink frequency at 19.75 GHz will be down converted into a standard IF for the VSAT modem. A typical IF value is assumed to be 140 MHz. Thus, the LO frequency for the down-conversion stage is selected to be 19.61 GHz.

In this topology, the VSAT baseband is connected to the LMDS baseband via a router or a switch. The dual stage converter is recommended instead of single stage converter because standard IF filters and amplifiers can be easily designed or cheaply purchased. The two-stage frequency planning of this topology can be seen in Figure 13, where downlink Ka-band frequency is down-converted to the first IF frequency at 910 MHz with the LO frequency of 18.80 GHz. The first IF frequency is then converted to a second IF at 140 MHz with a LO operating at 910 MHz.

3.3.3.2. Hardware Aspects

More components are required in this topology for the VSAT than in the first and second topologies. This results in higher cost earth terminals since additional baseband equipment is added at the VSAT. This topology's LTS and STL converters are the same as shown in two previous topologies, except that the second IF of the STL converter is fed directly onto the input port of the VSAT modem for baseband signal processing.

The VSAT baseband modem is proposed to be selective and provides extra degrees of freedom on the link budget designs. Different types of modulation techniques proposed in Chapter 2 will be adopted. This hybrid design can reconstruct the received signals and correct errors at the baseband. This improves signal transfer performance at downlink transmissions.

3.3.3.3. Link Budget Aspects

As mentioned in previous proposed topologies, the link budget analysis is affected directly by the modem characteristics at baseband. The downlink power budget between the satellite and the VSAT seems to be realistic when the VSAT modem can be characterized with desired features. To simplify the VSAT modem design, the VSAT modem is assumed to be the same as the LMDS modem. Different types of modulation, such as M-ary PSK and M-ary QAM, are examined to provide optimum BER performance.

This design uplink budget analysis is the same as those mentioned in Topology 1 (see Table 11). This concludes that the uplink is not feasible due to the given LMDS modem at the remote units running at a fixed 120 Mbps data rate.

The VSAT receiving antenna diameter was calculated to be around 2 meters providing data rate up to 4 Mbps with a reasonable transmitting power. The data rates of the VSAT modem are assumedly adjustable so that different capacities of signals can be delivered flexibly. The link budget analysis is not provided since the uplink power budget of this topology is not realistic.

3.3.3.4. Network Implementation Issues

The baseband coupling provides a feasible solution compared to the previous two topologies. For the downlink transmissions, the VSAT receiving modem is capable of demodulating the incoming satellite IEEE 802.3 (Internet environment) signals at the baseband. The baseband IEEE 802.3 signals will then be converted to IEEE 802.16 packets via a router or switch before being delivered to the LMDS subsystem. This router or switch can be purchased from many network equipment manufacturers. Occasionally, a couple of routers or switches are needed in order to provide proper protocol implementations. More details on the routers/switches appear in Chapter 5. The uplink transmissions still face the protocol compatibility issues as mentioned earlier. A modulator at the VSAT can overcome these network impairments.

3.3.4. Topology 4: Baseband-to-Baseband Coupling

This topology is to combine LMDS terrestrial system and Ka-band satellite system using baseband-to-baseband coupling. The VSAT consists of a two-stage frequency STL converter, a LTS converter, and a modem, shown in Figure 14 below. This design not only increases the components needed at the RF front-end and baseband sections, but also requires additional routers or switches in order to overcome the incompatibility of both network systems. Other techniques such as ad-hoc networks can be used to connect various network systems together, but a simple router or switch is proposed to simplify the network implementation design in this thesis.

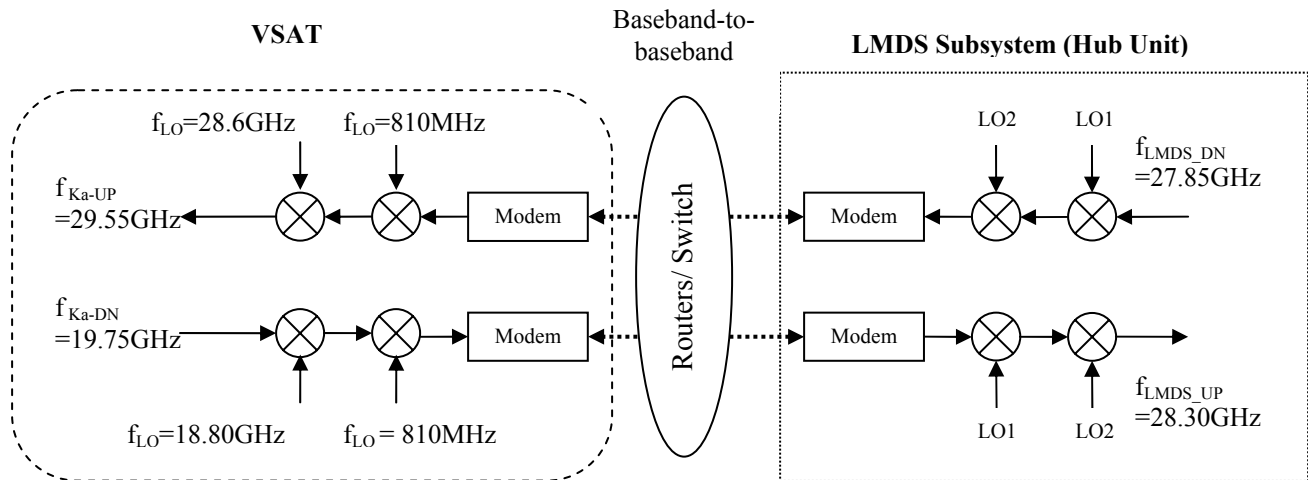


Figure 14 A Satellite-Terrestrial System Linked at baseband on Both Uplink and Downlink

3.3.4.1. Frequency Planning Aspects

The LTS converter of the VSAT converts the modem IF output frequency to the Ka-band uplink frequency via a two-stage frequency conversion. The modem IF is converted up to the Ka-band uplink frequency at 29.55 GHz with two LOs running at 810 MHz and 28.6 GHz. The STL converter of the VSAT will convert the satellite downlink frequency to the IF frequency at 140 MHz with LOs running at 18.80 GHz and 810 MHz. The VSAT modem is identical to the LMDS satellite modem. The IF input and output ports operate at 140 MHz. The difference

between the VSAT and LMDS modem is that the VSAT modem is flexible with different burst data rates and LMDS modem is fixed with the data rate of 120 Mbps.

Both satellite system and LMDS system are independent of each other since both system RF signals are isolated by the router or switch before communicating with each other. Thus, the networks can be compatible with each other via the router/switch.

3.3.4.2. Hardware Aspects

Apparently adding extra baseband equipment onto the VSAT increases the total cost for the VSAT and the complexity of VSAT design. However, the VSAT modem provides some flexibility that topologies one and two cannot provide. Multiple modulations, mentioned in Chapter 2, were selected for optimizing BER performance. Different data rates of the modem can be programmed and modeled to achieve the desired uplink and downlink BER values. The VSAT modem is modeled similarly to the LMDS modem for system design simplification.

The two-stage STL and LTS converters can be obtained off-the-shelf or be custom designed. For research purposes, LO signals can be generated by frequency synthesizers, whose frequency accuracy has to be treated cautiously. The antenna size and transmitting power of the VSAT are properly selected to provide at least BER of 10^{-6} . The trade-offs will be discussed in Chapter 4.

3.3.4.3. Link Budget Aspects

In this topology the downlink budget design is identical to Topology 3. The uplink link budget design now becomes realizable because a new transmitting modem placed before the LTS converter will be adopted for the VSAT. Since this topology is more feasible, the link budget analysis is extensively studied in Chapter 4. An inbound link (from the VSAT to a center hub) and outbound link (from a center hub to the VSAT) will be studied. Various case scenarios of the inbound and outbound link will be provided in Chapter 4.

3.3.4.4. Network Implementation Issues

As mentioned earlier, both satellite and terrestrial networks do not operate at the same protocol environment. The network incompatibilities between Ka-band satellite system and LMDS system can be resolved via MANET systems. For the same capabilities and lower prices, routers or switches are proposed. There might not be any standard routers or switches directly providing IEEE 802.3 and IEEE 802.16 protocol transformations. Thus, cascaded routers or switches are needed. This topology is selected because it can resolve the network impairment issues for the integrated systems, unlike topologies 1, 2, and 3.

3.4. Final Design Selection and Summary

In the aspect of hardware designs, all proposed topologies are feasible. Topology 1, RF-to-RF coupling design, provides the least hardware components among four topologies. On the other hand, no transmitting mixers and filters are available at such high frequency bands, and the networks are not compatible with each other.

Topology 2, allows lower frequency band hardware components, but the terrestrial and satellite networks are not compatible with each other. Topology 3, RF-to-baseband coupling, provides additional baseband equipment complicating the system design. The downlink transmission with the VSAT receiving modem for this integrated system is practical; however, the satellite uplink is done at RF, which suffers the same network incompatibility as described in Topology 1.

Topology 4 is the most feasible design among four proposed topologies. Not only can the frequency planning and hardware designs be done easily, but also the network implementation issues can be resolved via routers or switches at the baseband. The tradeoff with this topology is that the cost of VSAT is much higher and complex, but the VSAT can be constructed easily.

The fourth topology system design, reflector antenna design used by the VSAT, link budget analysis for various cases including rain attenuation, adjacent satellite interferences, other losses and interferences, engineering trade-offs, network implementation concerns, will be presented in the next two chapters.

Chapter 4: Final System Design Selection

Topology 4 was selected for the satellite-terrestrial integrated network design. The VSAT design, antenna design, and link budget analysis for the satellite system are presented in this chapter. Both outbound and inbound link budget designs including adjacent satellite interference, rain attenuation, and other losses for the Topology 4 are also included here.

4.1. System Design Block Diagram

As mentioned earlier, the Spaceway satellite operating in Ka-band serves as a backbone network of the LMDS terrestrial network system if the fiber optic cable network connection is not available. The final selected integrated terrestrial and satellite network system design was discussed in Topology 4 in the previous chapter. Figure 15 below presents the overall architecture of the integrated terrestrial-satellite network system.

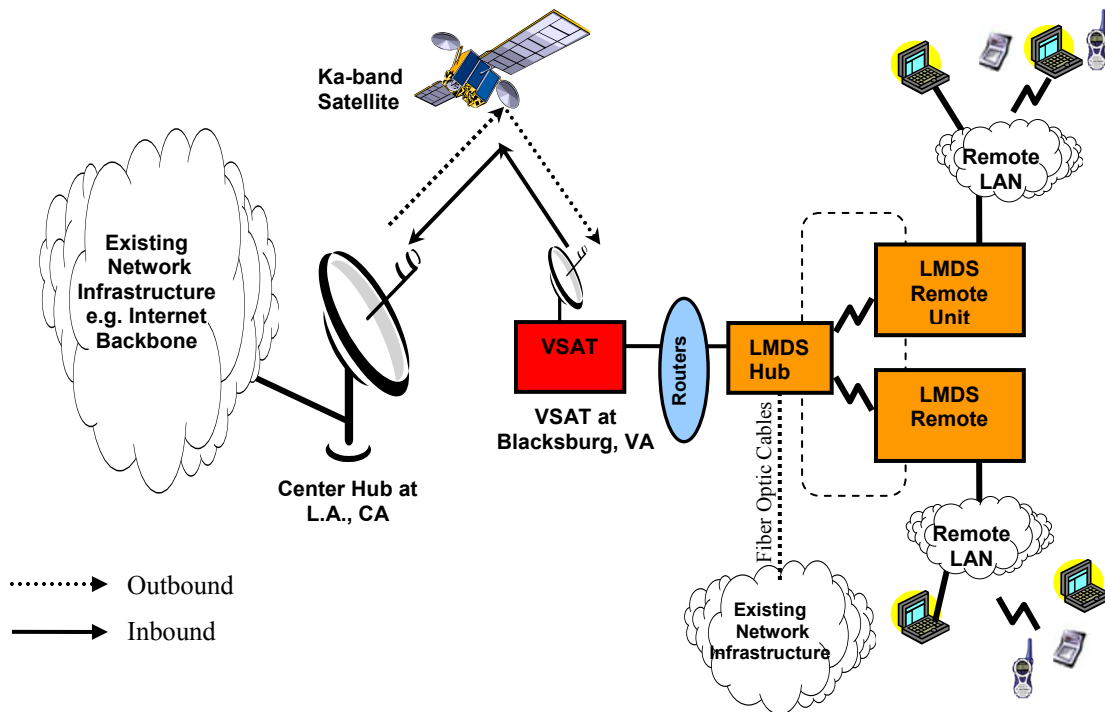


Figure 15 Integrated Terrestrial-Satellite Network Architecture

The VSATs for the Ka-band satellite networks are assumed to be placed at various locations in the U. S. The locations of the VSATs include Blacksburg (Virginia), Miami (Florida), New York City (New York), Chicago (Illinois), and Dallas (Texas) are chosen for the link budget design due to those locations' climates and VSATs' look angles. Two of Hughes' Ka-band center hubs, located at Los Angeles, California, and Littleton, Colorado, were licensed by the FCC for the Spaceway satellite systems. The center hub is typically connected to an existing network infrastructure, such as an Internet backbone or a broadcast server with 100BaseT interface.

An outbound link, known as a forward link, is defined as the signals that are delivered from a hub to a VSAT via the Spaceway Ka-band satellite. On the other hand, an inbound link, known as a return link, allows signals to be transferred from the VSAT to the hub via the Spaceway satellite. Usually, the inbound link will suffer degradations in heavy rain due to the VSAT's low transmitting power and small antenna. The VSAT design is required to have at least 10^{-6} BER performance for a disaster response communication system.

The characteristics of the VSAT modem were assumed to be similar to the LMDS modem, except that various data rates and modulation schemes for the VSAT modem were used to optimize the outbound and inbound link performance. This will be discussed in the link budget analysis section of this chapter.

In addition, as mentioned in the previous chapters, both satellite and terrestrial networks are independent of each other in term of RF transmissions. The end-to-end data are delivered from one network to the other network through routers or switches operating at baseband frequencies, as shown in Figure 15 above.

The satellite and center hub parameters are not changeable once the satellite and the hubs are placed for network services. In order to reach the desired BER performance, the antenna size and transmitting power of the VSAT can be adjusted. The antenna design will be discussed in the next section.

4.2. VSAT Antenna

Since the distance between an earth station in the US and a GSO satellite is typically 35,800 km, the signals are weak when arriving at the satellite receiver. Thus, a high gain antenna

is required to acquire the signals. Circular aperture parabolic reflector antennas are commonly used in VSAT designs. Most VSAT antennas have gains greater than 35 dB. For instance, an 18-inch Direct Broadcast System (DBS)-TV dish at 12 GHz has a gain of 35 dB. In this design, a low cost, small size, and high gain antenna is required in the VSAT designs, especially when operating in the frequency range between 20 GHz and 30 GHz.

A VSAT usually uses a parabolic reflector antenna. A typical gain value of a Ka-band reflector antenna is around 40-50 dB. The antenna pattern should also meet the FCC limitations. Another parameter limiting the antenna design is the EIRP value, defined by ITU. A Ka-band antenna normalized pattern is shown in Figure 18 below. The operating frequency was assumed to be 29.55 GHz, and the diameter of the antenna was 1 meter. The designed reflector antenna side-lobe is about 5 dB below the FCC antenna pattern envelope curve marked in thicker lines, and defined by sidelobe level = $29-25 \log(\theta)$ dBi, where dBi is decibels above isotropic level.

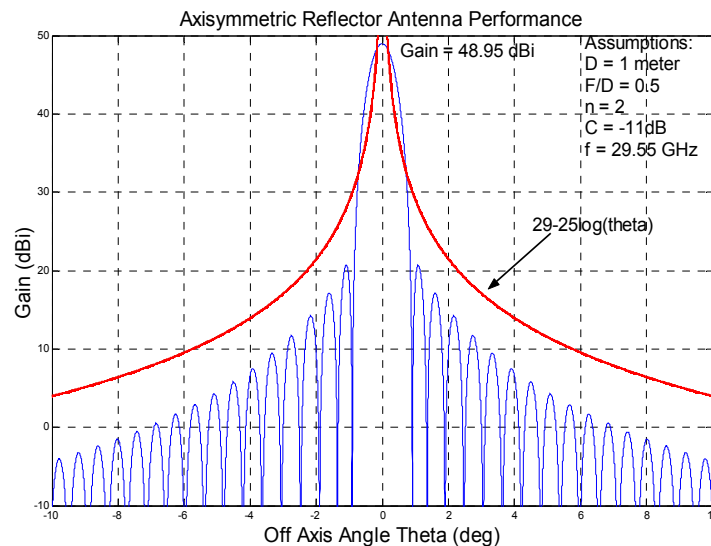


Figure 16 Theoretical Ka-band Reflector Antenna Pattern

In addition, the antenna gain for various sizes of reflector antennas aperture is tabulated in Table 13. The gain of the antenna is proportional to the diameter of the antenna. A higher gain antenna provides better link performance, especially when a Ka-band satellite operates in GEO orbit.

Table 13 Reflector Antenna Gain

Reflector Antenna Diameter	0.6 m	0.9 m	1 m	1.2 m	1.5 m	1.8 m	2 m
Transmitting Antenna Gain @ 29.55 GHz [dBi]	44.51	48.03	48.95	50.53	52.47	54.05	54.97
Receiving Antenna Gain @ 19.75 GHz [dBi]	41.01	44.53	45.45	47.03	48.97	50.55	51.47

Usually earth stations placed at different locations would have different look angles toward the same Ka-band satellite operating in GEO orbit. The look angle calculations of the earth station toward the satellite will be presented in the next section.

4.3. Elevation (EL) and Azimuth (AZ) Angle Calculations

In satellite communications systems, an earth station antenna has to point in the direction of a satellite in order to communicate with the satellite. The antenna’s pointing coordinates are called the look angles, and are expressed in azimuth (AZ) and elevation (EL). Both AZ and EL angles can be calculated only if both the satellite’s and the earth station’s locations are known.

The location of the satellite and the earth station are specified by latitudes and longitudes in degrees. The satellite’s location is defined by the sub-satellite point, located on the surface of the earth directly between the satellite and the center of the earth. For a GSO satellite, the latitude of the sub-satellite point will be zero because the GSO satellite is always located above the equator. For instance, the Spaceway satellite is located at longitude of 99° W, and the latitude of 0 degrees.

Figure 17 below [Pra02] presents the geometry between an earth station and a satellite, which is used to define EL and AZ angles of an earth station. For instance, if a VSAT is placed at Blacksburg, Virginia, the longitude of VSAT is 80.42° W and the latitude is 37.28° N.

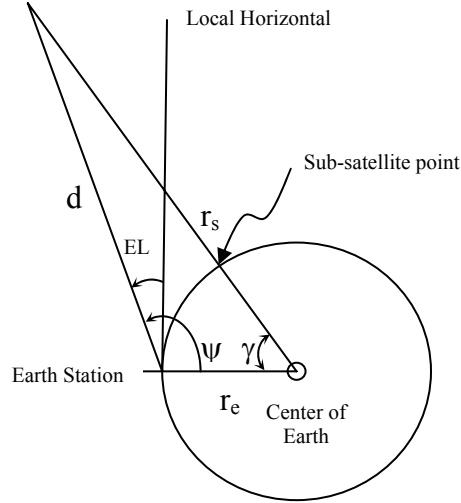


Figure 17 The Geometry of Elevation Angle Calculation

From Figure 19, the central angle (γ) can be obtained from (Eq. 14)

$$\cos(\gamma) = \cos(L_e) \cos(L_s) \cos(l_s - l_e) + \sin(L_e) \sin(L_s) \quad (\text{Eq. 14})$$

where γ = central angle [degree]

L_e = earth station north latitude [degree]

L_s = north latitude of the sub-satellite point [degree]

l_e = earth station west longitude [degree]

l_s = west longitude of sub-satellite point [degree]

The distance (d) between the earth station and the satellite can be calculated from (Eq. 15) when the central angle (γ), the orbital radius (r_s), and the earth radius (r_e = average earth's radius = 6378.137 km) are known.

$$d = r_s \left[1 + \left(\frac{r_e}{r_s} \right)^2 - 2 \left(\frac{r_e}{r_s} \right) \cos(\gamma) \right]^{1/2} \quad (\text{Eq. 15})$$

The elevation angle for an earth station with respects to a satellite can be obtained from (Eq. 16). For instance, the EL of a VSAT placed at Blacksburg, Virginia, was calculated to be 42.07 degrees for the Spaceway satellite located at 99° W.

$$\cos(EL) = \frac{r_s \sin(\gamma)}{d} \quad (\text{Eq. 16})$$

To find the azimuth angle between an earth station and a satellite, the intermediate angle (α) should be found first using (Eq. 17) below.

$$\alpha = \tan^{-1} \left[\frac{\tan |l_s - l_e|}{\sin(L_e)} \right] \quad (\text{Eq. 17})$$

The azimuth angle depends upon where the earth station is located and where the satellite's location is with respect to the earth station. For example, if the earth station is located in the Northern Hemisphere (north above the equator) and the satellite is to the southeast (SE) of the earth station, then Case I (a) in Table 14 below will be used to find out the azimuth angle of the earth station to the satellite. Table 15 illustrates different EL and AZ angles of earth stations located across the United States respected to the Spaceway satellite located at 99° W.

Table 14 Calculations for Azimuth Angle

Case I	Earth station in the Northern Hemisphere with	Azimuth Angle
a	Satellite to the SE of the earth station	Az = 180° - α
b	Satellite to the SW of the earth station	Az = 180° + α
Case II	Earth station in the southern Hemisphere with	
c	Satellite to the NE of the earth station	Az = α
d	Satellite to the NW of the earth station	Az = 360° - α
SE=Southeast, SW=Southwest, NE=Northeast, and NW=Northwest		

Table 15 EL and AZ Angles of Earth Stations Placed Across the United States

Earth Station Locations	Latitude [degrees]	Longitude [degrees]	Elevation Angle [degrees]	Azimuth Angle [degrees]
Blacksburg, Virginia	37.28	80.42	41.26	209.03
Miami, Florida	25.82	80.28	52.22	217.88
New York City, New York	40.78	73.97	34.92	215.56
Chicago, Illinois	41.85	87.65	38.95	196.74
Dallas, Texas	32.78	95.8	50.58	185.90
Los Angeles, California	34.08	118.09	44.16	174.10
Littleton, Colorado	39.01	105.01	43.13	174.10

4.4. Rain Attenuation Calculations

When designing a link budget for a satellite system, the atmospheric condition between the ground station and a space station is critical. A good (a clear sky day) or bad (a raining or cloudy day) atmospheric environment will determine how the signals propagate between ground

and space stations. The amounts of rain attenuation vary depending on the rain's characteristics, including raindrop sizes, raindrop temperatures, raindrop intensities, raindrop distributions, rain fall rates, and rain locations [Fen01].

The ITU provides a rain model that is used to predict the attenuation due to precipitation and clouds along a slant propagation path for a percentage ranged from 0.001% to 5% of an average year, which will be discussed below.

4.4.1. Prediction of Attenuation Statistics for an Average Year

The rain attenuation depends on many parameters, including the given earth station's elevation angle, latitude, and height above sea level estimated from [ITU1511], operating frequency, and effective earth's radius. The ITU rain model can be used for operating frequencies up to 55 GHz.

Figure 18 below shows an earth-to-space path giving the parameters that are used at the ITU-R rain attenuation prediction procedures. h_R represents the rain height in km, h_s presents the height above mean sea level (a.m.s.l) of the earth station in km, L_s represents the slant-path length between the earth station and the satellite in km, and L_G presents the horizontal projection of L_s in km [ITU618].

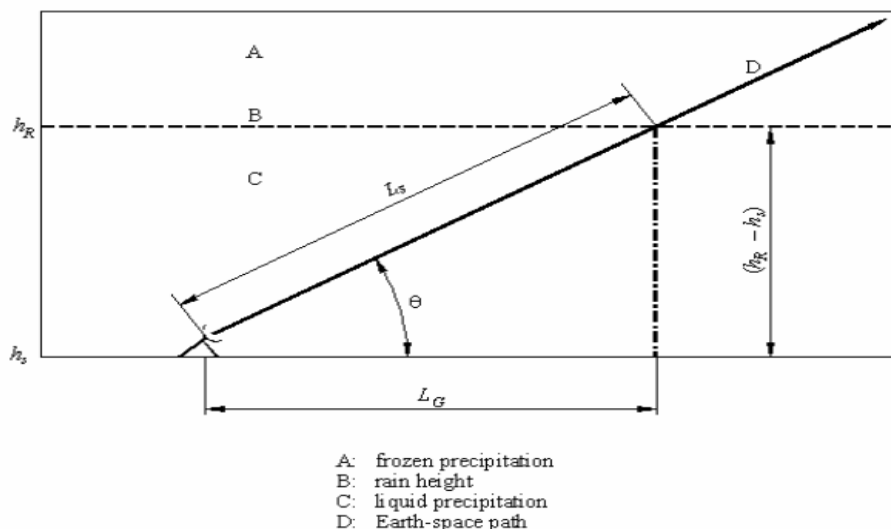


Figure 18 Schematic Presentation of an Earth-to-Space Path Giving the Parameters to be Input into the ITU-R Rain Attenuation Prediction Procedures

The ITU model procedure consists of 10 steps. Each step defines certain parameters before the rain attenuation is calculated. Each parameter will be introduced while the procedure is described in the following section.

In the **first step**, the rain height (h_R) has to be determined. The values of h_R can be calculated from the earth station latitude by (Eq. 18)

$$h_R = \begin{cases} 3.0 + 0.028 \phi, & 0^\circ < \phi < 36^\circ \\ 4.0 - 0.075(\phi - 36), & \phi \geq 36^\circ \end{cases} \quad [km] \quad (Eq. 18)$$

where ϕ is the earth station latitude. In the **second step**, the slant-path length (L_s) is defined in (Eq. 19) below as long as the elevation angle (θ) is greater or equal to 5° . If the elevation angle (θ) is less than 5° , (Eq. 20) should then be adopted.

$$L_s = \frac{(h_R - h_s)}{\sin \theta} \quad [km] \quad (Eq. 19)$$

$$L_s = \frac{2(h_R - h_s)}{\left(\sin^2 \theta + \frac{2(h_R - h_s)}{R_e} \right)^{1/2} + \sin \theta} \quad [km] \quad (Eq. 20)$$

where

- h_R = rain height [km] (typical value = 4 km)
- h_s = height above mean sea level of the earth station [km]
- θ = elevation angle [degrees]
- R_e = effective radius of the earth [8500 km].

If $(h_R - h_s)$ is less than or equal to zero, the predicted rain attenuation for any time percentage is zero. Thus, the rests of the steps in this section are not required. Otherwise, step three described below should be followed. In the **third step**, the relationship between the horizontal projection, L_G , and L_s can be derived from Figure 18 and defined as the following (Eq. 21):

$$L_G = L_s \cos \theta \quad [km] \quad (Eq. 21)$$

In the **fourth step**, the rainfall rate ($R_{0.01}$) exceeded for 0.01% of an average year (with an integration time of 1 min) is defined from a long-term statistical data collection and measurements. Figure 21 on the next page presents the overall rain climate zone of the Americas defined by ITU [ITU837]. The climate zone map is used for both propagation predictions and interference calculations. Other countries' climate zone maps can be found in [ITU837].

In **step five**, the rainfall intensities can also be found to correspond to particular time zones at the given percentage of time that is required for a satellite system link. Table 16 shows the rainfall rate intensities corresponded to particular rain climatic zones in Figure 21. For instance, the climatic zone code for Blacksburg, Virginia is M, and the rainfall rate intensity for 0.01% of the total amount of hours for an average year is 63 mm/hr.

Table 16 Rainfall Intensity Exceeded in mm/hr Corresponded to Rain Climate Zones

Percentage of Time	A	B	C	D	E	F	G	H	J	K	L	M	N	P	Q
	1	2	3	4	5	6	7	8	9	10	11	12	13	14	15
0.001	22	32	42	42	70	78	65	83	55	100	150	120	180	250	170
0.003	14	21	26	29	41	54	45	55	45	70	105	95	140	200	142
0.01	8	12	15	19	22	28	30	32	35	42	60	63	95	145	115
0.03	5	6	9	13	12	15	20	18	28	23	33	40	65	105	96
0.1	2	3	5	8	6	8	12	10	20	12	15	22	35	65	72
0.3	0.8	2	2.8	4.5	2.4	4.5	7	4	13	4.2	7	11	15	34	49
10	0.1	0.5	0.7	2.1	0.6	1.7	3	2	8	1.5	2	4	5	12	24

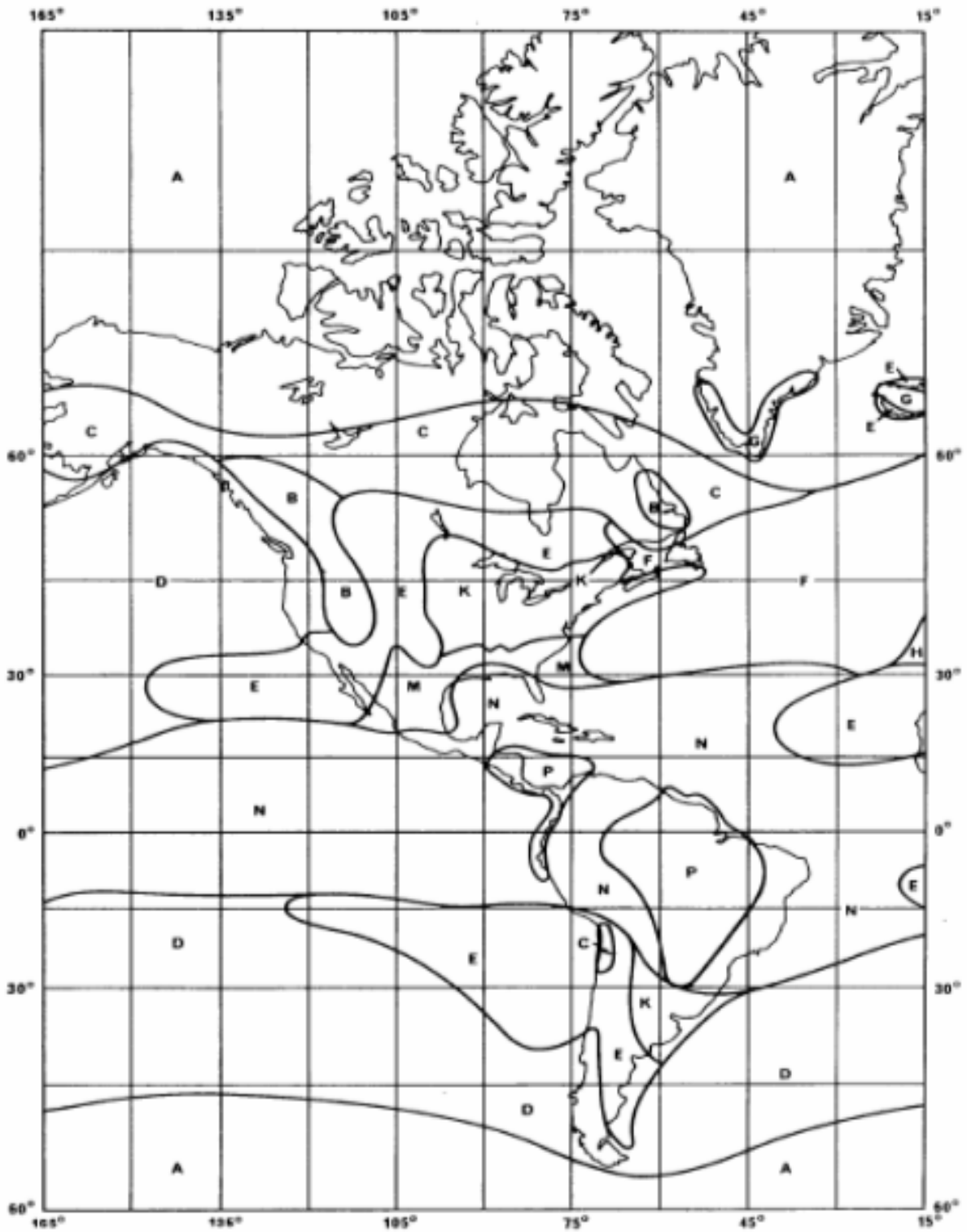


Figure 19 Rain Climatic Zones for the Americas [ITU837]

In **step six**, after the rainfall intensity is defined for a particular location and satellite system link availability for an average year, a specific attenuation (γ_R) can be determined using (Eq. 22) below [ITU838].

$$\gamma_R = k(R_{0.01})^\alpha \quad [dB / km] \quad (Eq. 22)$$

where $R_{0.01}$ = point rainfall rate for the location for 0.01% of an average year [mm/hr]
 α, k = regression coefficient for estimating specific attenuation

α and k are frequency dependent. The overall k and α can be calculated from (Eq. 24) and (Eq. 23) below from the vertical (V) and horizontal (H) polarization values of k and α , given in Table 17. In addition, k and α can also be calculated for other frequencies by an interpolation technique using a logarithmic scale for frequency, a logarithmic scale for k , and a linear scale for α .

$$k = [k_H + k_V + (k_H - k_V) \cos^2 \theta \cos 2\tau] / 2 \quad (Eq. 24)$$

$$\alpha = [k_H \alpha_H + k_V \alpha_V + (k_H \alpha_H - k_V \alpha_V) \cos^2 \theta \cos 2\tau] / 2k \quad (Eq. 23)$$

where θ = path elevation angle
 τ = polarization tilt angle relative to the horizontal ($\tau = 45^\circ$ for circular polarization)

Table 17 Regression Coefficients for Estimating Specific Attenuation, γ_R [ITU838]

Frequency (GHz)	k_H	k_V	α_H	α_V
1	0.0000387	0.0000352	0.912	0.880
2	0.000154	0.000138	0.963	0.923
4	0.00065	0.000591	1.121	1.075
8	0.00454	0.00395	1.327	1.310
10	0.0101	0.00887	1.276	1.264
12	0.0188	0.0168	1.217	1.200
15	0.0367	0.0335	1.154	1.128
20	0.0751	0.0691	1.099	1.065
25	0.124	0.113	1.061	1.030
30	0.187	0.167	1.021	1.000
35	0.263	0.233	0.979	0.963
40	0.35	0.31	0.939	0.929
45	0.442	0.393	0.903	0.897

Table 18 shows the k and α values for right hand and left hand circular polarization (when $\tau = 45^\circ$) for the system operating at the uplink frequency at 29.55 GHz and the downlink frequency at 19.75 GHz.

Table 18 Uplink and Downlink α and k Regression Coefficient

Locations	k_{up}	α_{up}	k_{dn}	α_{dn}
Blacksburg, VA	0.1664	1.0083	0.0682	1.0773
Miami, Florida	0.1704	1.0129	0.0694	1.0844
New York City, New York	0.1662	1.0080	0.0684	1.0769
Chicago, Illinois	0.1706	1.0131	0.0695	1.0848
Dallas, Texas	0.1660	1.0078	0.0681	1.0765
Los Angeles, California	0.1656	1.0073	0.0680	1.0759
Littleton, Colorado	0.1687	1.0109	0.0689	1.0814

After all the necessary parameters have been defined and introduced previously, the horizontal reduction factor, $r_{0.01}$, for 0.01% of an average year is

$$r_{0.01} = \frac{1}{1 + 0.78 \sqrt{\frac{L_G \gamma_R}{f}} - 0.38 (1 - e^{-2L_G})} \quad (Eq. 25)$$

where f = Operating center frequency [GHz]

In **step seven**, the vertical adjustment factor, $v_{0.01}$, for 0.01% of the time, can be calculated by a couple of sub-steps below. The values for ζ , L_R , ϕ and χ are found as follows:

$$\zeta = \tan^{-1} \left(\frac{h'_R - h_s}{L_G r_{0.01}} \right) \quad [\text{degrees}] \quad (Eq. 26)$$

If $\zeta > \theta$, (Eq. 27) should be used to find L_R ; otherwise, (Eq. 28) is used.

$$L_R = \frac{L_G r_{0.01}}{\cos \theta} \quad [\text{km}] \quad (Eq. 27)$$

$$L_R = \frac{(h_R - h_s)}{\sin \theta} \quad [\text{km}] \quad (Eq. 28)$$

In the **eighth step**, the latitude of the earth station (ϕ) is then used to determine the χ value. If $|\phi| < 36^\circ$, (Eq. 29) should be used to obtain the χ value; otherwise, the χ value equals to zero.

$$\chi = 36 - |\phi| \quad [\text{degrees}] \quad (Eq. 29)$$

Step nine now shows the vertical adjustment factor ($v_{0.01}$) that can be presented as the following (Eq. 30) when the ζ , L_R , ϕ and χ values are determined.

$$v_{0.01} = \frac{1}{1 + \sqrt{\sin \theta} \left(31 \left(1 - e^{-\theta/(1+\chi)} \right) \frac{\sqrt{L_R \gamma_R}}{f^2} - 0.45 \right)} \quad (\text{Eq. 30})$$

The effective path length (L_E), which will be used to calculate the prediction rain attenuation, can be obtained from (Eq. 31) when L_R was given previously.

$$L_E = L_R v_{0.01} \quad [km] \quad (\text{Eq. 31})$$

In the **tenth step**, the predicted attenuation exceeded for 0.01% of an average year is the products of L_E and γ_R , shown in (Eq. 32) below.

$$A_{0.01} = \gamma_R L_E \quad [dB] \quad (\text{Eq. 32})$$

The new estimated rain attenuation other than 0.01% of an average year can be calculated by (Eq. 33).

$$A_p = A_{0.01} \left(\frac{p}{0.01} \right)^{-(0.655 + 0.033 \ln(p) - 0.045 \ln(A_{0.01}) - \beta(1-p) \sin \theta)} \quad [dB] \quad (\text{Eq. 33})$$

p is the desired percentage of an average year other than 0.01%, and β can be calculated based on the desired p value, and the given ϕ and θ values, shown in Table 19.

Table 19 Parameter Status of p, ϕ , and θ to Find the β Value

If $p \geq 1\%$ or $ \phi \geq 36^\circ$	$\beta = 0$
If $p < 1\%$ and $ \phi < 36^\circ$ and $\theta \geq 25^\circ$	$\beta = -0.005(\phi - 36)$
Otherwise	$\beta = -0.005(\phi - 36) + 1.8 - 4.25 \sin(\theta)$

Table 20 and Table 21 present the uplink and downlink rain attenuation that are exceeded during the specified portion of an average year. The percentage on the tables represents the

tolerance of the link availability in an average year. For instance, 0.5% of 8760 hours in a year allows link outage of 43.8 hours, which is a moderate/reasonable tolerance to a satellite link performance.

Table 20 Uplink Estimated Rain Attenuation [in dB]

Location Percentage	Blacksburg, VA	Miami, FL	New York, NY	Chicago, IL	Dallas, TX	Los Angeles, CA	Douglas, CO
0.01	43.788	46.436	37.515	35.798	45.568	22.632	8.466
0.1	17.077	19.804	14.398	13.673	18.311	8.358	2.785
0.5	7.184	8.327	5.989	5.668	7.714	3.349	1.040
1	4.694	5.038	3.894	3.680	4.925	2.116	0.646
5	1.546	1.667	1.268	1.195	1.627	0.664	0.189
10	0.909	0.982	0.742	0.698	0.958	0.383	0.105

Table 21 Downlink Estimated Rain Attenuation [in dB]

Location Percentage	Blacksburg, VA	Miami, FL	New York, NY	Chicago, IL	Dallas, TX	Los Angeles, CA	Douglas, CO
0.01	22.051	22.999	18.931	17.967	22.560	11.054	3.896
0.1	8.009	9.120	6.769	6.389	8.428	3.790	1.183
0.5	3.206	3.645	2.680	2.520	3.374	1.442	0.417
1	2.050	2.157	1.706	1.601	2.108	0.891	0.253
5	0.643	0.678	0.529	0.494	0.662	0.266	0.070
10	0.370	0.391	0.303	0.283	0.381	0.150	0.038

Obviously, the uplink rain attenuation is much higher compared to that on the downlinks. Therefore, the uplink must be designed carefully. The above rain attenuation is considered to be a moderate/typical rain scenario for the inbound and outbound links. In addition, other interference (adjacent satellite interference, antenna pointing losses, needed implementation margin and link margin, etc.) presented in the next section will also degrade both uplink and downlink performance.

4.5. Interference from Adjacent Satellite Systems

The interference generated by either an earth station radiating into an adjacent satellite or an adjacent satellite radiating into an earth station depends on their respective antenna radiation patterns. Actual antenna patterns described above are considered for the system. The ITU also

defined the EIRP limited values for a VSAT operating in the 14 GHz frequency bands, shown in Table 22.

The ITU did not recommend EIRP limitation for Ka-band VSATs. Therefore, the EIRP limited values of 14 GHz (Ku-band) VSATs are assumed for the Ka-band VSATs because, with the same antenna gain, the Ka-band VSATs provide smaller antenna size and smaller beamwidth compared to the Ku-band VSAT. From the table, ϕ represents any angle off the main lobe axis of an earth station antenna, and N is equal to 1 when either TDMA or FDMA systems are adopted. For a CDMA system, N is the number of the earth stations transmitting simultaneously on the same frequency.

Table 22 VSAT Maximum EIRP Levels

Angle off-axis	Maximum EIRP in any 40-kHz band
$1.8^\circ \leq \phi < 7.0^\circ$	$19 - 25 \log \phi - 10 \log N$ [dBW]
$7.0^\circ < \phi \leq 9.2^\circ$	$- 2 - 10 \log N$ [dBW]
$9.2^\circ < \phi \leq 48^\circ$	$22 - 25 \log \phi - 10 \log N$ [dBW]
$\phi > 48^\circ$	$- 10 - 10 \log N$ [dBW]

4.5.1. Uplink Adjacent Satellite Interference Analysis

The uplink interference is analyzed from a case where a wanted satellite transponder receives a wanted carrier from an earth station located within the coverage of its receiving antenna, and where an interfering earth station normally transmits some undesired carrier power to the wanted satellite receiver, illustrated in Figure 20 below [Mar95]. Both wanted station and interfering station are assumed to operate at the same frequency.

N_{iU} refers to the uplink noise (or interference) from interfering stations arriving at the satellite transponders, and C_U is the uplink carrier power received by the satellite transponders from the wanted stations. For a worst case assumption, the wanted earth station is located at the edge of the satellite transmitting antenna coverage area, and the interference earth station is located at the center of the coverage.

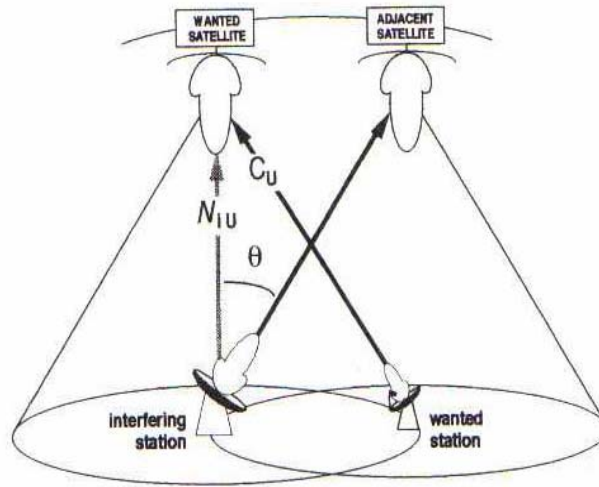


Figure 20 Uplink Interference from an Adjacent Satellite System [Mar95]

The adjacent satellite interference for uplink transmission can be mathematically analyzed as in (Eq. 34) below.

$$\frac{C}{I} \Big|_{dB_UP} = (EIRP_{esW} - G_{sat_r_W} - L_{p_W}) - (EIRP_{esI} - G_{sat_r_I} - L_{p_I}) \quad [dB] \quad (Eq. 34)$$

where $EIRP_{esW}$ = wanted earth station EIRP for the wanted carrier in the direction of the wanted satellite [dBW]
 $EIRP_{esI}$ = interfering earth station EIRP for the interfering carrier in the direction of the wanted satellite [dBW]
 L_{p_W} = uplink path loss for the wanted carrier [dB]
 L_{p_I} = uplink path loss for the interfering carrier [dB]
 $G_{sat_r_W}$ = satellite received antenna gain in the direction of the wanted earth station [dB]
 $G_{sat_r_I}$ = satellite received antenna gain in the direction of the interfering earth station [dB]

In addition, the antenna radiation pattern of the interfering earth station should obey the FCC antenna pattern given as $29-25\log \theta$ (dBi). The $EIRP_{esI}$ will then result as in the equation below.

$$EIRP_{es_I} = EIRP_{es_I,max} - G_{t_I,max} + 29 - 25 \log \theta \quad [dBW] \quad (Eq. 35)$$

where $EIRP_{es_I,max}$ = maximum EIRP of the interfering earth station [dBW]
 $G_{t,I,max}$ = maximum transmitting antenna gain of the interfering earth station [dB]
 θ = angular separation between two GEO satellites as seen by the earth station [degrees]
 [Usually it equals to 1.15 times the two satellites angular separation measured from the center of the earth)]

Considering the worst case described above, the wanted satellite receive antenna gain at the wanted earth station would be 3 dB less than the maximum earth station gain at the satellite. The uplink path losses for the wanted and interfering carriers are assumed to be the same. The resulting expression for overall $(C/I)_{up}$ is given as follows:

$$\left. \frac{C}{I} \right|_{dB_UP} = (EIRP_{esW} - EIRP_{es_I,max} - G_{t_I,max} - 32 + 25 \log(\theta)) \quad [dB] \quad (Eq. 36)$$

Based on (Eq. 4) in Chapter 2, the integrated C/N equation concerning the uplink adjacent satellite interference expressed as a ratio is given in (Eq. 37) below.

$$\frac{1}{\left(\frac{C}{N+I}\right)_{UP}} = \frac{1}{\left(\frac{C}{N}\right)_{UP}} + \frac{1}{\left(\frac{C}{I}\right)_{UP}} \quad [ratio] \quad (Eq. 37)$$

4.5.2. Downlink Adjacent Satellite Interference Analysis

Similarly to the uplink adjacent satellite interference calculations, the downlink adjacent satellite interference for the worst case is shown in Figure 23, where a wanted earth station is located at the edge of coverage of the wanted satellite and at the center of coverage of the interfering (adjacent) satellite.

N_{iD} refers to the downlink interference from the adjacent satellite arriving at the earth station, and C_D is downlink carrier power received by the wanted earth station from the wanted satellite. Both wanted satellite and adjacent satellite are separated by an angle of two or three degrees to the center of the earth. As to the results, the θ angle from Figure 23 will be 1.15 times larger than the 2 or 3 degrees separation angle [Mar95].

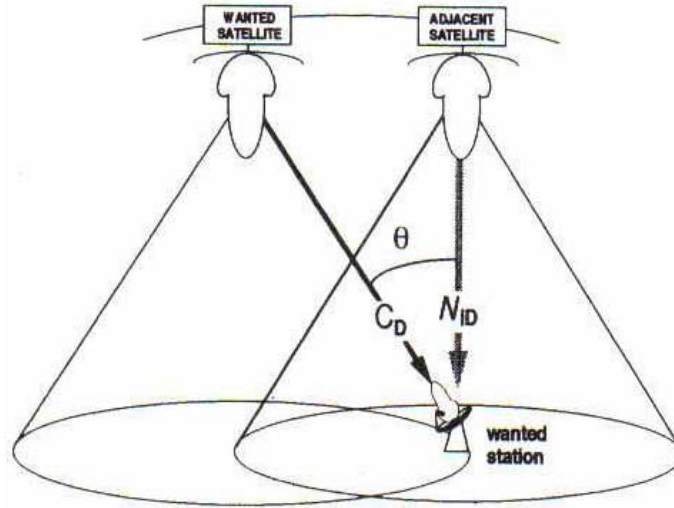


Figure 21 Downlink Interference from an Adjacent Satellite System [Mar95]

The expression for the carrier-to-interference power ratio for the downlink transmission would now be

$$\left. \frac{C}{I} \right|_{dB_DN} = (EIRP_{sat_W} - G_{es_r_W} - L_{p_W}) - (EIRP_{sat_I} - G_{es_r_I} - L_{p_I}) \quad [dB] \quad (Eq. 38)$$

where $EIRP_{sat_W}$ = wanted satellite EIRP for the wanted carrier in the direction of the wanted earth station [dBW]

$EIRP_{sat_I}$ = interfering satellite EIRP for the interfering carrier in the direction of the wanted earth station [dBW]

L_{p_W} = downlink path loss for the wanted carrier [dB]

L_{p_I} = downlink path loss for the interfering carrier [dB]

$G_{es_r_W}$ = earth station received antenna gain in the direction of the wanted satellite [dB]

$G_{es_r_I}$ = earth station received antenna gain in the direction of the interfering satellite [dB]

The antenna patterns of the wanted earth station can be expressed as

$$G_{es_r_I} = G_{es_r_W} - G_{es_r_W,max} + 29 - 25 \log \theta \quad [dBW] \quad (Eq. 39)$$

$G_{es_r_W,max}$ is the maximum received gain of the wanted earth station. The final expression of the overall downlink C/I is presented as

$$\left. \frac{C}{I} \right|_{dB_DN} = EIRP_{sat_W} - EIRP_{sat_I} + G_{es_r_W,max} - 32 + 25 \log(\theta) \quad [dB] \quad (Eq. 40)$$

Similarly to the uplink integrated C/N expression, the downlink integrated C/N with the adjacent satellite interference is expressed in (Eq. 41) below.

$$\frac{1}{\left(\frac{C}{N+I}\right)_{DN}} = \frac{1}{\left(\frac{C}{N}\right)_{DN}} + \frac{1}{\left(\frac{C}{I}\right)_{DN}} \quad [ratio] \quad (Eq. 41)$$

As introduced in earlier chapters, the adjacent satellite interference has significantly decreased the carrier-to-noise performance. (Eq. 37) and (Eq. 41) are applied to both OBP and bent-pipe transponders, although the OBP uplink and downlink are independent of each other as mentioned in Chapter 2. Hrycenko, et al., have proposed four methods that can decrease the adjacent satellite interference. The four basic approaches are frequency isolation, spatial isolation, polarization isolation, and signal processing. For more details refer to [Hry89].

4.6. Other Losses

Other losses that will degrade the satellite link performances include antenna pointing loss, atmospheric gaseous loss, beam spreading loss, etc. Implementation margin and link margin are selected to be 1 dB and 3 dB, respectively. Both margins are added to the link power budget analysis for the other unconsidered losses, such as antenna waveguide losses, cable losses between the ODU and IDU, and other hardware losses.

In addition, the atmospheric gaseous loss is chosen to be 0.5 dB. The accuracy of earth station antenna pointing is defined to be 0.5 dB for a 0.6 meter dish-antenna. Pointing errors less than a degree could result in harmful interference with neighboring systems. It is essential that the transmitting earth stations are installed precisely and the pointing angles are carefully monitored and maintained. As the size of an antenna increases, the pointing losses increase because the residual satellite motion causes the satellite to move out of the VSAT antenna beamwidth. Figure 24 shows the pointing losses for the Ka-bands and Ku-bands satellite station-

keeping requirements, corresponding to $\pm 0.05^\circ$ and $\pm 0.08^\circ$ angular excursions as seen from the ground [Hug93].

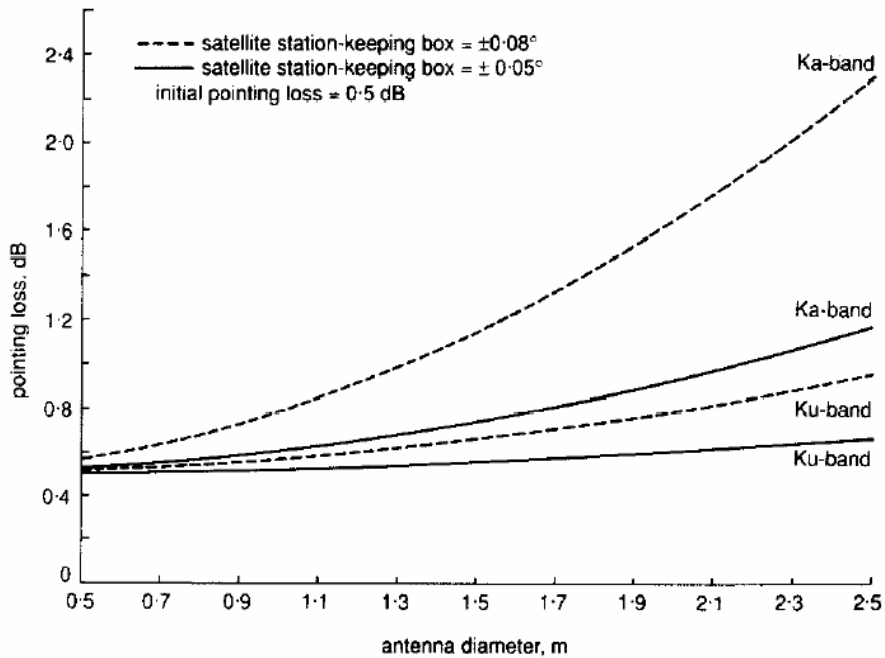


Figure 22 Pointing Losses as a Function of VSAT Antenna Diameter

4.7. Uplink and Downlink Noise Temperatures

The noise captured by the satellite antenna is the noise from the earth and from outer space. The major source of noise is from the earth system. In this system design, the noise temperature for the uplink transmission was chosen to be around 575 K.

The noise captured by the earth station antenna includes the noise from the sky conditions and the noise from the earth due to radiations. To simplify the design, the downlink noise temperature at the VSAT receiver was selected to be 275 K.

4.8. Link Budget

Since both bent-pipe and on-board processing transponders were discussed in the previous chapters, the Spaceway OBP transponders will be treated as conventional bent-pipe

transponders for link budget analysis. The inbound link and outbound link among the center hub, the transponder, and a VSAT will be analyzed under clear sky and moderate rain. As the bent-pipe transponder is assumed, multiple VSATs can fully utilize the transponder's bandwidth. The inbound and outbound links are either power or bandwidth limited because the transponder transmitting power and bandwidth is limited. This depends on the selectivity of the bandwidth and power of each channel.

4.8.1. Inbound Link Design

Table 23 shows an example of the inbound power budget between Blacksburg, Virginia and Los Angeles, California. The 1-watt 0.6-meter VSAT is placed in Blacksburg and the 8-meter center hub is placed at Los Angeles. Since the satellite carries a bent-pipe transponder, the noise bandwidth used in the link budget will be the IF bandwidth of the receiver, and both uplink and downlink noise bandwidths are the same.

The moderate rain attenuation was assumed to provide the link availability of 99.5% in an average year (or the outage of 43.80 hours) for both locations. For a 29.55-GHz uplink operating frequency, the rain attenuation for Blacksburg is 7.2 dB and for Los Angeles is around 3.4 dB. The downlink rain attenuation at Blacksburg is 3.2 dB, and at Los Angeles is around 1.4 dB with the operating center frequency at 19.75 GHz. The rain attenuation for other desired link availabilities can be referred to Tables 20 and 21 in this chapter.

The VSAT is assumed to operate with flexible burst rates. As stated in the earlier chapters, the VSAT modem is assumed similarly to the VT LMDS modem, providing QPSK modulation, and forward error correction. The coding gain for the VSAT modem is claimed to be 6.6 dB. Extra 1 dB implementation margin is counted for the link budget for other unconsidered losses. This results 8.0 dB for the threshold C/N value for this topology as the BER of 10^{-6} is desired.

Table 23 Topology 4: Inbound Link Budget Example (Blacksburg, VA-Los Angeles, CA)

Major Parameters	Rain	Clear Sky	
Uplink Frequency (Hz)	29.55E+9	29.55E+9	Hz
Downlink Frequency (Hz)	19.75E+9	19.75E+9	Hz
VSAT Diameter	0.60	0.60	m
VSAT Transmitting Antenna Gain	44.51	44.51	dB
VSAT Receiving Antenna Gain	41.01	41.01	dB
UPLINK: VSAT to satellite			
VSAT Pt	0.0	0.0	dBW
VSAT Gt	44.5	44.5	dB
Satellite Gr	41.5	41.5	dB
Free Space Path Losses	-212.9	-212.9	dB
Atmosphere Gaseous Losses	-1.0	-1.0	dB
Antenna Pointing Losses	-0.5	-0.5	dB
Other Losses	-0.5	-0.5	dB
Rain Attenuation Losses (0.5% outage at Blacksbug)	-7.2	0.0	dB
Pr (Received Power at Satellite Transponder Input)	-136.1	-128.9	dBW
Boltzmann's constant k	-228.6	-228.6	dBW/K/Hz
Satellite Input Noise Temperature Ts =575K	27.6	27.6	dBK
Satellite Receiver Bandwidth Bn = TBD MHz (421 kHz for rain & 2.23 MHz for clear sky)	56.3	63.5	dBHz
N (Noise Power at Satellite Transponder Input)	-144.7	-137.5	dBW
Uplink C/N	8.6	8.6	dB
Uplink C/I	16.6	16.6	dB
Uplink C/(N+I)	8.0	8.0	dB
DOWNLINK: Satellite to HUB			
Satellite EIRP	54.0	54.0	dBW
HUB Gr	61.8	61.8	dB
Free Space Path Losses	-209.4	-209.4	dB
Atmosphere Gaseous Losses	-1.0	-1.0	dB
Antenna Pointing Loss	-0.5	-0.5	dB
Other Losses	-0.5	-0.5	dB
Rain Attenuation Losses (0.5% Outage at Los Angeles)	-1.4	0.0	dB
Pr (Received Power at Hub Input)	-97.1	-95.6	dBW
Boltzmann's constant k	-228.6	-228.6	dBW/K/Hz
HUB Input Noise Temperature Ts = 275K	24.4	24.4	dBK
Hub Receiver Bandwidth Bn = TBD MHz (421 kHz for rain & 2.23 MHz for clear sky)	56.3	63.5	dBHz
N (Noise Power at HUB Receiver Input)	-147.9	-140.7	dBW
Downlink C/N	50.8	45.1	dB
Downlink C/(N+I)	38.6	37.9	dB
For Bent-Pipe Transponder:			
QPSK Required C/N @ 10e-6	13.6	13.6	dB
Implementation Margin	1.0	1.0	dB
Turbo Code Coding Gain	6.6	6.6	dB
Threshold C/N	8.0	8.0	dB
Overall (C/N+I)	8.0	8.0	dB

At the inbound uplink, in order to achieve 10^{-6} BER performance and meet the minimum threshold C/N value of 8 dB, the maximum data rate of the VSAT modem is calculated to be 2.2 Mbps under clear sky and 421 kbps under moderate rain at Blacksburg and Los Angeles. Higher data rates can be obtained under moderate rain when uplink power control (UPC) is incorporated in VSAT, described in Chapter 2, or when the VSAT transmitting power is increased.

Figure 25 illustrates that the data rate of the QPSK VSAT increases as the antenna size increases given that the VSAT transmitting power is 1W for the uplink transmissions. Figure 23 also shows that the overall inbound link data rate of the bent-pipe transponder under clear sky atmosphere is higher than those under moderate rain providing that the link availability is around 99.5% in an average year.

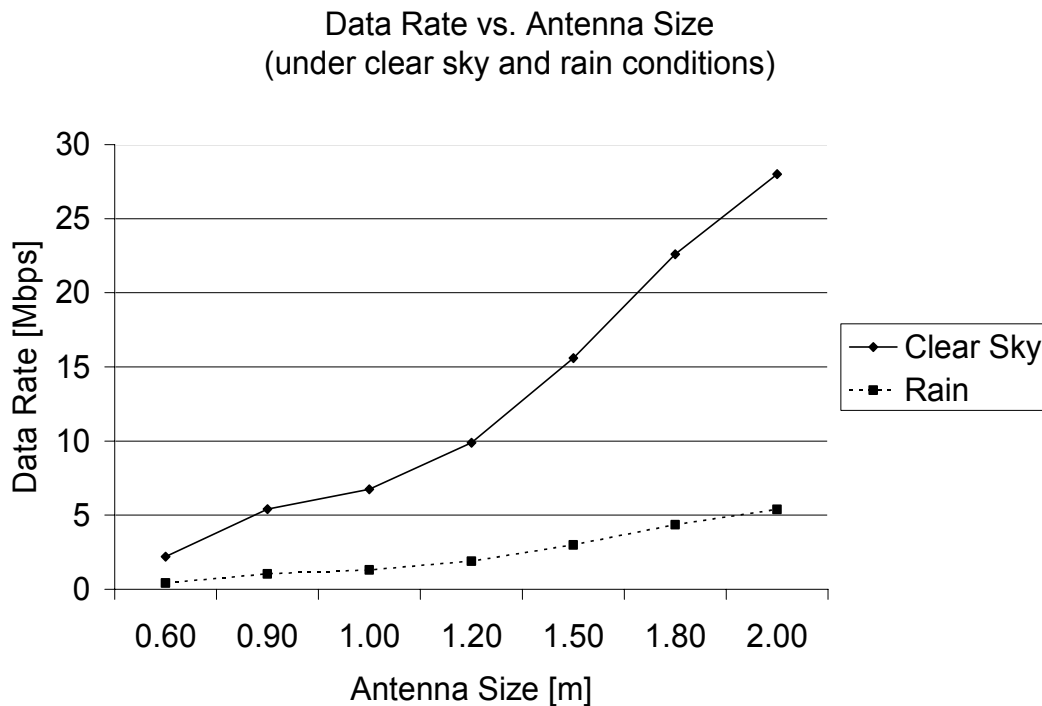


Figure 23 Inbound Data Rate vs. VSAT Transmitting Power

Rain decreases the data rate that can be used. The link performance therefore decreases also. Since the center hub and satellite parameters are not adjustable in the link budget, the VSAT transmitting power is another variable that can be adjusted to provide higher C/N link values. Increasing VSAT transmitting power can increase the uplink C/N value and BER

performance. On the other hand, higher power amplifiers will be required. The cost of the VSAT will also increase.

Figure 26 shows that when the antenna size of the BPSK VSAT increases, the data rate of the link also increases for any given transmitting power and any given weather conditions. As the transmitting power of the VSAT increases, the antenna size will decrease for any desired data rate. Certainly, the data rate, antenna size and VSAT transmitting power are proportional to each other.

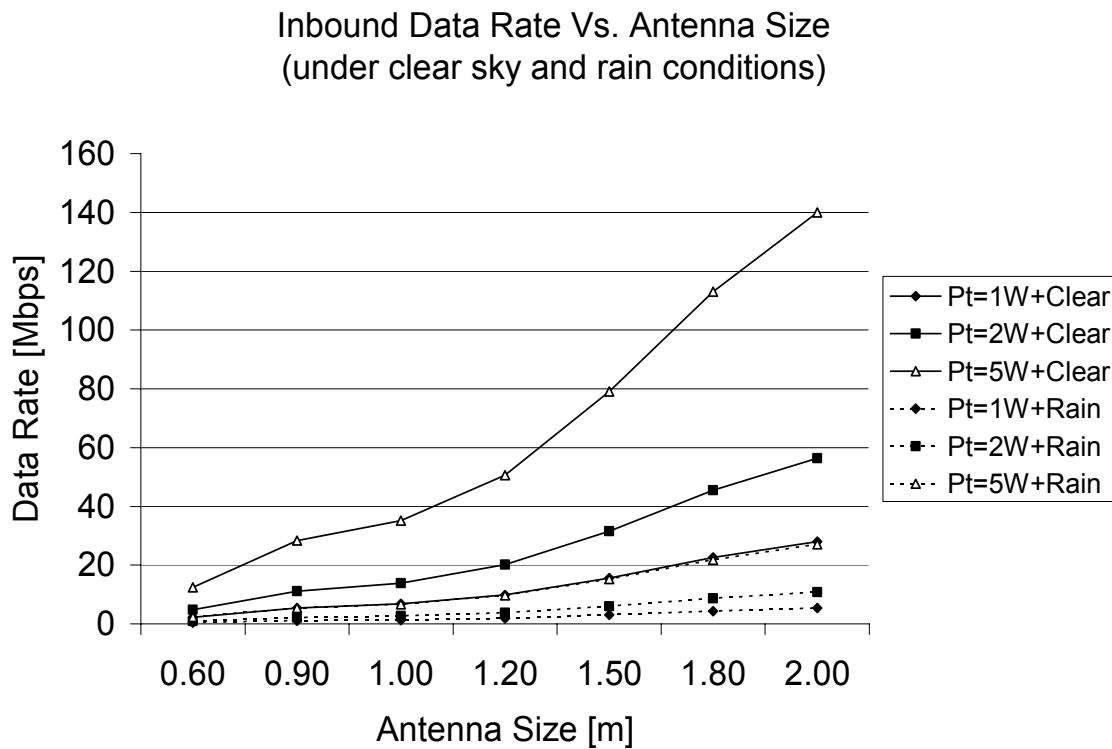


Figure 24 Inbound Data Rate Vs. Antenna Size for Given Various Pt

Figure 26 also shows that a 5W BPSK VSAT under rain has the same performance as a 1W VSAT under clear sky for the same antenna size at the inbound link of the Topology 4 design.

Different types of modulation were adopted for the inbound link budget analysis. The results show that the data rates for other modulations are less than the data rate with BPSK modulation. Figure 27 shows the inbound maximum data rate that the system can operate under clear sky and moderate rain assuming the transmitting power of VSAT is 1W and the antenna size is 1m. The data rate also depends on the type of modulation that is adopted. The higher the

order of the modulation, the lower the maximum data rate for the inbound link design. For a given bandwidth, the higher order modulation can deliver larger amount of information via the transmission link. For instance, the QPSK system can deliver twice the symbol rate of information compared to the BPSK system at the same bandwidth availability. The drawback for higher order modulation system is that larger amount of power is required to deliver those data bits.

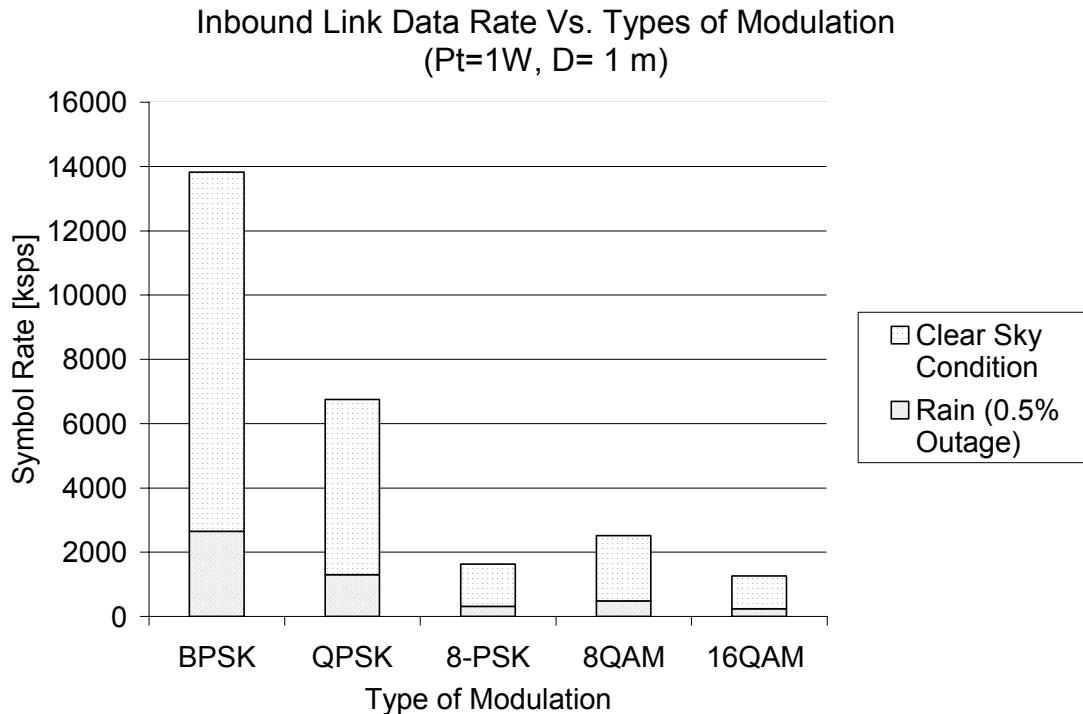


Figure 25 Inbound Data Rate vs. Antenna Size with Pt=1w and Different Modulations

Higher order modulation schemes, such as 8PSK and 16QAM, can be adopted, but they require higher C/N values to provide 10^{-6} BER performance. Some satellite manufacturers have proposed using 8PSK and 16QAM for the new satellite communication systems. From the figure above, higher order modulation, such as 8-PSK, 8QAM, and 16QAM, are not feasible for the Topology 4 designs since the data rate of the modulation is too low for broadband Internet service or for connecting to the LMDS terrestrial system. To maximize the bandwidth usage, the QPSK modulation is chosen for the VSAT. In addition, the LMDS modem was initially modeled for the VSAT modem because of the optimum usage of the transponder bandwidth.

In the U.S., the predicted link availability ranges from 95% to 99.9% depending upon the earth station's location and the desired data rate of the system. Figure 28 below shows the link availability of the inbound uplink for Topology 4. Larger VSAT antenna size is required for higher link availability. For instance, a VSAT with the burst rate of 1.544 Mbps providing T1-line broadband service was assumed here. The VSAT transmitting power was set to be 1W. The inbound downlink was not shown here since the center hub is capable of providing sufficient link margins. Moreover, Figure 28 concludes that when 96.5% of the link availability is desired, in order to provide the same BER performance, Miami and Dallas require 1.2-meter antennas for the VSAT, but Blacksburg, New York, and Chicago only need to use 0.6 meter antenna for the VSAT. Thus, when the VSATs are placed in different locations, the size of the antenna will be various due to the location rain intensity.

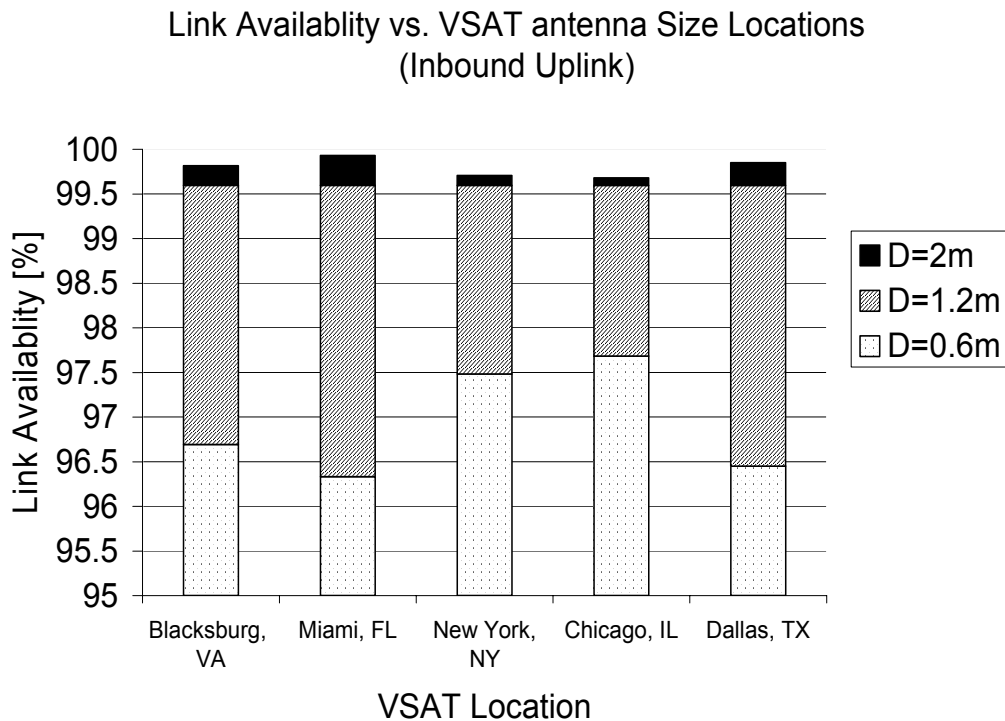


Figure 26 Inbound Link Availability vs. Antenna Size for Different Locations

4.8.2. Outbound Link Design

The outbound (from the center hub to the VSAT) link budget design is presented in this section. The outbound uplink usually will not be so critical due to the higher EIRP and antenna gain values of the center hub. The small size of VSAT usually limits the downlink performance of the outbound link. As the result, the downlink C/N value is dominated over the uplink C/N value for the overall C/N value, as shown in Table 24.

For the overall C/(N+I) equals the minimum C/N threshold value of 8.0 dB, the noise bandwidth of the receiver for both uplink and downlink are set to be 41 MHz under moderate rain, and 85.5 MHz under clear sky. The uplink C/(N+I) is 36.1 dB for moderate rain, and the downlink C/(N+I) is 8.0 dB. The downlink C/(N+I) value from the satellite to the hub is dominated compared to the uplink C/(N+I) value. No parameter of the satellite station and the hub station can be changed. In order to provide better BER performance or maintain the overall C/(N+I) value, the bandwidth of the receiver as the antenna size should increase.

Table 24 Topology 4: Outbound Link Budget Example (Los Angeles, CA-Blacksburg, VA)

Major Parameters	Rain	Clear Sky	
Uplink Frequency (Hz)	29.55E+9	29.55E+9	Hz
Downlink Frequency (Hz)	19.75E+9	19.75E+9	Hz
VSAT Diameter	0.60	0.60	m
VSAT Transmitting Antenna Gain	44.51	44.51	dB
VSAT Receiving Antenna Gain	41.01	41.01	dB
UPLINK: Hub to Satellite			
	Rain	Clear Sky	
HUB EIRP	89.5	89.5	dBW
Satellite Gr	41.5	41.5	dB
Free Space Path Losses	-212.9	-212.9	dB
Atmosphere Gaseous Losses (dB)	-1.0	-1.0	dB
Antenna Pointing Loss	-0.5	-0.5	dB
Other Losses	-0.5	-0.5	dB
Rain Attenuation Losses (0.5% outage at Los Angeles)	-3.3	0.0	dB
Pr (Received Power at Satellite Transponder Input)	-87.3	-83.9	dBW
Boltzmann's constant k	-228.6	-228.6	dBW/K/Hz
Satellite Input Noise Temperature Ts = 575K	27.6	27.6	dBK
Satellite Receiver Bandwidth Bn = TBD Mbps (41 MHz for rain & 85.5 MHz for clear sky)	76.1	79.3	dBHz
N (Noise Power at Satellite Transponder Input)	-124.9	-121.7	dBW
Uplink C/N	37.6	37.8	dB
Uplink C/I	41.5	41.5	dB
Uplink C/(N+I)	36.1	36.2	dB
DOWNLINK: Satellite to VSAT			
	Rain	Clear Sky	
Satellite EIRP	54.0	54.0	dBW
VSAT Gr	41.0	41.0	dB
Free Space Path Losses	-209.4	-209.4	dB
Atmosphere Gaseous Losses (dB)	-1.0	-1.0	dB
Antenna Pointing Losses	-0.5	-0.5	dB
Other Losses	-0.5	-0.5	dB
Rain Attenuation Losses (0.5% outage at Blacksburg)	-3.2	0.0	dB
Pr (Received Power at VSAT Input)	-119.6	-116.4	dBW
Boltzmann's constant k	-228.6	-228.6	dBW/K/Hz
VSAT Input Noise Temperature Ts = 275K	24.4	24.4	dBK
Satellite Receiver Bandwidth Bn = TBD Mbps (41 MHz for rain & 85.5 MHz for clear sky)	76.1	79.3	dBHz
N (Noise Power at VSAT Input)	-128.1	-124.9	dBW
Downlink C/N	8.5	8.5	dB
Downlink C/I	18.1	18.1	dB
Downlink C/(N+I)	8.0	8.0	dB
For Bent-Pipe Transponder:			
	Rain	Clear Sky	
QPSK Required C/N @ 10e-6	13.6	13.6	dB
Implementation Margin	1.0	1.0	dB
Turbo Code Coding Gain	6.6	6.6	dB
Threshold C/N	8.0	8.0	dB
Overall (C/N+I)	8.0	8.0	dB

Once again, increasing the size of the VSAT antenna will provide high data rate and reach the targeted BER performance. Figure 27 below shows that when the VSAT antenna size increases, higher data rate can be obtained for the QPSK system under clear sky and moderate rain. If a 2-m antenna is used, the outbound downlink can provide more than 30 Mbps of data rate link transmission. However, because rain attenuation between Blacksburg and Los Angeles degrades the signal performance, the data rate degrades to 5 Mbps to reach 10^{-6} BER performance. The transmitting power of the satellite is not controllable; thus the link performance all depends on the VSAT antenna receiving gain values.

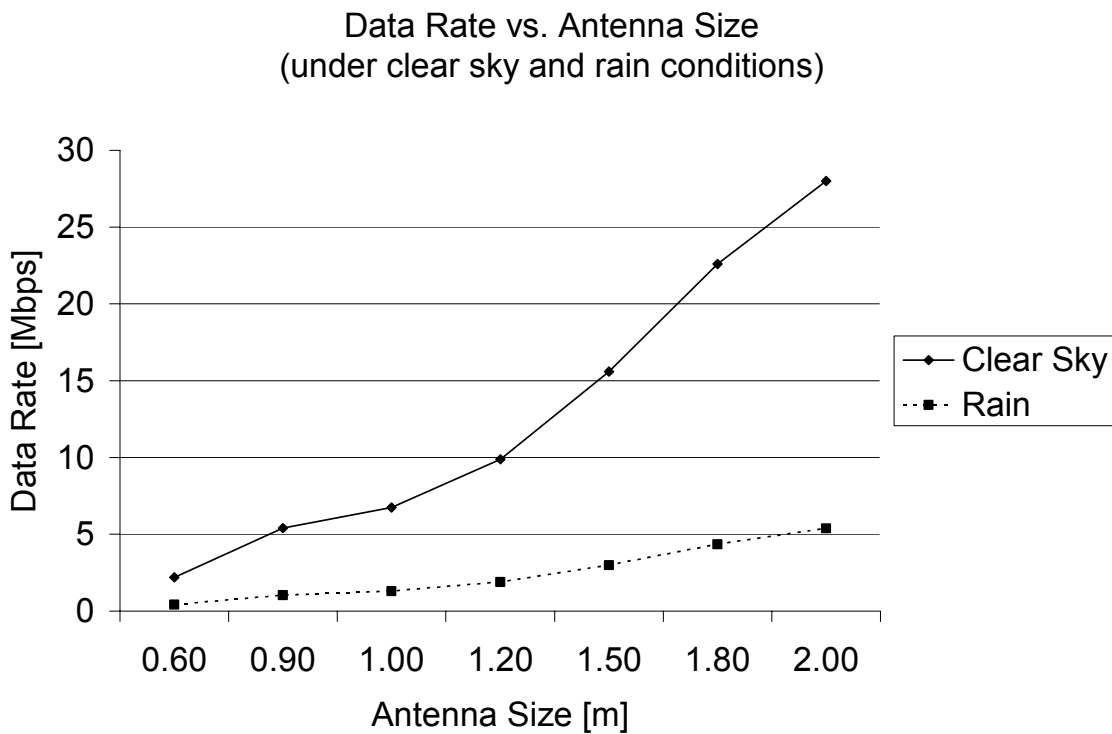


Figure 27 Data Rate versus VSAT Antenna Size for the Outbound Link Design

As higher order types of modulation are adopted, the data rate of the system will drop as expected in the previous inbound link design. QPSK is adopted for the outbound link design since it carries twice of the information at the given limited bandwidth. The satellite power or bandwidth might be limited depending on the channel power and bandwidth selections.

The inbound and the outbound link design can be very flexible and selective since the VSAT modem was assumed to be programmable with any desired data rate. The selectivity of

the VSAT antenna size and transmitting power will affect the BER link performance for the OBP transponder and the C/N values for the bent-pipe transponder. A QPSK modulation scheme was selected for Topology 4. The smaller the VSAT antenna size and transmitting power, the lower the VSAT costs. The estimated cost of the VSAT hardware will be given in the next chapter after the integrated system network implementation issues are addressed.

Table 23 below presents the overview technical specifications of center hub, satellite station, and LMDS hub and remote unit. The selected VSAT design specification is also included in the table.

Table 25 An Overview of All Terminals/Stations Technical Specifications

	Center Hub Station	Satellite Station	LMDS Hub/ Remote Unit	VSAT
Location	Los Angeles, CA	GEO/GSO	Blacksburg, VA	Blacksburg, VA
Latitude	34.08° N	0° W	37.28° N	37.28° N
Longitude	118.09° W	99° W	80.42° W	80.42° W
Uplink Frequency	29.75 GHz	29.75GHz	29.3 GHz	29.75GHz
Downlink Frequency	19.70 GHz	19.70 GHz	28.5 GHz	19.70 GHz
Antenna Type	Dish	Dish	Horn	Dish
Antenna Size	8 m	N/A		0.6-2 m
TX Antenna Gain	64.5 dB	41.50 dB	12.5 dB	44.51-54.97 dB
RX Antenna Gain	61.8 dB	41.50 dB	33.5 dB	41.01-51.47 dB
Total EIRP	89.5 dBW	60 dBW	-0.5 dBW	44.51–64.97 dBW
Type of Modulation	QPSK	QPSK	QPSK	QPSK
Type of Multiple Access	FDM/TDMA	FDM/TDMA	TDMA	FDM/TDMA
Supported Data Rate	Up to 120 Mbps	N/A	120 Mbps	Various

4.9. Summary

This chapter provided the detail design of Topology 4 for the terrestrial-satellite integrated system. The reflector antenna design with sub-efficiencies was provided for more accurate reflector antenna design. The adjacent satellite interference analysis for the satellite system was given for the worst case power budget analysis. The 10-step ITU rain model was used to calculate the link attenuation for various cities across the U.S. The different percentage of link availability was also provided in the chapter for designing a lower cost, higher data rate earth station. The VSAT modem was assumed to be the same as the LMDS modem but the VSAT modem data rate and modulation scheme is more selective. The tradeoffs among VSAT's antenna sizes, transmitting power, and costs were considered.

Chapter 5: System Network Issues and Hardware Selection

5.1. Terrestrial-Satellite Network and Protocols Concerns

The Virginia Tech LMDS system was assumed based on the standard IEEE 802.16 protocol. The end-users at the remote unit carries IEEE 802.11a and 802.11b standard protocols for wireless network accesses. The proposed Spaceway's OBP networks are capable of providing Internet services. Information exchange over the Internet network is governed by the TCP/IP Internet Protocol Suite. TCP/IP belongs to the IEEE 802.3 protocols for Internet access applications.

In the Topology 4 design, the satellite system is assumed to provide IEEE 802.3 protocols, and the existing LMDS system is assumed to operate at the IEEE 802.16 environment. As a result, both systems are not compatible with each other due to unrecognized protocols and different information data. As the packets from the terrestrial networks are sent via the satellite networks, the packets will not be recognized unless the satellite transponders' baseband modems are programmed to recognize IEEE 802.16 packets. Thus, the terrestrial network packets should be formatted onto satellite TCP/IP network packets transmission to the satellite. The satellite IEEE 802.3 packets should be translated to IEEE 802.16 packets when arriving at the earth station, and before coupling onto the LMDS system at baseband. All packet transformation should be done at the baseband instead of IF or RF bands. That is the reason why Topology 4 is the most feasible among all four topologies given in Chapter 3.

5.2. Open System Interconnection (OSI) Layers

The Transmission Control Protocol (TCP) and the Internet Protocol (IP) are packet-based protocols designed to support communications over data networks. TCP/IP belongs to the transport layer (layer 4) and network layer (layer 3) of the International Organization for Standards' (ISO) Open System Interconnection (OSI) protocol stacks. The TCP/IP connection uses the lower four layers of the ISO model and the Internet application will treats the upper three layers as a single application layer. Figure 28 below presents the overall ISO OSI layer

architecture and the TCP/IP implementation into those layers. The ISO OSI reference model is divided into seven layers.

	OSI	TCP/IP
Layer 7	Application	Application
Layer 6	Presentation	
Layer 5	Session	
Layer 4	Transport	TCP
Layer 3	Network	IP
Layer 2	Datalink	Access Network
Layer 1	Physical	Physical

Figure 28 A comparison of the TCP/IP and OSI protocol architecture [Ngu03]

Layer 1 is the physical layer, which is a medium that physically carries the signals through a twisted-paired wire, coaxial cable, fiber optic link, microwave link, or satellite link. This layer is concerned with all aspects of bit transmission, such as bit error rate, bit rate, forward error correction encoding and decoding, modulation and demodulation, etc. In general, this layer is built to meet existing transmission standards and allow interfacing between two different media types.

Layer 2 is known as a data link layer. This layer is referred to the physical network's protocols. The network access layer in the TCP/IP protocol stacks is related with the exchange of data between an end system and the network to which it is connected. Some of the layer standards are circuit switching, packet switching, and others. The Internet Protocol (IP) operates at Layer 3. IP is responsible for transporting datagrams across the Internet. Datagrams are short data packets, and each packet is labeled with an IP source and destination address. IP does not provide guaranteed datagram delivery.

Layer 4 is known as the transport layer, which can take care of the imperfections of network and lower layers by providing end-to-end reliability function if the TCP is used. For instance, TCP sends and tracks all datagrams, retransmits lost datagrams, and re-assembles datagrams at the destination in the same order in which they were sent. TCP can also respond to

link congestion by adjusting the data transmission rate. In TCP, a transmitter, such as a VSAT, sends a TCP packet and waits for an acknowledgement (ACK) from the receiver, such as a satellite station, to indicate that the packet is arrived correctly.

Layers 5, 6, and 7 at the TCP/IP protocol environment are treated as a single application layer. This combined layer supports various user applications, such as file transfer and browsing. To be in more details, Layer 5 is a session layer that provides specifications for managing the communications session between two applications across the network by facilitating the dialogue and inserting checkpoints in a large sequence of data bits. Layer 6 is known as a presentation layer, which provides information syntax and formatting specifications to facilitate communications between applications. Layer 7 is the last layer, so-called application layer, which provides specifications to design application program interfaces.

5.3. Overall Terrestrial-Satellite System Network Design

Figure 31 below illustrates the overall architecture of the satellite-terrestrial system network. Since the Spaceway satellite system was proposed for broadband Internet access, it carries IEEE 802.3 packet and protocols. The LMDS system was assumed to carry IEEE 802.16 standard data frame and protocol for the hub unit, and IEEE 802.11 packets and protocols for the end-users at the remote units. In order to interconnect three different networks together, the standard routers, switches, or bridges are adopted, as mentioned in Chapter 3.

Phys. = Physical Layer/link 802.3=IEEE 802.3 Standard for Ethernet application
 Appl. =Application Layer 802.16=IEEE 802.16 standards for LMDS broadband application
 ISP= Internet Service Provider 802.11=IEEE 802.11 standards for 2.4GH and 5-6GHz application

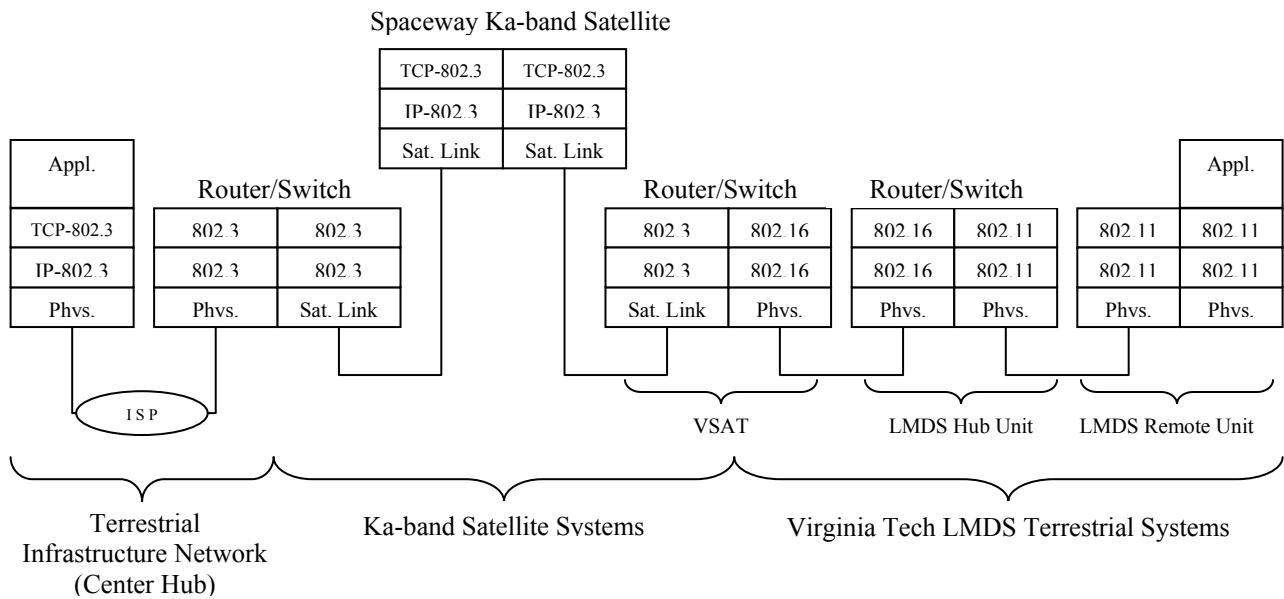


Figure 29 The Terrestrial-Satellite Integrated System OSI Model Architecture

Figure 31 shows that the network transformation between the LMDS remote units and hub unit was taken care of at the LMDS terrestrial system. The uplink internetworking connection between the VSAT and the satellite can be done by using a router or a switch. This router or switch will formulate a standard IEEE 802.16 packet and encapsulate the packet in an IEEE 802.16-compatible frame for transmitting over the IEEE 802.16 medium. At the router or the switch that is placed at the VSAT, the frame strips off its IEEE 802.16 header at the sub-layer of the link layer, and the frame is subsequently passed up to the upper sub-layer for further processing. Then, the IEEE 802.16 packet is passed to an IEEE 802.3 implementation, which encapsulates the packet in an IEEE 802.3 header for transmission on the IEEE 802.3 network to the IEEE 802.3 host at a Spaceway Ka-band transponder.

On the other hand, the downlink from the satellite to the VSAT network compatibility is also done by the same router or switch. The satellite IEEE 802.3 Internet protocol packets will be delivered down to the VSAT, and the packet will again be formulated and encapsulated into IEEE 802.16 packet on the OSI layers. These OSI model processes can be done with software at the application layer and proper inter-network implementation algorithms. In general, this type of

router or switch can be purchased off-the-shelf. If the direct IEEE 802.16 to IEEE 802.3 transformation is not available on the router or switch, multiple routers or switches can be cascaded until the desired end-to-end network are obtained.

The proposed Spaceway satellite uses packet switching technology on its OBP transponders. The OBP packet switch will automatically process any incoming standard information data (including frames, packets, datagrams) to the desired standard packets, such as IEEE 802.3 packets, before transmitting to end-users. In addition, the transformations between two networks will cause network errors and packet delays, and therefore degrade the network performance. Sometimes the network transformation is known as the protocol conversion between two networks or as the protocol emulation. The details on formatting the information at the OSI layers are beyond the scope of this thesis.

5.4. VSAT Commercial Hardware Components

Figure 32 below represents the VSAT block diagram of the Topology 4 design, including the RF, IF, and baseband sections. The RF front-end and IF sections were described in the Topology 4 design. The baseband section is simply the VSAT modem proposed in the earlier chapters. The QPSK modulation scheme with turbo coding with FEC Ω rate is adopted for the VSAT modem. The router or switch used for coupling VSAT and LMDS modem is shown in the figure below. A computer and controller connected to the VSAT baseband interface unit is responsible for informing the demodulator and modulator of what frequencies, coding rate, symbol rate, and coding type, and burst rate to use.

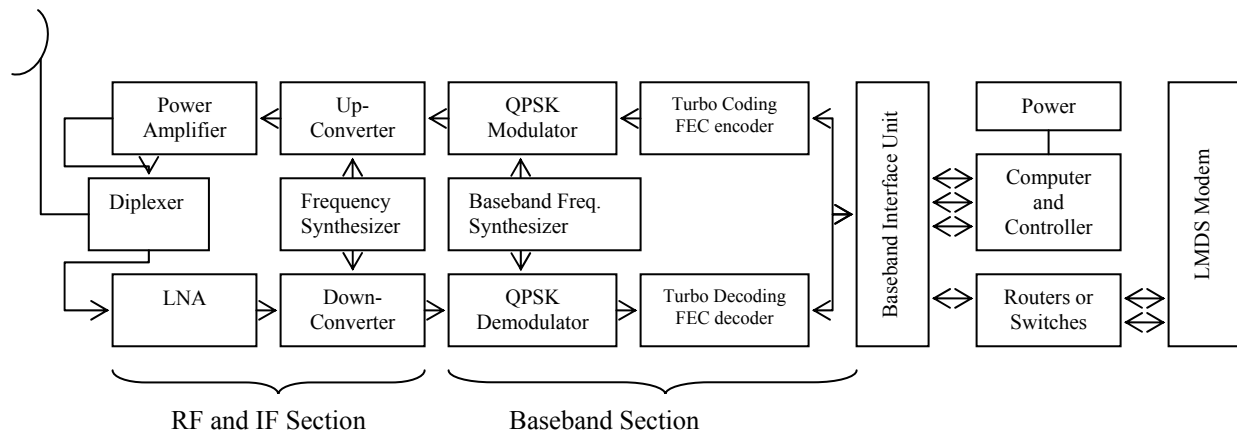


Figure 30 Topology 4 VSAT Block Diagram

From the block diagram above, it is noticeable that the hardware components of the VSAT can be purchased off-the-shelf easily from RF microwave and satellite equipment manufacturers. A standard commercial reflector antenna used for the VSAT is shown in Figure 33. Figure 34 shows the commercial existing satellite-to-LMDS and LMDS-to-Satellite frequency converters. More details of each component can be directly found on the manufacturers' websites [ITS03a & ITS03b]. The reflector antenna and the up- and down-frequency converters are the major cost of the whole VSAT design. The baseband hardware will not be described here since it is widely available on the market with a lower cost. The estimated cost of this VSAT for Topology 4 design will be greater than \$2000 depending on the desired features of the in-door and out-door units.



Figure 31 A Typical VSAT Commercial Reflector Antenna



Figure 32 Selected Commercial STL Frequency Up-converter (Left) and LTS Frequency Down-Converters (right)

5.5. Summary

The ISO model was introduced in this chapter. Since the LMDS network was not compatible with the Spaceway satellite network, a router or switch was proposed. The ISO model for the terrestrial and satellite network end-to-end users were given. The incompatible packets transferring between both terrestrial and satellite networks were processed through the router or switch at the VSAT or at the Spaceway satellite on-board packet switches. The VSAT hardware components, including antenna, power amplifier, frequency converters for Satellite-to-LMDS (STL) and LMDS-to-Satellite (LTS) conversions, were selected from the RF microwave manufacturers.

Chapter 6: Conclusion and Future Work

This chapter summarizes the thesis's contributions and overall integrated system design between the Ka-band satellite system and the terrestrial LMDS system. Future work and suggestions are given here for further integrated network development between a terrestrial system and a satellite system.

6.1. Conclusion and Contribution

The Virginia Tech LMDS broadband system was developed to provide last-mile broadband communication services for disaster recovery and response via a fiber optic infrastructure network. Alternatively, the fiber optic network backbone can be replaced by a satellite network backbone to achieve a shorter time period of equipment setup, higher data rate delivery, and lower cost of integrated equipment.

The first motivation for designing an integrated terrestrial-satellite network between an adjacent LMDS terminals and a Ka-band satellite system was economy and simplicity. The studies on four possible topologies to incorporate the LMDS system and satellite system showed that it was more complicated than the initial system design idea. The satellite VSAT could not operate at the desired 120 Mbps satellite modem speed because the VSAT has to meet the ITU and FCC maximum EIRP permitted limitations, the network protocols between both terrestrial and satellite networks have to be recognizable, and the link budget analysis for the satellite system has to be feasible in the face of adjacent satellite interference, propagation effects, and other losses. Thus, a new satellite modem supporting various data rate delivery and different types of modulation was designed for the this thesis.

Four terrestrial-satellite integrated system topologies were studied, and the Topology 4 design was selected to be most feasible and practical for the integrated system. The VSAT consists of both satellite-to-LMDS (STL) and LMDS-to-satellite (LTS) frequency converters. Both converters' planning frequencies were selected carefully to minimize channel interference, provide image cancellation, and avoid spurs and higher order modulations. The characteristics of the VSAT were designed based on the inbound and outbound link budget analysis. The ITU rain

model, EIRP limitation of the VSAT, adjacent satellite interference, and other noise and attenuation sources were considered at the link budget design.

The tradeoffs in the VSAT design were analyzed in the link budgets. To achieve better BER performance, either VSAT antenna size or the VSAT transmitting power has to be increased. For better bandwidth use, higher order modulation can be used; however, QPSK modulation is proposed to use in the Topology 4 design. Turbo codes with FEC $\frac{1}{2}$ rate providing additional 6.6 dB coding gain was adopted for the link budget design of Topology 4. That leads the minimum C/N threshold to be 8.16 dB. In addition, the router/switch was selected for network impairments between two incompatible protocol systems, and the routers/switches provide protocol conversion (emulation) and promise packets delivery between both terrestrial and satellite networks.

6.2. Future Work

The fundamental and theoretical system designs of the VSAT for the satellite system were studied in this thesis. This work can become practical and feasible. The Topology 4 design's hardware components can be purchased and assembled together for a feasible VSAT.

Multiple VSATs with either a star network or a mesh network can be analyzed for full use of the satellite transponder, although the Topology 4 link budget analysis was only based on a single VSAT operation. Multiple VSAT networks are more realistic and economical to the satellite system investors.

The proposed and designed VSAT can be built easily but proper inter-networking implementation algorithms must be written for the inter-network protocol conversion and implementation between the Spaceway Ka-band satellite network and LMDS terrestrial networks. An additional software algorithm is also required for controlling the functionalities of the VSAT modem. This suggested future work will practically provide additional interoperability to the Virginia Tech LMDS system.

References

- [Bal82] Balanis, C. A., *ANTENNA THEORY: Analysis and Design*, Harper & Row, Inc., New York, 1982.
- [Bar95] Barker, L., and Maxwell, S., “Telecommunications resource management for disaster response and recovery”, *MILCOM '95*, Vol. 2, pp. 853 -857, 5-8 Nov. 1995.
- [Bos02] Bostian, C. W., Midkiff, S. F., Kurgan, W.M., Carstensen, L. W., Sweeney, D.G., Gallageher, T., “Broadband communications for disaster response”, *Space Communications* (International Edition). Vol. 18, Issue 3-4, pp. 167-177, 2002.
- [Cra80] Crane, R.K., “Prediction of Attenuation by Rain”, *IEEE Transactions on Communications*, Vol. COM-28, No. 9, pp. 1717-1735, Sept. 1980.
- [Com01] Comparetto, G., and Marshall, J., “Small-diameter Earth terminal transmission issues in support of high data rate mobile satellite service applications”, *MILCOM 2001, IEEE Journals*, Vol. 1, pp.321 –325, Oct. 2001.
- [Cou01] Couch, L. W., *Digital and Analog Communications Systems*, Prentice Hall, NY, 6th ed., 2001.
- [Csm03] Ohio Consortium for Advanced Communications Technology, <http://www.csm.ohiou.edu/ocact>, 2003.
- [CWT01] Eshler, T. J., “Proposed Multiple Access Scheme for the LMDS Modem”, CWT documentation, Rough Draft, March 29, 2001.
- [CWT02] “Proposed Multiple Access Scheme and Data Link Protocol”, CWT documentation, February 25, 2002.
- [Dis97] Dissanayake, A.W., “Application of open-loop uplink power control in Ka-band satellite links”, *IEEE Journals*, Vol. 85, Issue 6 , pp. 959 -969, June 1997.
- [Ega82] Egami, S., “Individual closed-loop satellite access power control system using overall satellite up-link quality level”, *IEEE Trans. Commun.*, Vol. COM-30, pp. 1806-1808, July 1982.
- [Elb00] Elbert, B. R., *Ground Segment and Earth Station Handbook*, Artech House, Inc., Norwood, MA, 2000.
- [Esh02] Eshler, T. J., “Adaptive protocols to improve TCP/IP performance in an LMDS network using a broadband channel sounder”, *Masters Thesis*, Virginia Polytechnic Institute and State University, 2002. <http://scholar.lib.vt.edu/theses/available/etd-04252002-115751/>

- [Eva91] Evans, B. G., *Satellite Communications Systems*, 2nd Edition, Peter Peregrinus Ltd., 1991.
- [Eva98] Evans, J. V., “Proposed U.S. Global Satellite Systems Operating at Ka-band”, *IEEE Aerospace Conference Proceedings*, 1998.
- [Eva00] Evans, J. V., “The U.S. filling for multimedia satellite: a review”, *International Journal of Satellite Communications*, Vol. 18, pp. 121-160, 2000.
- [Far01] Farserotu, J. “Integration of Terrestrial and Satellite Networks: Technology, Services and Applications”, *Wireless Personal Communications*, Vol. 17, pp. 283-290, 2001.
- [FCC00] “Redesignation of the 17.7-19.7 GHz Frequency Band, Blanket Licensing of Satellite Earth Stations in the 17.7-20.2 GHz and 27.5-30.0 GHz Frequency Bands, and the Allocation of Additional Spectrum in the 17.3-17.8 GHz and 24.75-25.25 GHz Frequency Bands for Broadcast Satellite-Service Use”, *FCC Report and Order*, IB Docket No. 98-172 or FCC No. 00-212, released 22 June 2000.
- [FCC02a] Federal Communications Commission, Radio Station Authorization: Hughes Network Systems, Inc., Callsign: E020241, File No. SES-LIC-20020829-01460, Nov. 25, 2002.
- [FCC02b] Federal Communications Commission, Radio Station Authorization: Hughes Network Systems, Inc., Callsign: E020242, File No. SES-LIC-20020829-01461, Nov. 25, 2002.
- [Fen01] Feng, Y., “Resource Allocation in Ka-band Satellite Systems”, *Masters Thesis*, University of Maryland, College Park, Maryland, U.S.A., 2001.
http://techreports.isr.umd.edu/reports/2001/MS_2001-2.pdf
- [Fit95] Fitzpatrick, E., “SPACEWAY™ System Summary”, *Journal of Space Communications*, Vol. 13, Issue 1, pp. 7-23, 1995.
- [Gar99] Gargione, F., Iida, T., Valdoni, F., and Vatalaro, F., “Services, technologies, and systems at Ka band and beyond-a survey”, *Communications, IEEE Journal*, Vol. 17 (2), pp. 133 –144, Feb. 1999.
- [Gua02] Guarnera, M., Villari, M., Zaia, A., and Puliafito, A., “MANET: possible applications with PDA in wireless imaging environment”, *IEEE International Symposium*, Vol. 5, pp. 2394-2398, 15-18 Sept. 2002.
- [Gom02] Gomez, J. M., *Satellite Broadcast Systems Engineering*, Artech House, Inc., Norwood, MA, pp. 48, 2002.
- [Ha86] Ha, T. T., *Digital Satellite Communications*, Macmillan, New York, 1986.

- [Hry89] Hrycenko, G., and Dulac, S., “Adjacent Satellite and Ground Station Interference”, *SMPTE Journal*, Vol. 98, Issue 12, pp. 890-5, Dec. 1989.
- [Hug93] Hughes, C.D., et al., “Satellite system in A VSAT environment”, *IEEE Electronics & Communication Engineering Journal*, Vol. 5, Issue 5, pp 285-291, Oct. 1993.
- [ITU02] ITU, *Handbook on Satellite Communications*, 3rd ed., Wiley, New York, 2002.
- [ITU618] Recommendation ITU-R P.618-7, “Propagation Data and Prediction Methods Required for the Design of Earth-Space Telecommunications Systems”, 2003.
- [ITU728] Recommendation ITU-R S.827, “Maximum permissible level of off-axis e.i.r.p. density from very small aperture terminals (VSATs)”, 2003.
- [ITU837] Recommendation ITU-R P.837, “Characteristics of precipitation for propagation modeling”, 2003.
- [ITU838] Recommendation ITU-R P.838, “Specific attenuation model for rain for use in prediction”, 2003.
- [ITU839] Recommendation ITU-R P.839, “Rain height model for prediction methods”, 2002.
- [ITU1329] Recommendation ITU-R S.1329, “Frequency sharing of the bands 19.7-20.2 GHz, and 29.5-30.0GHz between systems in the mobile-satellite service and systems in the fixed-satellite service”, 1997.
- [ITU1511] Recommendation ITU-R S.1511, “Topography for Earth-to-Space Propagation Modeling”, 2001.
- [ITS03a] ITS Electronics Inc., Ka-band Frequency Down-converter, http://www.itselectronics.com/prod/pdf/Datasheet_K-Band_BDC-19-20GHz.pdf, 2003.
- [ITS03b] ITS Electronics Inc., Ka-band Frequency Up-converter, http://www.itselectronics.com/prod/pdf/Datasheet_Ka-Band_BUC-29-30GHz.pdf, 2003.
- [Liv99] Livieratos, S.N., Ginis, G., and Cottis, P.G., “Availability and performance of satellite links suffering from interference by an adjacent satellite and rain fades”, *Communications, IEE Proceedings*, Vol. 146 (1), pp. 61-67, Feb. 1999.
- [Loc01] “Virginia Tech 120 Mbit/s Modem Interface Card: Interface Control Document MIC to Modem”, Lockheed Martin, Doc. No. ICD00093 Rev. 02, April 11th, 2001.
- [Luk99] Luka, G., “Government Use of Commercial Satellite Systems for Disaster Response”, *MILCOM 1999, IEEE*, Vol. 1, pp. 117 -119, 31 Oct. - 3 Nov. 1999.

- [Mar95] Maral, G., *VSAT Networks*, John Wiley & Son, NY, 1995.
- [Ngu03] Nguyen, H. N., *Routing and Quality-of-Service in Broadband LEO Satellite Network*, Kluwer Academic Publishers, MA, U.S.A., 2003.
- [Pan02] Panagopoulos, A.D., Margoni, M., and Kanellopoulos, J.D., “Carrier-to-interference ratio statistics of an Earth-space system interfered by an adjacent satellite system and a point-to-point microwave system under rain fades”, 6th Africon Conference in Africa, 2002, *IEEE AFRICON*, Vol. 1, pp.343 –346, Oct. 2002.
- [Phi95] Phillip, G., and Hodge, R., “DISASTER ARE: Telecommunications Support to Disaster Response and Recovery”, *MICOM '95, IEEE*, Vol. 2, pp. 833-837, 5-8 Nov. 1995.
- [Pra86] Pratt, T., and Bostian, C., *Satellite Communications*, John Wiley & Son, New Jersey, 1986.
- [Pra02] Pratt, T., Bostian, C., Allnutt, J., *Satellite Communications*, John Wiley & Son, New Jersey, 2002.
- [Raz98] Razavi, B., *RF microelectronics*, Prentice Hall, New Jersey, 1998.
- [Ors99] Ors, T., Chotikapong, T., and Sun, Z. “Geo Satellite Network Characteristics”, Public Final, Esprit Project EP 28425, BISANTE Consortium, U.K., Mar. 1999.
- [Saa89] Saam, T. J., “Uplink Power Control Technique for VSAT Networks”, *Southeastcom '89 Proceedings, 'Energy and Information Technologies in the Southeast', IEEE*, 9-12 April 1989, Vol. 1, pp. 96 -101, 1989.
- [Sko01] Skolnik, M. I., *Introduction to Radar Systems*, McGraw-Hill, New York, 2001.
- [Str02] Strother, J.B., “A contrast in responses to the unspeakable events of September 11: American Airlines vs. United Airlines”, *IPCC 2002, Proceedings IEEE*, 17-20 Sept. 2002, pp. 423 -436, 2002.
- [Stu88] Stutzman, W., and Thiele, G., *Antenna Theory and Design*, John Wiley & Sons, New York, 2nd edition, 1988.
- [Yen00] Yen, L., “Satellite communications for the millennium”, *IEEE Antennas and Propagation Society International Symposium*, Vol. 2, pp. 530 -533, July 2000.
- [Yoh99] Yoh, J., Wang, C.C., and Goo, G.W.; “Survey of Ka-band satellites for wideband communications”, *IEEE*, Vol. 1, pp. 120 –125, 1999.

Appendix A: Elevation and Azimuth Angle Calculations

Location	VSAT Locations						Hub Locations	
	Blacksburg, VA	Miami, FL	New York, NY	Chicago, IL	Dallas, TX	Los Angeles, CA	Douglas, CO	
Geosynchronous Radius Rs	42164.17	42164.17	42164.17	42164.17	42164.17	42164.17	42164.17	km
Earth Radio re	6378.137	6378.137	6378.137	6378.137	6378.137	6378.137	6378.137	km
ES North Latitude Le	37.28	25.82	40.78	41.85	32.78	34.08	39.01	N
ES West Longitude le	80.42	80.28	73.97	87.65	95.8	118.09	105.01	W
Subsatellite Point North Latitude, Ls	0	0	0	0	0	0	0	N
Subsatellite Point West Longitude ls	99	99	99	99	99	99	99	W
COS(gamma)	0.75	0.85	0.69	0.73	0.84	0.78	0.77	radians
gamma	41.04	31.51	46.68	43.09	32.92	38.49	39.40	degrees
distance from ES to sat, d	37587.74	36877.49	38071.89	37758.26	36972.91	37383.32	37454.77	km
cos(EL)	0.74	0.60	0.81	0.76	0.62	0.70	0.71	radians
Intermediate angle alpha	29.03	37.88	35.56	16.74	5.90	-31.70	-9.50	degrees
EL	42.56	53.30	36.32	40.29	51.70	45.41	44.40	degrees
AZ	209.03	217.88	215.56	196.74	185.90	211.70	189.50	degrees
Location Defined	SW	SW	SW	SW	SW	SE	SE	
Case I: Earth Station in the Southern Hemisphere for AZ								
(a) Southern Hemisphere Satellite to the NE of the ES	NE	37.88	35.56	16.74	5.90	-31.70	-9.50	degrees
(b) Southern Hemisphere Satellite to the NW of the ES	NW	330.97	322.12	324.44	343.26	391.70	369.50	Degrees
Case II: Earth Station in the Northern Hemisphere for AZ								
(a) Northern Hemisphere Satellite to the SE of the ES	SE	150.97	142.12	144.44	163.26	211.70	189.50	degrees
(b) Northern Hemisphere Satellite to the SW of the ES	SW	209.03	217.88	215.56	196.74	148.30	170.50	degrees

Appendix B: (a) Uplink Rain Attenuation Calculations

	VSAT Locations						Hub Location		
	Blacksburg, VA	Miami, FL	New York, NY	Chicago, IL	Dallas, TX	Los Angeles, CA	Douglas, CO		
Frequency	29.55	29.55	29.55	29.55	29.55	29.55	29.55	29.55	GHz
Re Effective Radius of the Earth	8500	8500	8500	8500	8500	8500	8500	8500	km
Polarization	Circular	Circular	Circular	Circular	Circular	Circular	Circular	Circular	
Tau (Circular Polarization)	90	90	90	90	90	90	90	90	degrees
Earth Station Latitude Le (phi)	37.28	25.82	40.78	41.85	32.78	34.08	39.01	39.01	degrees
Rain Height h'(R)	3.904	3.72296	3.6415	3.56125	3.91784	3.95424	3.77425	3.77425	km
Height of earth station (above sea level), hs	0.6096	0.05	0.04	0.181	0.183	0.2995	1.6969	1.6969	km
Rain Climate Regions Zone	M	M	K	K	M	E	B	B	
Uplink Availability	99.99	99.99	99.99	99.99	99.99	99.99	99.99	99.99	%
R(0.01)	63	63	42	42	63	22	12	12	mm/hr
Elevation Angle, Theta	42.56	53.30	36.32	40.29	51.70	45.41	44.40	44.40	degrees
k (circular)	0.1664	0.1704	0.1662	0.1706	0.166	0.1656	0.1687	0.1687	
alpha (circular)	1.0083	1.0129	1.008	1.0131	1.0078	1.0073	1.0109	1.0109	
Slant Path Length, Ls	4.87	4.58	6.08	5.23	4.76	5.13	2.97	2.97	km
Horizontal Projection of slant-path length, LG	3.59	2.74	4.90	3.99	2.95	3.60	2.12	2.12	km
gamma (R)=k(R0.01)^alpha	10.85	11.32	7.19	7.52	10.80	3.73	2.08	2.08	dB/km
Horizontal Reduction Factor (r 0.01)	0.66	0.70	0.68	0.71	0.70	0.87	1.08	1.08	
curve symbol	54.30	62.32	47.26	50.00	61.11	49.30	42.23	42.23	degrees
LR (if curve symbol > EL, Theta)	3.21	3.22	4.13	3.72	3.33	4.48	2.91	2.91	km
X=36-phi when phi <36	0.00	10.18	0.00	0.00	3.22	1.92	0.00	0.00	degrees
v0.01	1.25	1.27	1.25	1.27	1.27	1.35	1.44	1.44	
Effective path length, LE	4.01	4.09	5.15	4.71	4.21	6.03	4.17	4.17	
Predicted Attenuation for A0.01	43.4624	46.3724	37.0215	35.4499	45.4815	22.4694	8.6810	8.6810	dB
Desired link availability percentage, p	0.5000	0.5000	0.5000	0.5000	0.5000	0.5000	0.5000	0.5000	%
Beta	0.0000	0.0509	0.0000	0.0000	0.0161	0.0096	0.0000	0.0000	
Predicted Attenuation for Ap	7.121	8.323	5.897	5.603	7.699	3.322	1.071	1.071	dB
Number of Hours for Outage per year	43.800	43.800	43.800	43.800	43.800	43.800	43.800	43.800	hrs

Appendix B: (b) Downlink Rain Attenuation Calculations

Downlink Rain Attenuation Calculation	VSAT Locations						Hub Location	
	Blacksburg, VA	Miami, FL	New York, NY	Chicago, IL	Dallas, TX	Los Angeles, CA	Douglas, CO	
Frequency	19.75	19.75	19.75	19.75	19.75	19.75	19.75	GHz
Re Effective Radius of the Earth	8500	8500	8500	8500	8500	8500	8500	km
Polarization	Circular	Circular	Circular	Circular	Circular	Circular	Circular	
Tau (Circular Polarization)	90	90	90	90	90	90	90	degrees
Earth Station Latitude Le (phi)	37.28	25.82	40.78	41.85	32.78	34.08	39.01	degrees
Rain Height h'(R)	3.904	3.72296	3.6415	3.56125	3.91784	3.95424	3.77425	km
Height of earth station (above sea level), hs	0.6096	0.05	0.04	0.181	0.183	0.2995	1.6969	km
Rain Climate Regions Zone	M	M	K	K	M	E	B	
Uplink Availability	99.99	99.99	99.99	99.99	99.99	99.99	99.99	%
R(0.01)	63	63	42	42	63	22	12	mm/hr
Elevation Angle, Theta	42.56	53.30	36.32	40.29	51.70	45.41	44.40	degrees
k (circular)	0.0682	0.0694	0.0684	0.0695	0.0681	0.068	0.0689	
alpha (circular)	1.0773	1.0844	1.0769	1.0848	1.0765	1.0759	1.0814	
Slant Path Length, Ls	4.87	4.58	6.08	5.23	4.76	5.13	2.97	km
Horizontal Projection of slant-path length, LG	3.59	2.74	4.90	3.99	2.95	3.60	2.12	km
gamma (R)=k(R0.01)^alpha	5.92	6.20	3.83	4.01	5.89	1.89	1.01	dB/km
Horizontal Reduction Factor (r 0.01)	0.70	0.74	0.72	0.76	0.74	0.93	1.13	
curve symbol	52.69	61.00	45.42	48.25	59.72	47.57	40.84	degrees
LR (if curve symbol > EL, Theta)	3.41	3.41	4.41	3.95	3.52	4.76	2.91	km
X=36-phi when phi <36	0.00	10.18	0.00	0.00	3.22	1.92	0.00	degrees
v0.01	1.08	1.09	1.11	1.12	1.08	1.22	1.36	
Effective path length, LE	3.69	3.70	4.87	4.43	3.82	5.79	3.94	
Predicted Attenuation for A0.01	21.8443	22.9305	18.6428	17.7576	22.4811	10.9572	3.9895	dB
Desired link availability percentage, p	0.5000	0.5000	0.5000	0.5000	0.5000	0.5000	0.5000	%
Beta	0.0000	0.0509	0.0000	0.0000	0.0161	0.0096	0.0000	
Predicted Attenuation for Ap	3.171	3.636	2.632	2.485	3.362	1.427	0.429	dB
Number of Hours for Outage per year	43.800	43.800	43.800	43.800	43.800	43.800	43.800	hrs

Vita

Suem Ping Loo was born in 1978 in Malaysia. She came to the U.S. on August 14, 1996. She attended Northern Virginia Community College, Annandale, Virginia before transferring to Virginia Polytechnic Institute and State University (Virginia Tech) in January 1998. She obtained her bachelor's degree in Electrical Engineering in December 2001 at Virginia Tech. During her undergraduate study, she worked at General Electric (GE) Company at Salem, Virginia as a Sourcing Engineer and Engineering Assistant for three academic semesters. She has continued to pursue her master's degree in Electrical Engineering, and is planning to obtain her M.S. degree with this thesis research. Her research interests are satellite telecommunications systems, solid state radio engineering, and electronics circuit hardware designs.

Loo is also a student member of the Eta Kappa Nu National Engineering Honor Society, Tau Beta Pi National Engineering Honor Society, IEEE Society, Golden Key National Honor Society, and Phi Theta Kappa Fraternity Society. She has received the Personal Communications Industry Association (PCIA) Ardizzone Family Foundation Scholarship, William Webber Scholarship, and Center of Power Electronics System (CPES) Assistantship and Fellowship in her undergraduate study at Virginia Tech. She was also awarded a graduate teaching assistantship under the Bradley Electrical and Computer Engineering (ECE) Department at Virginia Tech, and a graduate research assistantship under the Center for Wireless Telecommunications at Virginia Tech during her graduate study.